IOWA STATE UNIVERSITY
Digital Repository

Retrospective Theses and Dissertations

Iowa State University Capstones, Theses and Dissertations

1962

Mechanisms of the electrical resistivity of rare earth alloys at low temperatures

Fred August Smidt Jr.
Iowa State University

Follow this and additional works at: https://lib.dr.iastate.edu/rtd

 Part of the Physical Chemistry Commons

Recommended Citation
Smidt, Fred August Jr., "Mechanisms of the electrical resistivity of rare earth alloys at low temperatures " (1962). *Retrospective Theses and Dissertations*. 2076.
https://lib.dr.iastate.edu/rtd/2076

This Dissertation is brought to you for free and open access by the Iowa State University Capstones, Theses and Dissertations at Iowa State University Digital Repository. It has been accepted for inclusion in Retrospective Theses and Dissertations by an authorized administrator of Iowa State University Digital Repository. For more information, please contact digirep@iastate.edu.

www.manaraa.com

This dissertation has been 62-4178
microfilmed exactly as received

SMIDT, Jr., Fred August, 1932-
MECHANISMS OF THE ELECTRICAL RESISTIVITY OF RARE EARTH ALLOYS AT LOW TEMPERATURES.

Iowa State University of Science and Technology
Ph.D., 1962
Chemistry, physical

University Microfilms, Inc., Ann Arbor, Michigan

MECHANISMS OF THE ELECTRICAL RESISTIVITY OF RARE EARTH ALLOYS AT LOW TEMPERATURES

by

Fred August Smidt, Jr.

A Dissertation Submitted to the
Graduate Faculty in Partial Fulfillment of
The Requirements for the Degree of
DOCTOR OF PHILOSOPHY

Major Subject: Physical Chemistry

Approved:

Signature was redacted for privacy.

In Charge of Major Work

Signature was redacted for privacy.

Head of Major Department

Signature was redacted for privacy.

Dean of Graduate College

Iowa State University
Of Science and Technology
Ames, Iowa

1962

TABLE OF CONTENTS

I. INTRODUCTION

Recent years have seen tremendous strides made in the knowledge and understanding of the solid state. An important factor in this advance has been the use of high speed electronic computers which have allowed the theoretician to apply the principles of quantum mechanics to the problems of the solid state and get solutions quickly which would otherwise be impossible or would require years of tedious work. The burden of testing the theories so obtained now falls upon the experimentalist who must carefully examine various materials to determine where the theories are valid, where they fail and where they must be slightly modified. High on the list of those materials under investigation are the metals, which include approximately three-fourths of the known elements.

Chief contributors to the advance in knowledge about the solid state have been the disciplines of physics, metallurgy, and chemistry. The contributions have been so intertwined that one cannot discern exactly where the artificial academic boundaries of discipline should be placed and to do so would be a waste of time.

In outlining the present research, two articles from the area of solid state research were influential in delineating the problem studied. The first was by B. R. Coles (1960)

who said, in part

> There can be little doubt that, if as much attention had been given to the electrical and magnetic properties of alloys as has been to their phase equilibria, we should probably understand the alloying behavior of metals very much better than we do. It is a forlorn hope to expect that the determination of more and more equilibrium diagrams more and more accurately will, without extra information, enable us to understand why they take the forms they do; but intelligently conducted experiments on the physical properties of alloys can always be expected to reveal aspects of the electronic structures on which, in part, their phase constitution must depend.

A constructive suggestion to metallurgists in general was made by J. C. Slater (1956) in a paper presented at the 37th National Metal Congress. He very aptly summed up the plight of many metallurgists when he said:

> . . . the theory has advanced far beyond the point which most metallurgists seem to be aware of. If they would put themselves in the front of the advancing theory, instead of living with the theory of twenty years ago, they would stand a better chance of making real progress in the study of the theory of metals.

These viewpoints were foremost in outlining the scope of a literature survey of the state of knowledge of physical properties of metals and alloys which might yield information pertaining to their electronic structure.

At the present time the behavior of the alkali metals, which have the simplest electronic structure, is just reaching a quantitative stage of understanding. The behavior of the transition metals, however, is not well understood even though they have been the subject of a great many investiga-

tions and many of them are the metals of greatest industrial importance. One avenue to a better understanding of the transition metals might be a study of the rare earth group, including scandium and yttrium, since they form a bridge between the divalent alkaline earth metals and the polyvalent transition metals. According to the "aufbau" principle, one would expect the free atoms of Sc, Y, La, and Lu to have one d electron in their unfilled d shells, while Ti, Zr, and Hf have two d electrons in their unfilled d shells, etc. through the transition series. Across the rare earth group, elements 58 to 71, the 4 f shell must first be filled with electrons before the next electron is added to a 5 d orbital, as in the element hafnium. Thus elements 58 to 71 form a "transition series within a transition series."

The electronic structure of the metallic state is not as simple as that indicated by the "aufbau" principle. The outermost, or valence electrons, form a conduction band and are free to move throughout the whole solid. Those energy levels occupied by d electrons in the neutral transition metal atom broaden into bands or form hybrid orbitals, depending upon which explanation one chooses, in the metallic state. Either approach leads to a concept of direct interaction between atoms via the d electrons. Electrical and magnetic measurements on alloys indicate that the empty states in the d band are filled between Ni, Pd, and Pt of Group VIII, and

Cu, Ag, and Au of Group I B. Many studies have been directed toward characterizing the electronic structure at the end of the series where the d band is nearly filled, but few have examined the electronic structure at the beginning of the transition series. An examination of such properties in rare earth metals and alloys might be helpful in determining how the electronic structure changes between the divalent alkaline earth metals and the beginning of the transition series.

The rare earth metals have been investigated in detail only in recent years because they were not available in sufficient quantity or purity until about 1944. Through the efforts of F. H. Spedding and his co-workers at the Ames Laboratory, improved techniques for separating the rare earths (F. H. Spedding and J. E. Powell (1954)) and preparing the metals (F. H. Spedding and A. H. Daane (1954)) have been devised and the metals made accessible in a state of purity not hitherto attained. Spedding early recognized the significant contributions to knowledge that a study of the rare earths might provide and instituted a program to systematically investigate their properties. This program has now proceeded to the point where many of the physical, metallurgical and thermodynamic parameters of these elements are now available.

The present picture of these metals which has unfolded

is that of a trivalent metal with the appropriate number of 4 f electrons buried deeply within the ion core. The number of 4 f electrons is not strictly as one would predict from the "aufbau" principle since europium and ytterbium are divalent. These two elements should possess respectively one less than a half-filled f shell and one less than a completely filled f shell. However, the half filled and filled 4 f shell apparently are the more energetically favorable configurations, and one of the conduction electrons is required to meet this specification in europium and ytterbium. Cerium too, displays anomalous behavior in its low temperature or high pressure α - Ce allotrope. According to K. A. Gschneidner and R. Smoluchowski (1961), this allotrope is best characterized by a valence of 3.62 at 116°K. and 1 atm. pressure, and is pressure and temperature dependent. Magnetic susceptibilities of the rare earths show that in the metallic state Hund's rules are followed quite closely and there is little or no quenching of the orbital angular momentum as is the case in the transition metals. Thus the 4 f electrons do not directly enter into interactions in the metallic state and are considered to be localized on the ion cores. The effects of their presence is visible in the physical properties, however, and such mechanisms as exchange interactions with the conduction electron and super-exchange have been proposed to treat the indirect interactions.

The rare earth metals, then, provide excellent subjects for a study which can be expected to yield information leading to a better understanding of the metallic state in at least three specific areas. The first area deals in general with the change of properties from the alkaline earth metals to the Group IV metals at the beginning of the transition series. The second area considers the change of properties across the rare earth series from lanthanum to lutetium as the 4 f shell progressively fills with electrons. The third area is concerned with a better understanding of magnetic properties of metals by a comparison and contrast between the magnetism of the rare earth type arising from localized electrons and the magnetism of the transition metals arising from collective electron effects.

Alloy studies of metals have proved useful in gaining knowledge applicable to the interpretation of the electronic structure. If the electronic structure of a particular metal is not easily interpreted from its physical properties, clues may often be gleaned from the change in properties upon alloying. A judicious choice of the materials to be studied is required, however, so as to change as few parameters as possible outside the one under investigation. Here again the uniqueness of the rare earths offers many advantages. Subtle changes in physical properties, which might be obscured by large size or valence differences between components, may be

more evident in studies of intra-rare earth alloys.

The information to be gained by the use of rare earth alloys in a study such as that proposed by B. R. Coles (1960) appeared promising. Solid solution alloys were particularly appealing because several of the unique properties of the rare earths could be exploited, such as the similarity in their metallic size, valence, crystal structures, and the slight changes of properties across the series. This reduces the number of parameters which must be considered and should simplify the interpretation of the results. The same advantages might be cited for a study of isostructural intermetallic compounds, but these materials are presently the subject of several investigations, while the area of solid solution alloys remains virtually untouched. There are several distinct advantages in choosing alloys among the heavy rare earth metals Gd, Tb, Dy, Ho, Er, Tm, Lu, and Y, rather than the light rare earths or the whole series for that matter. The need for a single crystal structure to obtain complete solid solubility between two rare earth metals obviously limits the choice to either the heavy or light group of rare earths. Not only does the heavy group contain more metals with the same crystal structure, but the crystal structure is less complex and the nature of the magnetic properties is better understood. An added advantage is that the heavy rare earths are less reactive than the light

group and may be handled in air at room temperature without serious oxidation problems, thus simplifying the preparation of the samples.

The electronic structure of the rare earth metals has been a subject of speculation since their first preparation. Although the more obvious features are known, there are several aspects not completely understood, and for this reason a property which might reflect changes in the electronic structure of the alloy system under consideration was sought. Several properties which appeared to be particularly applicable to such an investigation were magnetic susceptibility, conductivity, thermo-electric power, and Hall effect. The magnetic susceptibility reflects changes in the inner electronic structure, while the last three are influenced mostly by the conduction electrons. Actually, the specific influence of the electronic structure on these properties is not fully understood even in the case of pure metals; that it has some effect is unquestioned. Ideas presented by several authors discussing the behavior of the electrical conductivity (or its reciprocal the resistivity) in terms of the electronic structure appeared to have aspects which could profitably be explored in an investigation using solid solution alloys.

A. H. Wilson (1936) had a rather low regard for the information to be gained from a study of the electrical

resistivity of metals for he said in the first edition of his book,

> It is perhaps unfortunate that so much attention has been paid to the resistance of metals, since it is probably one of the least characteristic properties of the substance, and depends on the electronic distribution and the elastic constants in a very complicated way.

D. K. C. Mac Donald (1956), however, profiting by 20 years of progress in science had a more optimistic attitude, and replied in rebuttal,

> From some points of view this outlook might still be maintained, but we should not forget that one of the most striking and valuable properties of a metal is its ready conduction of electricity. It is true that a complete fundamental understanding of electrical resistance in metals is still lacking today despite unremitting experimental investigation for at least a century; however, the wealth of useful information on metals gained by studies of electrical conductivity appears unequalled by any other comparable measurement. It is of course the rather subtle dependence of the electron scattering on the characteristic parameters of a metal that renders a full theoretical interpretation so difficult; nonetheless, it appears a fortunate fact that so sensitive and informative a parameter can be so readily measured.

Several interesting aspects of the problem were apparent before the present investigation began, while others appeared as the investigation progressed. Although these aspects will be developed in detail in a later section it is perhaps in order to mention them briefly at this point.

There are several questions regarding conduction phenomena in rare earth metals that are not fully understood.

Why are resistivities of the rare earth metals among the highest known for metals? Why are the temperature coefficients of the resistivity so different for the various metals? An observation of this latter property prompted B. R. Coles (1958) to postulate different conduction electron configurations within the rare earth series. A gradual change of these properties across a solid solution system might prove to be helpful in answering these questions since any change in the electronic structure would be seen.

Information pertinent to the magnetic interactions in a metal or alloy can also be gained from a study of the resistivities, because the ordering temperature is seen as a sharp change in slope of the resistivity vs. temperature curves. Therefore, the ordering temperatures can be obtained as a function of composition in the alloy system.

The rare earth magnetism arising from localized electrons represents an idealized model for a study of spin-disorder effects in the resistivity. In contrast to this, a recent study by A. I. Schindler et al. (1956, 1957) on Ni-Pd solid solution alloys characterized the resistivity behavior in a system possessing collective electron magnetism. N. F. Mott and K. W. H. Stevens (1957) made some predictions about the differences in resistivity behavior near the Curie point for the contrasting models of magnetism which were based upon a comparison of the resistivity of a ferromagnetic metal and

the resistivity of one of its ferromagnetic alloys. As the investigation progressed it became apparent that a characterization of the interaction of the conduction electrons with the 4 f electrons would be possible and the scope of the investigation was accordingly broadened.

To summarize then, this investigation was conducted to determine how a physical property, the resistivity, changed as a function of composition in solid solution alloys of the rare earth metals, and hopefully, to interpret the results in terms of the electronic structure. Specific objectives included comparison of the results with those for the pure rare earth metals and also with information on the transition metals and their alloys, an examination of the influence of composition on the magnetic ordering temperature, and a test of Mott and Steven's proposal concerning the behavior of the localized electron model magnetism. Results obtained in accomplishing the above objectives led to the investigation of the conduction electron-magnetic ion interaction which represents the most important contribution of this study.

II. LITERATURE SURVEY

The following survey of the literature covers previous studies of the variation of resistivity as a function of composition in solid solution alloys, studies of physical properties in rare earth - solid solution alloys, and measurements of the electrical transport properties of the rare earth metals. Papers dealing with interpretation of the resistivity phenomena and conduction electron - magnetic ion interactions are cited in Section IV dealing with theory.

A. Studies of Resistivity in Solid Solution Alloy Systems

M. Hansen (1958) lists approximately 50 binary alloy systems that form continuous solid solutions over some temperature range. In addition to those listed in Hansen, there are about thirty-five more binary systems based upon rare earth components which satisfy the requirements for complete solid solubility. The bulk of this group consists of alloys among the heavy rare earths, but there are a few among the light rare earths, and also a few with non-rare earth elements as one component, such as Yb-Ca, Yb-Sr, Sc-Zr, Sc-Hf, and Ce-Th. Of the systems cited in Hansen, many have been studied by resistivity methods, especially in the earlier

literature, where resistivity techniques were used to establish the presence of ordered structures and continuous solid solutions before x-ray equipment was commonly available. If the resistivity is examined as a function of composition at some given temperature two general patterns of behavior are apparent; the first shows a symmetrical inverted parabola while the second is unsymmetrical. For those cases in which there was no change in electronic structure across the system, L. Nordheim (1931) proposed the relation, $\rho = Cx(1-x)$, for the symmetrical case. In this equation ρ is the resistivity, C is a constant characteristic of the alloy system and x is the mole fraction of one component. Deviations giving rise to the unsymmetrical curves were explained in the case of the transition metals by N. F. Mott and H. Jones (1936).

Several typical examples of both types of behavior were described by Mott and Jones and have since been reproduced in many articles pertaining to the subject, for example Ag-Au and Pt-Pd represent examples of the symmetrical case and Cu-Pd, Ag-Pd, and Au-Pd the unsymmetrical case. A listing of these and other systems is given in Table 1. The list is not intended to be comprehensive but does include examples of the solid solution systems listed in Hansen for which applicable data have been published.

Many of the workers prior to 1930 published only the data at room temperature taken on annealed samples. In

Table 1. Examples of resistivity studies of complete solid solution systems

Alloy system	Reference
Ag-Au	Beckman (1911)
Ag-Pd	B. Svensson (1932)
Au-Cu	C. H. Johansson and J. O. Linde (1936)
Au-Pd	W. Geibel (1911a)
Au-Pt	C. H. Johansson and J. O. Linde (1930)
Co-Ni	H. Masumoto (1927)
	W. Broniewski and W. Pietrek (1935)
Co-Pd	G. Grube and H. Kästner (1936)
Co-Pt	E. Gebhardt and W. Koster (1940)
Cr-Fe	F. Adcock (1931)
Cs-K	E. Rinck (1936)
Cs-Rb	E. Rinck (1937)
Cu-Mn	R. S. Dean et al. (1945)
Cu-Ni	P. Chevenard (1926)
Cu-Pd	B. Svensson (1932)
	C. H. Johansson and J. O. Linde (1927)
Cu-Pt	C. H. Johansson and J. O. Linde (1927)
	J. O. Linde (1937)
Ge-Si	A. Levitas (1955)
Ir-Pd	F. E. Carter (1928)
Ir-Pt	W. Geibel (1911b)
K-Rb	N. S. Kurnakow and A. J. Nikitinsky (1914)
Mn-Ni	S. Valentiner and G. Becker (1934)
Mo-W	North American Philips Co. (ca. 1948)
Ni-Pd	A. I. Schindler et al. (1956, 1957)
Ni-Pt	V. Esch and A. Schneider (1944)
Pd-Pt	W. Geibel (1911a)
Pt-Rh	F. E. Carter (1928)
Ta-W	H. Braun et al. (1959)
Ti-Zr	J. H. De Boer and P. Clausing (1930)
Ti-Mo	R. R. Hake et al. (1961)
Ti-Nb	S. L. Ames and A. D. Mc Quillan (1954)
Ti-V	H. K. Adenstedt et al. (1952)
U-Mo	L. F. Bates and R. D. Barnard (1961a)
U-Nb	L. F. Bates and R. D. Barnard (1961b)

systems where ordered phases occurred, the curves, of course, were not smooth but showed the presence of ordered phases. Other deviations from symmetrical curves appeared when one of the components was magnetic or where the temperature coefficients of resistance were not equal, because, to be strictly valid, the Nordheim relation should be applied only to that portion of the resistivity due to the effects of alloying. To eliminate the other factors which contribute to the resistivity the measurements should be made at helium temperatures, a technique available only in recent years. A. I. Schindler *et al.* (1956) is the lone example found which employed this technique over the whole composition range, although there have been several studies at helium temperatures over restricted composition ranges.

The work of A. I. Schindler *et al.* (1956, 1957) on Ni-Pd is notable because it demonstrates the type of information to be gained from such a study and provides an example of the resistivity behavior for a solid solution system of transition metal alloys. The system was judiciously chosen to simplify the interpretation of the results, for both Ni and Pd have approximately the same band structure with 0.6 hole in the d band and 0.6 electron in the s band. A maximum in the ρ vs. composition curves was observed at 70 a/o Pd at temperatures below the Curie temperature in all alloys, but this shifted to 50 a/o Pd at temperatures above the Curie

temperature of all alloys. This was interpreted as evidence for a change in occupancy of spin states in the d band, since in Pd the number of occupied spin states in the d band is equally divided between spin up and spin down, while for Ni in the magnetic state, all states with one spin are believed to be occupied; thus leaving only half as many vacant states into which the conduction electrons could be scattered. Above the magnetic transition temperature in Ni the distribution of occupied spin states is the same as that found in Pd.

A. Levitas (1955) characterized the behavior of semiconductor solid solutions in the intrinsic conduction region in his study of the Ge-Si system.

A subject which is of current interest is the anomalous behavior of meta-stable bcc solid solutions of Ti and U in the systems indicated. Such alloys do not follow Nordheim's relation and have a negative temperature coefficient of resistivity. The behavior is not entirely understood at present. Examples of this behavior are the systems Ti-V, Ti-Nb, U-Mo, U-Nb, and Ti-Mo.

B. Studies of Physical Properties in Rare Earth Solid Solution Alloys

E. M. Savitskii and V. F. Terekhova (1958) report the only ρ vs. composition data for a rare earth - rare earth

system, La-Ce, which has been published in the literature. They cite no x-ray data which leaves some question as to whether the alloys were exclusively the fcc structure of cerium. In addition, the techniques used to prepare the metals did not appear to be likely to yield pure metals. The ρ vs. composition curve for the alloys was approximately symmetrical.

L. F. Bates and M. M. Newmann (1958) investigated the magnetic susceptibility and resistivity of alloys in the Ce-Th system. Resistivities were reported for 5 alloys as a function of temperature from 90°K. to 273°K. The results, when plotted as a function of composition, are somewhat difficult to interpret because of the low temperature modification of cerium and the change in electronic structure associated with it; but they appear to follow an approximately symmetrical curve. The magnetic susceptibilities also showed the effects of the change in electronic structure as the susceptibility showed a sudden drop at low temperatures. The effective moment per cerium atom in the alloys was higher than the effective moment for pure cerium in all the samples.

W. C. Thoburn et al. (1958) studied the magnetic properties of Gd-La and Gd-Y alloys, of which the Gd-Y alloys show complete solid solubility. They found that in these alloys gadolinium had a higher effective moment per gadolinium atom than the theoretical moment for pure gadolinium. The

magnetic ordering changed from ferromagnetic to antiferromagnetic at about 60 atom percent gadolinium, while the paramagnetic Curie temperatures showed an approximately linear decrease with gadolinium content.

L. M. Roberts and J. M. Lock (1957) investigated four alloys in the La-Ce system by means of magnetic susceptibility and specific heat measurements. They observed peaks in the specific heat curves for alloys of 27.0, 37.6 and 78.9 weight percent cerium which they attributed to antiferromagnetic ordering, although the alloys showed double peaks rather than the single peak observed in pure cerium. Anomalous behavior in the magnetic susceptibility appeared to be associated only with the lower peak. The effective moment per cerium atom in the alloys was higher than the moment for pure cerium in all the samples.

G. S. Anderson *et al.* (1958a) studied the change in the superconducting transition temperature as a function of composition and crystal structure in some lanthanum rich La-Y and La-Lu alloys.

J. M. Lock (1957) studied the magnetic susceptibility of three La-Nd alloys. The Néel point and effective moment per neodymium atom were found to increase as the neodymium content of the alloys decreased for 60 a/o and 40 a/o neodymium alloys, but further dilution to a 20 a/o neodymium alloy caused both the Néel point and effective moment to decrease.

C. Measurements of Electrical Transport Properties of Rare Earth Metals

Knowledge of the electrical transport properties of the rare earth metals is essential to the interpretation of the resistivity behavior of the alloys. Data on high and low temperature resistivities, Hall coefficients, thermo-electric power, and pressure coefficients of resistivity are available for most of the rare earth metals.

The first measurements of low temperature resistivities on polycrystalline materials were reported by N. R. James et al. (1952) for La, Ce, Nd, and Pr, and S. Legvold et al. (1953) for Gd, Dy, and Er. More recent measurements on materials of higher purity by R. V. Colvin et al. (1960) on Gd, Tb, Dy, Ho, Er, Tm and Lu; M. A. Curry et al. (1960) on Eu and Yb; and J. K. Alstad et al. (1961a) on La, Pr, Nd, and Sm; and (1961b) on Y, represent the best data presently available. The results in all the above papers are presented as a function of temperature over the range from helium temperatures to 300°K. The curves for the weakly paramagnetic metals Lu and Y are linear from 40°-300°K. while La and Yb, which are also weakly paramagnetic, show a curvature toward the temperature axis over this temperature range.

The curves for Pr, Nd, and Sm show two changes in slope at the magnetic ordering temperatures and are fairly linear

in the paramagnetic region. The curve for Eu shows a peak at 90°K., associated with a magnetic ordering point, but the peak is followed by a 50° range over which the slope of the curve is negative. The curves for Gd, Tb, Dy, Ho, Er, and Tm are similar in showing a sharp change in slope at the transition point from magnetic ordering to paramagnetism; however, they differ in the behavior immediately above the transition point, for Dy, Ho, Er, and Tm show a pronounced minimum over a 10-20° temperature range. In addition Tb and Dy show anomalies at lower temperatures associated with a ferromagnetic-antiferromagnetic transition. Although all the curves are linear in the paramagnetic region their slopes are not the same, Gd having the lowest and Tm the highest. The magnitudes of the resistivities at room temperature are higher than usual for a metal, being exceeded only by Mn, Bi, and Pu. Ytterbium is an exception in that it has a lower resistivity, but its other physical properties are also exceptions to the behavior typical of rare earth metals. Part of the excess resistivity is obviously associated with the magnetic properties of the metals, a point which will be further explored in Section IV, but La, Y, and Lu which are not magnetic still have resistivities of about 55 micro ohm-cm. at room temperature. In comparison, copper has a resistivity of 1.673 micro ohm-cm. at 20°C.; aluminum, also a trivalent metal, has a resistivity of 2.655 micro ohm-cm. at

20°C.; and among the typical metals only titanium and hafnium, with resistivities of 42 and 40 micro ohm.-cm. respectively, approach the values of the rare earths.

Single crystal measurements of the resistivity over the temperature range 4°K. to 300°K. have been made by P. M. Hall et al. (1959a) on Y, and (1959b) on Dy; R. W. Green et al. (1961) on Er; D. L. Strandburg (1961) on Ho; H. E. Nigh* on Gd; and D. E. Hegland** on Tb. The most striking features of these curves are the large anisotropies in the resistivity parallel and perpendicular to the c axis and the marked effects of the magnetic ordering on the resistivity parallel to the c axis.

The case of Er is especially striking for it shows three distinct changes at points where the magnetic ordering is known to change. In general, the anisotropies in the regions of magnetic order are less than in the paramagnetic region and the resistivity curve perpendicular to the c axis shows only one anomaly, a simple change in slope at the transition point from magnetic ordering to lack of ordering.

The high temperature resistivities of polycrystalline

---

*Nigh, H. E., Physics Department, Iowa State University, Ames, Iowa. Information about the resistivity of gadolinium single crystals. Private communication. 1961.

**Hegland, D. E., Physics Department, Iowa State University, Ames, Iowa. Information about the resistivity of terbium single crystals. Private communication. 1961.

samples of several rare earths have been reported by F. H. Spedding et al. in several papers listed in Table 2.

Table 2. Investigations of high temperature resistivities of rare earth metals

Metal	Temperature range	Reference
La, Ce, Pr, Nd	25°C. - m.p.	F. H. Spedding et al. (1957)
Y	25°C. - m.p.	C. E. Haberman (1960)
Gd, Tb, Lu	900°C - m.p.	F. H. Spedding et al. (1961)
Eu	28°C. - 208°C.	F. H. Spedding et al. (1958)
Sc	room temperature	F. H. Spedding et al. (1960)

These results show the resistivity - temperature curve to be fairly linear near room temperature with increasing curvature toward the temperature axis above 300°C. A discontinuous change in slope of the curve is observed at the temperature at which a crystallographic transformation occurs in La, Ce, Pr, Nd, Gd, Tb, and Y, and a much smaller anomaly is observed in Lu.

The Hall effect has been studied by C. J. Kevane et al. (1953) for Y, La, Ce, Pr, Nd, Gd, Dy, and Er and by G. S. Anderson et al. (1958b) for Lu, Yb, Tm and Sm. The temperature range covered in the investigations was from 20°K.

to 300°K. except for Gd which was measured to 350°, but the data for the magnetic materials was evaluated only in the paramagnetic region. Anomalies associated with the magnetic ordering temperature were observed as well as a large hysteresis in cerium believed to be associated with the change in electronic structure. The number of effective carriers calculated for a one band model were reported, but both authors believed that a more sophisticated model was necessary to explain the results. The number of carriers calculated was approximately -3 for La, Y, and Lu, +0.7 for Yb, -2 for Gd, Dy, Er, and Tm and +2 for Ce, Pr, and Nd, where the - indicates electrons and the + indicates holes.

The thermoelectric powers of polycrystalline samples of Y, La, Pr, Nd, Sm, Gd, Tb, Dy, Ho, Er, Tm, Yb, and Lu were measured by H. J. Born et al. (1961) over the temperature range 7°K. to 300°K. Anomalies in the TEP vs temperature curves were observed at the magnetic ordering temperatures of many of the metals. With the exception of Sm and Yb, the TEP's of the metals are negative throughout most of the temperature range covered, and with the same exceptions, the curves have about the same slope near room temperature.

L. R. Sill* has measured the TEP of single crystals

*Sill, L. R., Physics Department, Iowa State University, Ames, Iowa. Information about the TEP of holmium single crystals. Private communication. 1961.

of Ho cut with the long axis of the crystals parallel to the a, b, and c axes respectively. Anomalies were observed both at the Néel point and the anti-ferromagnetic to ferromagnetic transition point; in addition, anisotropy in the TEP was observed between the c and a directions.

P. W. Bridgman has measured the resistivity as a function of pressure over the range 0-100,000 kg/cm^2 (1952) for La, Ce, Pr, and Nd; (1953) for Gd; (1954) for Sm, Dy, Ho, Er, Tm, Yb and Lu; and (1955) for Y. All except Y, Nd, Sm, Tm, and Lu show some type of anomalous behavior but the most striking are the cases of Ce and Yb. A discontinuous decrease in the Rp/Ro vs pressure curve is observed at the point where cerium changes to its low temperature collapsed fcc structure. The behavior of ytterbium is most unusual in that the resistivity increased to a maximum value at 50,000 kg/cm^2 which is 13 times greater than its value at normal pressure and then drops with increasing pressure to 3/4 of its initial value. Bridgman measured the temperature coefficient of the resistivity between 0^o and 200^{o}C. under pressures up to 7,000 kg/cm^2 and found an inversion of the temperature coefficient characteristic of semi-conductor behavior.

III. EXPERIMENTAL PROCEDURES AND APPARATUS

The following section describes the techniques used for preparation of the alloys, the apparatus for measuring the resistivities, the method by which the x-ray data were obtained and processed, and an analysis of the errors inherent in the measurements. The apparatus used to measure the resistivities of the samples was made available for use by Dr. S. Legvold and was designed, built, and originally described by R. V. Colvin (1958). The description of the apparatus here includes a few minor modifications of the original design but is included in this thesis only to assure the reader a complete description of the techniques involved in the investigation. The x-ray program for calculating precision lattice constants was written in conjunction with D. H. Dennison to satisfy a frequently recurring demand for such a tool.

A. Sample Preparation

1. Materials

The metals used to prepare the alloys for this study, with the exception of yttrium, were prepared by C. E. Habermann. The lutetium, gadolinium, and terbium were taken from the same stock as that used to prepare the resistivity

samples for R. V. Colvin et al. (1960). All the metals, except yttrium, were prepared by the standard fluoride reduction with calcium described by F. H. Spedding and A. H. Daane (1954). In addition, the dysprosium, erbium, and holmium had been distilled by a process used by A. H. Daane et al. (ca. 1962) to distill rare earth metals. Although most of the other rare earth metals have been distilled in small quantities, it was not feasible to so produce the quantities required in this investigation. The yttrium was prepared by F. A. Schmidt by a magnesium-calcium reduction process described by O. N. Carlson et al. (1960). Analyses of the metals are listed in Table 3.

Analysis showed the "as reduced" metals contained appreciable amounts of unreduced fluoride and calcium metal as well as some tantalum. An arc melt treatment under reduced pressure was found to be effective for removing the volatile impurities. For example, the fluoride content of the lutetium was reduced from 1050 ppm. to 48 ppm. by arc melting. This was preferred to a vacuum casting which would have increased the tantalum content.

2. Alloy preparation and casting

The constituents for each alloy were mixed together and homogenized by arc melting. The weighed samples were placed in the arc melter and the arc melter evacuated. An argon atmosphere was bled in and thoroughly "gettered" by melting a

Table 3. Analysis of metals

Impurity	Lu	Gd	Tb	Er	Y
C	106 ppm.	160 ppm.	137 ppm.	120 ppm.	115 ppm.
N_2	800 ppm.	147 ppm.	496 ppm.	24 ppm.	56 ppm.
F_2	48 ppm.	170 ppm.	895 ppm.	80 ppm.	159 ppm.
O_2	735 ppm.	1150 ppm.	1360 ppm.	60 ppm.	430 ppm.
C_2	.02%	.005%	W	.01%	400 ppm.
Fe	.005%	.015%	VW	W	200 ppm.
Ni	VW	T	T	-	-
Mg	.03%	.02%	-	VFT	45 ppm.
Si	.025%	.025%	FT	-	-
Ta	VV	.05%	-	-	-
Ti	-	-	-	-	20 ppm.
Ho	-	.02%	-	.01%	-
Yb	.005%	-	-	.0001%	-
Dy	-	.01%	-	.005%	-
Tb	-	.01%	-	-	-
Eu	-	.001%	-	-	-
Sm	-	.02%	-	-	-
Nd	-	.05%	-	-	-
Tm	.002%	-	-	.001%	-
La	-	VW	-	-	-

"button" of zirconium before the alloys were melted. Each alloy "button" was melted, turned over, and remelted a total of six times to insure a homogeneous sample. Weight losses on arc melting and in the succeeding casting operation were monitored to detect any gross change of composition which might have occurred with some of the more volatile metals.

The highly directional cooling in the arc melting process introduces a high degree of preferred orientation in the samples and it is necessary to further treat the samples to obtain random orientation. This is perhaps the most important step in the sample preparation process because of the large anisotropies observed in the single crystal studies of resistivities of the rare earth metals. The most pronounced anisotropy is that of yttrium as was shown by P. M. Hall et al. (1959a). Two methods have been used to remove the preferred orientation; a swaging and annealing technique and a pressure-differential vacuum casting technique.

The swaging and annealing technique was recently used to prepare the samples used by J. K. Alstad et al. (1961b) and it was successful in removing preferred orientation. Previous attempts by C. E. Habermann* to prepare samples by this technique were not uniformly so successful. The samples used

*Habermann, C. E., Chemistry Department, Iowa State University, Ames, Iowa. Information about the preparation of resistivity samples. Private communication. 1960.

by Alstad et al. were cut from much larger size arc melts (70 lbs. vs. 30 gr.) and this probably was a factor in their success. One distinct advantage of the method is that it introduces no more tantalum into the sample.

The pressure-differential vacuum casting technique used in this work was previously used to prepare the polycrystalline samples used by R. V. Colvin et al. (1960) and J. K. Alstad et al. (1961a). The success achieved in randomizing the orientation in the samples can be judged by comparing the results obtained by the authors cited above with the results of P. M. Hall et al. (1959a)(1959b) and R. W. Green et al. (1961) on single crystals of Y, Dy, and Er respectively. If one applies the averaging rule, ρ poly = $(2\rho_{\perp} + \rho_{\parallel})/3$, to the resistivities for samples cut perpendicular and parallel to the c axis, one obtains the theoretical resistivity for a polycrystalline sample; the validity of this rule for the rare earths has been shown in a paper by J. K. Alstad et al. (1961b). There is little deviation between the curves predicted from single crystal studies and the experimental results on polycrystalline samples. It was, of course, also desirable to prepare the alloy samples used in this study in the same manner as that used to prepare the pure metal samples because a comparison of the results was of interest. The samples were molten in the tantalum containers for only a brief period and since they already contained some tantalum

the small amount taken into solution in this step was not deemed to be of major importance.

The pressure differential vacuum casting method consists of melting the alloy under vacuum in a tantalum crucible and forcing the molten metal up into another inverted crucible suspended in the melt. The pressure-differential necessary to accomplish this is produced by bleeding 1/3 atm. of argon into the system. The inverted crucible, being at a lower pressure, is immediately filled with metal. The equipment is illustrated in Figure 1. The inverted crucible was made from a 2½ inch length of tantalum tubing sealed at the upper end. This crucible was held above the melt with a length of tantalum tubing coupled to a brass rod which extended to the top of the vacuum system and out through an "o" ring seal which allowed vertical motion. As soon as melting of the alloy was detected, the rod and crucible were pushed below the surface of the melt and positioned so that the lower lip of the inverted crucible was about ¼ inch above the bottom of the melt. The vacuum system was then sealed off and about 1/3 atm. of argon was bled into the system. The solidification in this type of casting occurs first at the top of the casting and proceeds downward rather than the usual case where the first solidification takes place at the outer walls of the crucible and leaves a shrinkage cavity in the center of the casting.

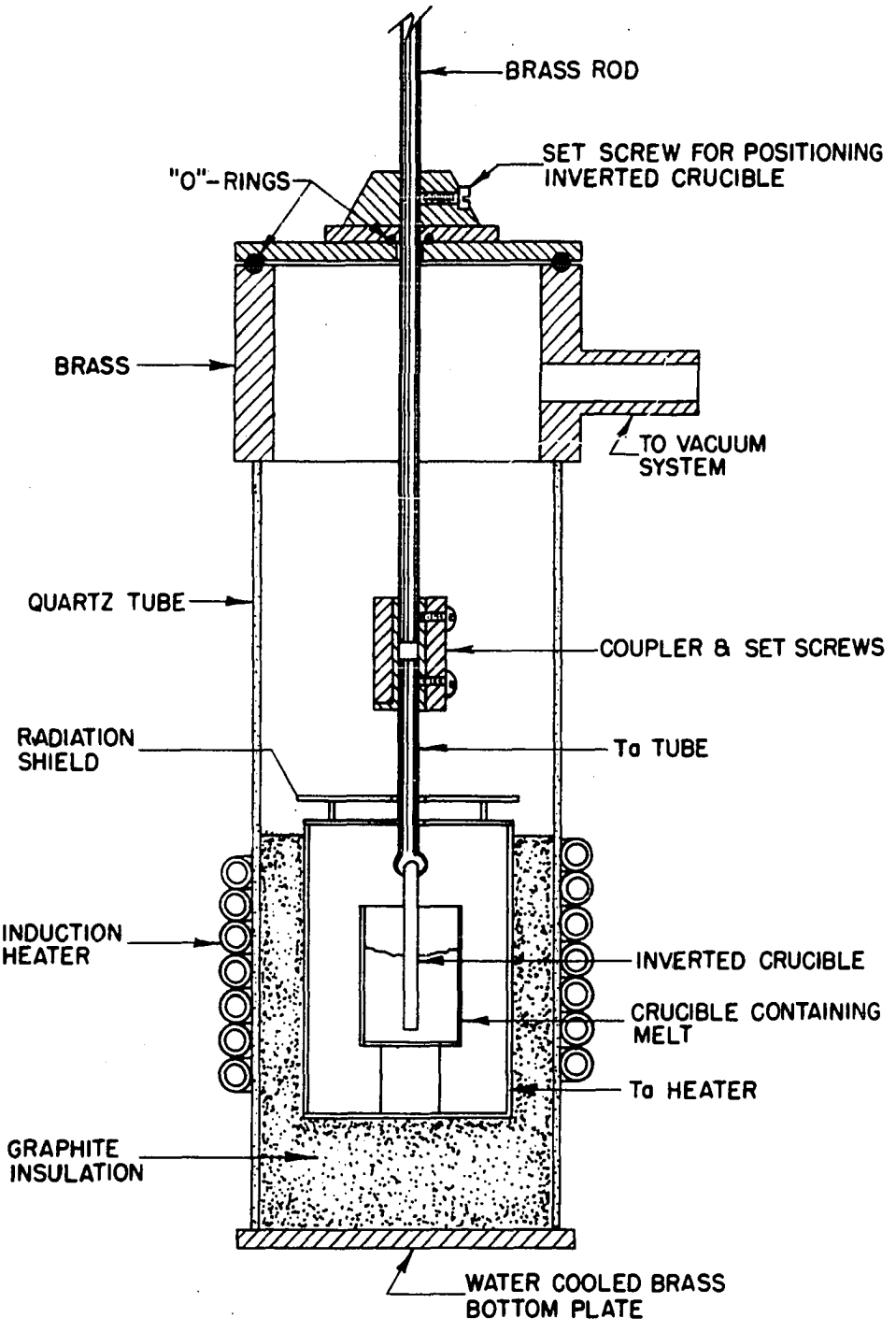

Figure 1. Casting furnace showing inverted crucible in position for casting

The samples were furnace cooled after the casting operation. The graphite insulation in the furnace cooled rather slowly and about two hours were required to cool the furnace to room temperature. Thus, after the first sharp drop in temperature from the melting point, the samples cooled more slowly and were left in an annealed condition.

3. Machining of the sample to shape

The tantalum tubing and excess sample were removed by maching in a lathe. The resulting sample was a cylinder about 3/16 inch in diameter and two inches in length. It was later discovered that this machining introduced some strain in the samples which was detectable in the measurement of the residual resistivities. This was removed by a strain anneal at 350°C. for three hours.

The pressure-differential vacuum casting method described in Section 2 was not universally successful and several of the samples high in lutetium content were found to contain small holes. All samples were examined for holes with a radiograph employing an iridium gamma ray source. To conserve the limited stock of lutetium a smaller rectangular parallelepiped was cut from the solid portion of the faulty castings rather than preparing additional samples of the larger geometry. This was then formed to final shape by the techniques used to prepare single crystal samples. This technique involves the use of sanding block, sanding table, and manual labor to

abraid and polish the sample to the desired geometry. The resistivity of several samples was measured on both geometries and the agreement was well within the limits of experimental error. It was also necessary to strain anneal samples formed in this way to remove the effects of cold work.

4. Dimension measurement

The diameters of the two inch long cylindrical samples were measured with a micrometer at four points along the length of the sample with three measurements at each point. The average of these twelve measurements was taken as the average diameter from which the cross sectional area was calculated.

The dimensions of the rectangular parallelepiped samples were measured with a Sheffield depth gauge at three points along the length on each side. The average of the readings along each pair of parallel sides was used to determine the two dimensions required for the calculation of the cross-sectional area.

B. Resistivity Apparatus

1. Electrical resistance measurement

The electrical resistance of the sample was measured by the standard dc four probe method with current reversal. A simplified circuit is illustrated in Figure 2. The current

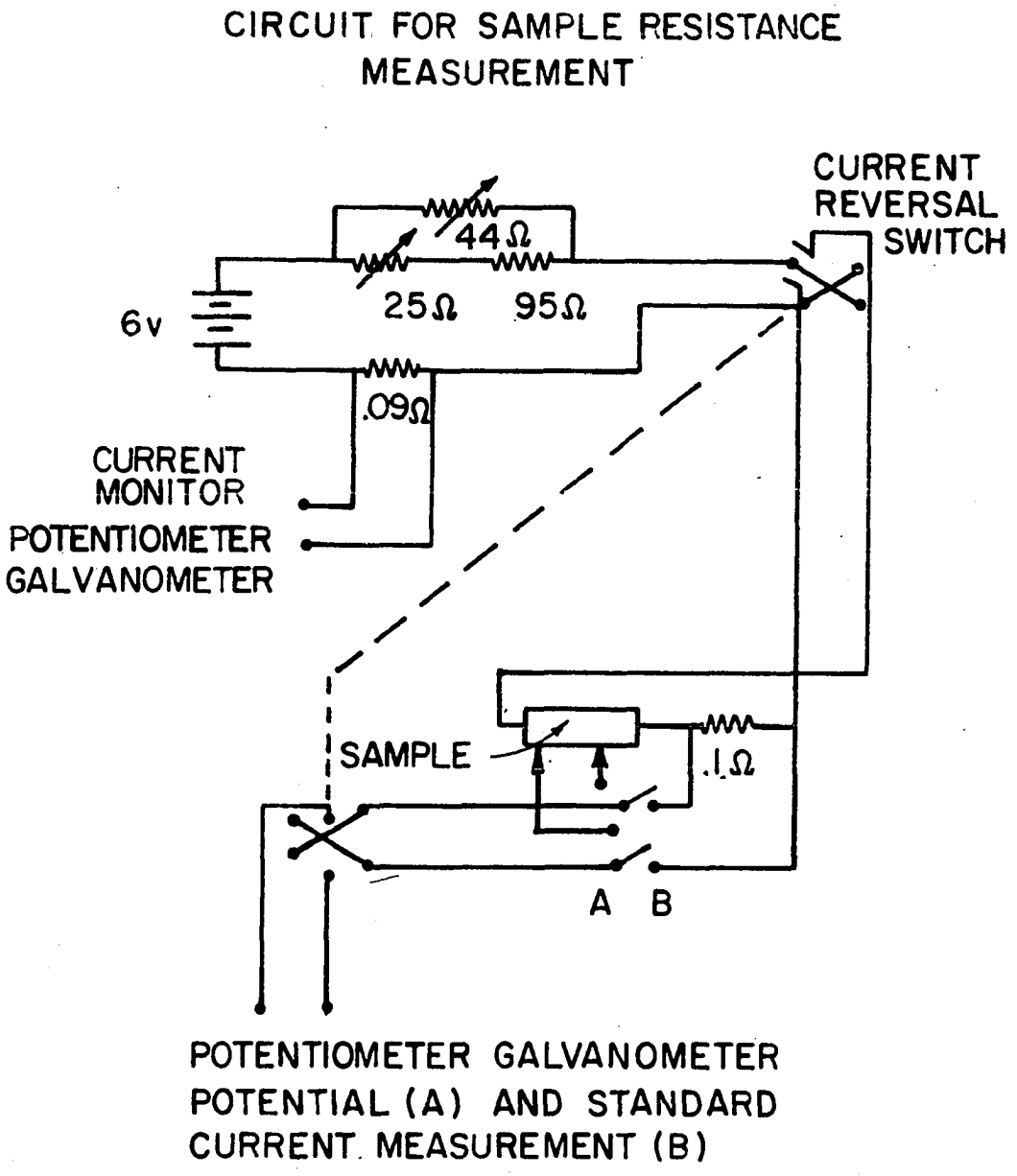

Figure 2. Electrical circuit for measuring the sample resistivity

was supplied by a 6 volt storage battery which provided a sufficiently steady current of 0.1 or 0.3 amp.; the choice depending upon the current required to provide a measurable potential drop across the sample. The current was adjusted to the desired value by a variable resistor in a series-parallel connection with the current limiting resistor. The current was measured precisely by the voltage drop across a standard 0.1 ohm resistor in series with the sample. The current was thereafter monitored continuously during a run with a separate potentiometer-galvanometer circuit and any small compensations required were effected as described above.

The potential across the potential contacts was measured with a Rubicon type B potentiometer using a Leeds and Northrup type 2430 galvanometer with a sensitivity of approximately 0.5 microvolt per mm. for the null indicator. To eliminate the effects of any small temperature gradients across the sample, two measurements of the potential were made at each temperature. The average of the two, before and after current reversal, was used to determine the resistivity. A voltage stabilizer employing a Zener diode which had been designed and built by the Ames Laboratory electronics shop was used to supply the battery voltage for the potentiometers. This unit provides a more stable voltage source than a battery and hence reduced the drift in the potentiometer. The exclusive use of copper or manganin wire and shielding of

switch contacts from air currents kept the thermal emfs small and reasonably constant in time.

2. Temperature measurement

The temperature of the sample was measured by means of a copper-constantan thermocouple. The wires used to make the thermocouples were taken from spools of wire calibrated by W. C. Thoburn et al. (1958) and R. V. Colvin (1958) against a platinum resistance thermometer. The thermocouple was calibrated at the boiling point of nitrogen and the boiling point of helium and appropriate corrections applied to the data so as to give correct readings from the calibration curves against the platinum resistance thermometer.

For the cylindrical samples the thermocouple was glued directly to the sample but insulated by a thin sheet of paper. For the smaller rectangular samples the thermocouple was glued into the sample holder in close proximity to the sample. Some error was undoubtedly introduced by not having the thermocouple in direct contact with the sample but the reproducibility of the resistivity-temperature curves was excellent and indicates the temperature was known to a few tenths of a degree except below 20°K. where the uncertainty was somewhat greater. The same type potentiometer and galvanometer as previously described were used to measure the thermocouple emf above or below an ice bath reference point.

3. Sample holder

Two types of sample holders were used as necessitated by the different sizes and geometries of the samples. Both were held in position in the sample chamber by a stainless steel tube with the appropriate fittings to make the sample chamber vacuum tight. The copper wires supplying current, the maganin wires to the potential probes, and the thermocouple wires all ran down the center of this tube.

The sample holder which accomodated the two inch long cylindrical samples is illustrated in Figure 3. Copper blocks served the dual role of sample mount and current contact, the sample being held firmly in place by Allen screws. The potential probes consisted of two sharpened brass wedges mounted on a quartz bar. The probes were held in contact with the sample by a spring under tension.

The sample holder for the rectangular parallelepiped samples was a modification of one described by D. L. Strandburg (1961) and is pictured in Figure 4. The sample geometry is somewhat distorted in the perspective drawing in Figure 4 as the actual dimensions were about 1.5 X 1.5 X 20 mm. The fiber base was attached to an adapter and this in turn was mounted to the stainless steel tube. The sample was held in place between bronze strips used as current contacts. The upper strip was bent to a right angle, sharpened, and held against the sample by tension. The knife edges were made by

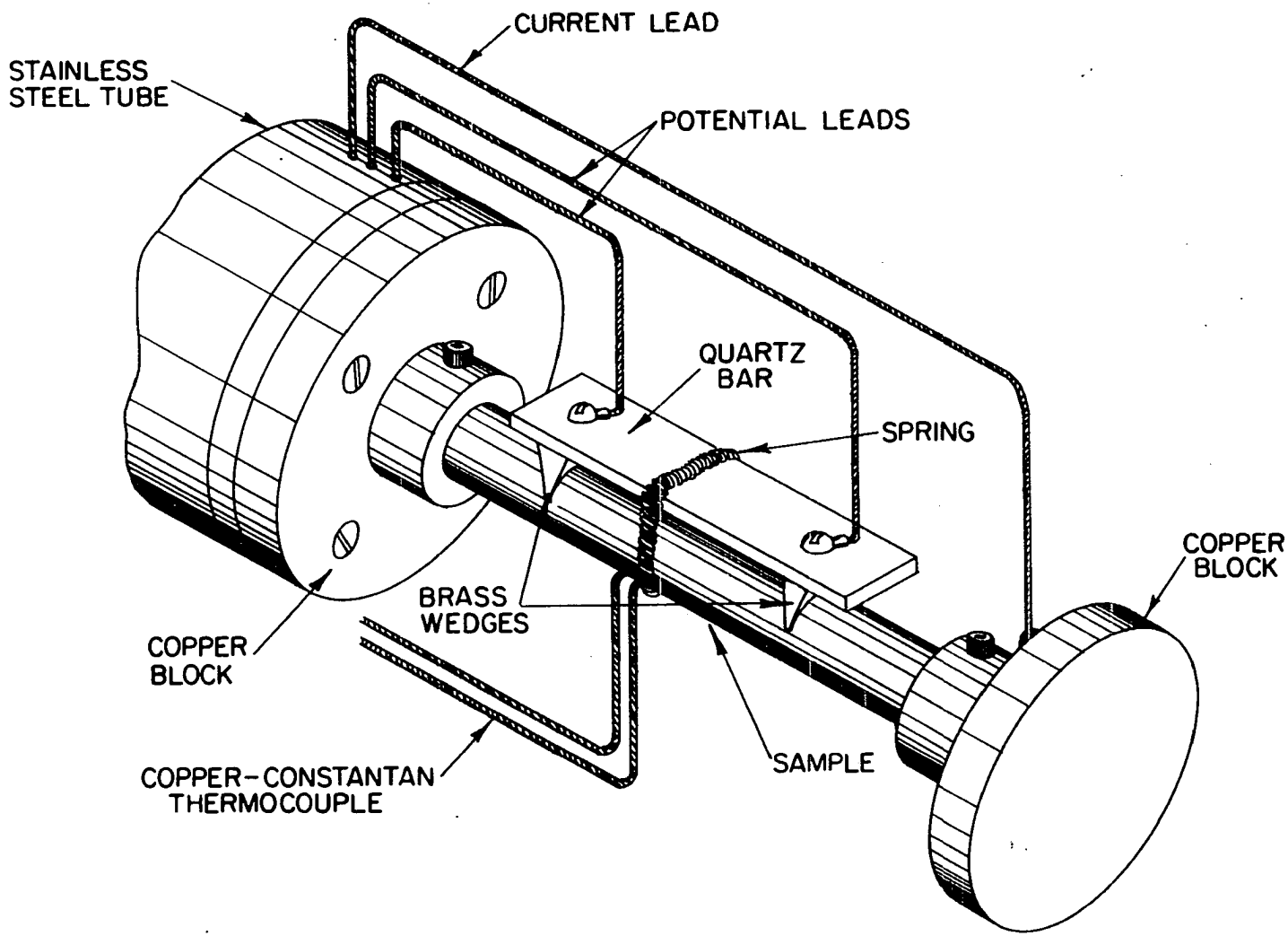

Figure 3. Sample holder for cylindrical samples

Figure 4. Sample holder for rectangular parallelepiped samples

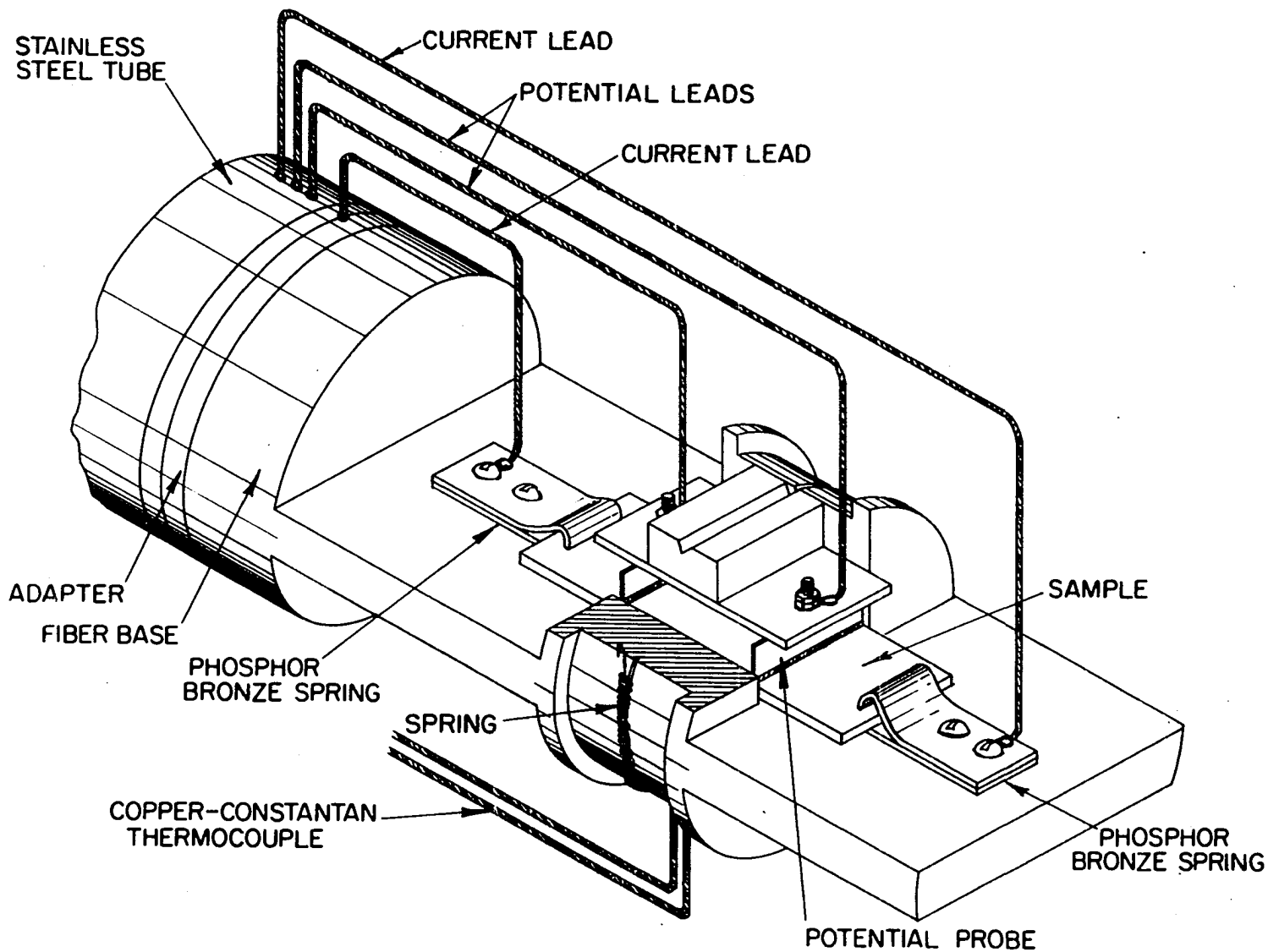
STAINLESS
STEEL TUBE
CURRENT LEAD
POTENTIAL LEADS
CURRENT LEAD
ADAPTER
FIBER BASE
PHOSPHOR
BRONZE SPRING
SAMPLE
SPRING
COPPER-CONSTANTAN
THERMOCOUPLE
PHOSPHOR
BRONZE SPRING
POTENTIAL PROBE

soldering sections of razor blades into screw heads which were in turn mounted on a strip of fiber reinforced in the center by a plastic block. The assembly was held in contact with the sample by a spring under tension.

The distance between the knife edges was measured with a traveling microscope; directly on the probe for the brass wedges, and from the marks on the sample for the razor blades.

4. Cryostat

The cryostat, which consisted of a heat leak chamber and system of Dewars, is pictured in Figure 5. The outer glass Dewar was filled with liquid helium for measurements in the temperature range 4.2°K. to 77.4°K. and liquid nitrogen for measurements at higher temperatures.

The heat leak chamber was immersed in the liquid contained in the inner Dewar. The outside copper tube on the heat leak chamber kept the joint to the Cu-Ni tube (point A in Figure 5) at the bath temperature even when the liquid level was below the joint. When heat was applied to the copper sample chamber by the 140 ohm heater wound around it, a temperature gradient was set up between point A and the sample chamber, thus raising the temperature of the sample chamber above that of the bath.

After initially evacuating the heat leak chamber, sample chamber and walls of the inner Dewar to approximately 2×10^{-5} mm. of Hg, the sample chamber and heat leak chamber were

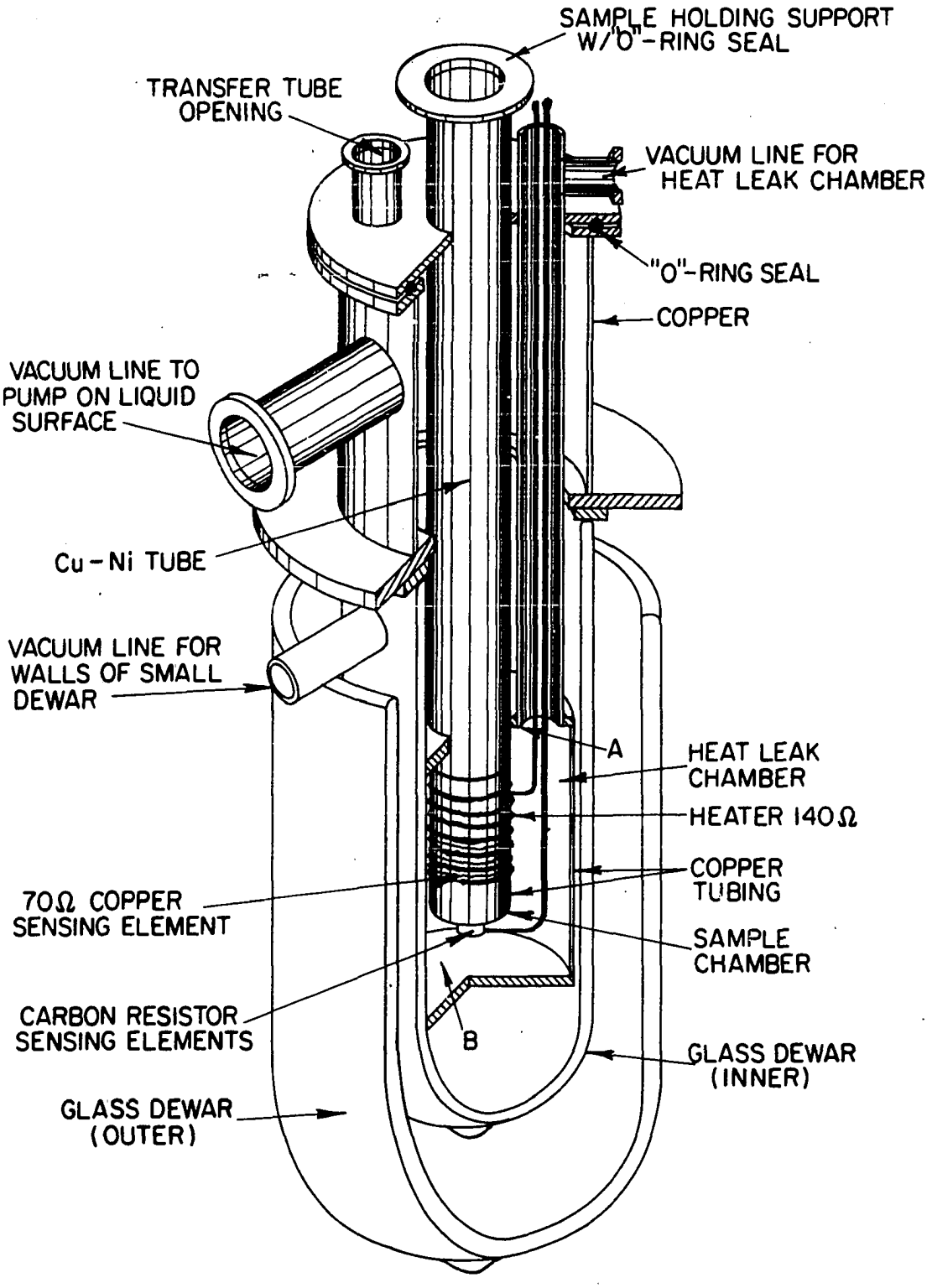

Figure 5. Cryostat

pressurized to about 0.1 mm. of mercury with helium exchange gas. After cooling the apparatus to nitrogen bath temperature and then helium bath temperature, the measurements at bath temperature were made and the heat leak chamber again evacuated. Temperatures above bath temperature were obtained by sending pulses of current through the heater coil. By proper adjustment of the magnitude and time of the current pulses, temperature equilibrium could be attained in about 5 to 10 minutes or at least approached closely enough so that the temperature change during the time required to make the two measurements was essentially nil.

Measurements on the series of dilute alloys in lutetium were made only at the ice point, nitrogen bath temperature, and helium bath temperature. For this series of experiments the cryostat was not used; instead the sample was immersed directly in a liquid nitrogen bath and then into the liquid helium storage Dewar. This practice conserved liquid helium and nitrogen and insured the same temperature for each measurement. It also provided more rapid cooling than could be attained in the cryostat.

5. Temperature controller

An automatic temperature controller designed and built by the Ames Laboratory electronics shop was used to automatically maintain any desired temperature. A copper or carbon sensing element on the sample chamber formed one leg of a Wheatstone

bridge. Unbalance of the bridge when the temperature dropped below some pre-set value operated a servo-mechanism which in turn caused pulses of current to be sent through the heater coil until the sample chamber temperature rose above the desired value. Unbalance in the opposite direction shut off the current and the cycle repeated. The sensitivity was such that a constant temperature could be maintained during the time required to make the two potential measurements and the thermocouple reading.

C. Lattice Constant Determinations

1. X-ray diffraction measurements

X-ray data for the lattice constants of the alloys were obtained from 114.6 mm. diameter Debye-Scherrer powder patterns. The filings, taken directly from the resistivity sample, were strain annealed at a temperature of 375°C. for three hours. To prevent oxidation, the filings were placed in a small Ta container previously outgassed and these in turn were sealed in Pyrex tubes under a partial atmosphere of helium.

2. Computer program

Lattice constants were evaluated with an I.B.M. 650 computer using a program which basically was an application of Cohen's method to determine precision lattice constants.

The diffraction equations for the hexagonal system give $\sin^2\theta = \lambda^2/3a_o^2\ (h^2+hk+k^2) + \lambda^2/4c_o^2\ (l^2) + \text{const.}\ \frac{1}{2}\ (\cos^2\theta/\sin\theta + \cos^2\theta/\theta)$, for each line of the pattern, or symbolically $Z = AX + BY + CW$. The last term in the above equation represents the error from the true $\sin^2\theta$ value for the line. The normal equations are

$$XZ = X^2A + XYB + XWC$$

$$YZ = XYA + Y^2B + YWC$$

$$WZ = WXA + WYB + W^2C$$

Data for the values of θ, (h^2+hk+k^2), and l^2 for each line were fed into the computer and the normal equations for each line calculated, summed over the n lines of the pattern and solved simultaneously for the best values of A and B from which the lattice constants were calculated. The deviation of each line from the calculated value was also computed.

The Nelson - Riley function, $\frac{1}{2}\ (\cos^2\theta/\sin\theta + \cos^2\theta/\theta)$, provides an accurate extrapolation function for lines greater than $20^\circ\ 2\theta$, but only lines above 40° were used for the present computation. All $K_{\alpha 2}$ lines and lines where $K_{\alpha 1}$ and $K_{\alpha 2}$ were not clearly resolved were converted to a value appropriate for $K_{\alpha 1}$ wavelength radiation since the program could only handle data for radiation of one wavelength. The program can compute lattice constants for crystals of the cubic, hexagonal and tetragonal systems as presently written and is an invaluable aid in carrying out this tedious

calculation.

D. Analysis of Errors

The errors inherent in resistivity - temperature measurements in this work arose from errors in measurement of dimensions, potentials, current, and temperature. Variables influencing the sample itself, such as composition and preferred orientation, were probably as great a source of error. The analysis of errors which follows represents a calculation for a pure metal sample, and hence shows a greater error in the potential measurement than was present in the measurements on higher resistivity alloy samples. Table 4 shows the influence of the various sources of error on the resistivity as a function of temperature for both sample geometries.

The potentiometer used for measuring the voltage was readable to $\pm$ .1 microvolt, but due to internal thermal voltages was probably only accurate to $\pm$ .5 microvolt, or a total error of 1 microvolt. The percentage error caused in the reading was of course dependent upon the magnitude of the potential measured. The lowest potential measured for any sample was 20 microvolts while the highest ranged up to several thousand microvolts.

The current was measured and monitored to better than

Table 4. Maximum errors in resistivity

	4.2°K.		273°K.	
	%	$\rho\mu\Omega$ cm.	%	$\rho\mu\Omega$ cm.
Cylindrical sample				
Potential	4.0	0.1	0.2	0.1
Current	0.07	0.002	.07	.04
Probe separation	.2	0.005	.2	.04
Cross sectional area	0.8	0.01	0.8	0.4
Overall	4.4	0.11	1.1	0.5
Rectangular parallelepiped sample				
Potential	1.2	.04	.07	.04
Current	.08	.002	.08	.04
Probe separation	.4	.01	.4	.2
Cross sectional area	1.2	.04	1.2	.65
Overall	2.8	.09	1.7	.9

.0001 amp. for currents of .1 or .3 amp.

The diameters of the cylindrical samples were measured with a micrometer readable to $\pm$ .001 mm. but the greatest source of error was the taper in the samples which at most amounted to $\pm$ .01 mm. The calculated error shown in the table was determined for 0.02 mm. taper on a 4.80 mm. diameter sample. The rectangular parallelepiped samples were measured with a Sheffield depth gauge readable to $\pm$ .00001 inch or $\pm$ .00025 mm. The tolerances on the standard gauge blocks were observed to be $\pm$ .0001 inch or .0025 mm. Again the taper of the sample was a greater source of error amounting to $\pm$ .005 mm. maximum.

Typical dimensions were 1.750 mm. x 1.750 mm.

The probe separations were measured with a traveling microscope which could be read to ± .001 mm. The probable error was assessed as the width of the knife edge or the indentation in the sample which was at most ± .025 mm. The separations were about 25.00 mm. for the cylindrical samples and 12.90 mm. for the rectangular cross section samples.

Errors in the temperature measurement with the copper constantan thermocouple varied from ± 0.1°K. at room temperature to ± .25°K. at temperatures below 20°K. The uncertainty in temperature for those samples immersed in the liquid bath should have been less than this.

The compositions of the alloys containing Ho and Er were determined by a spectrophotometric method accurate to ± .2%. The compositions of the Tb-Lu and Y-Lu alloys were determined by spectrographic methods accurate to ± .1% for the dilute alloys and ± 2% for the others.

Although the errors in the resistivity of a given sample did not exceed 1.7% at 273°K., the deviation from the value for a true polycrystalline sample may have been 5% (the difference quoted by P. M. Hall *et al.* (1959a) between the predicted and experimental values of the resistivity of yttrium).

Other errors, such as holes in the sample, were less easily analyzed but were potentially the source of much

greater errors. For example, one sample with a hole had a resistivity 15% greater than the value subsequently measured on a solid sample. All samples were examined radiographically to detect imperfect samples; such samples were rejected to eliminate any errors of this type.

No correction was made for the thermal contraction of the sample because such a correction was not applied to the data for pure metals with which a comparison was made. Such a correction is less than the experimental error in the measurements.

IV. THEORY

The various aspects of the theory of electrical conductivity in metals and alloys discussed in this section are confined to those applicable to the phenomena observed in this investigation. The presentation is begun with the least complex situation, a pure metal, and is developed through increasing stages of complexity to the case of a solid solution alloy with one magnetic component.

A. Mechanisms of the Resistivity in Metals and Alloys

1. Resistivity of a non-magnetic metal

A perfect metal at absolute zero would be made up of an infinite periodic lattice with the ion cores situated exactly on the lattice points and the valence electrons free to move throughout the whole lattice. Such a metal would have no resistance. Any deviation from the perfect periodicity of the lattice, however, will give rise to a scattering of the conduction electrons and hence a resistance. A typical resistivity - temperature curve for a real metal is pictured in Figure 6 and is seen to consist of two parts, ρ_I and ρ_T, the resistivity due to imperfections and the resistivity due to thermal vibrations of the lattice.

The terminology, imperfection resistivity, is used in

Figure 6. Resistivity-temperature curve for a typical metal

Figure 7. Resistivity-temperature curve for a typical magnetic rare earth metal

Figure 8. Resistivity-temperature curve for a typical disordered solid solution alloy

Figure 9. Resistivity-temperature curve for a typical disordered solid solution alloy with one magnetic component

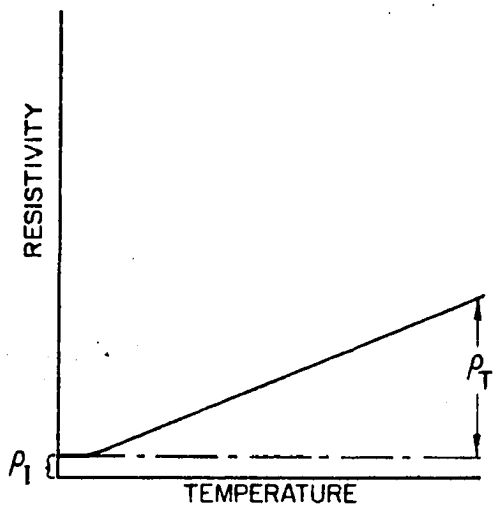
RESISTIVITY
ρ_T
ρ_1
TEMPERATURE

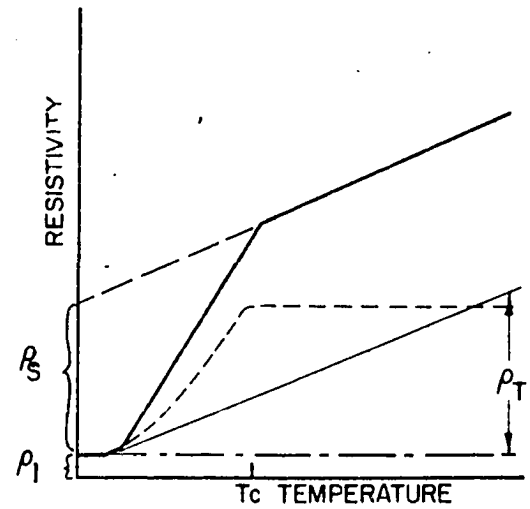
RESISTIVITY
ρ_S
ρ_T
ρ_1
Tc TEMPERATURE

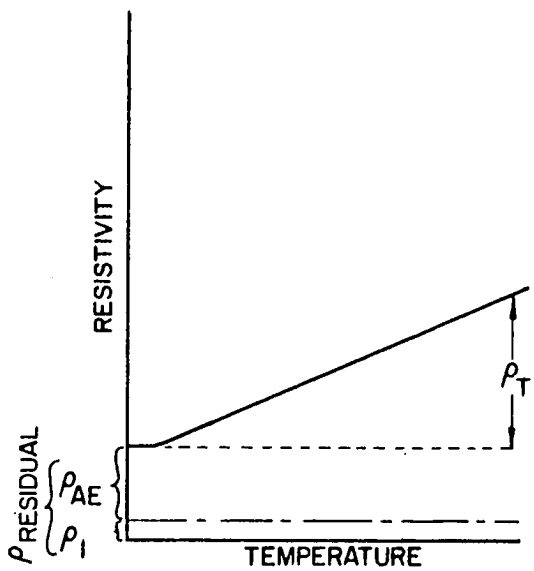
RESISTIVITY
ρ_T
$\rho_{RESIDUAL}$
ρ_{AE}
ρ_1
TEMPERATURE

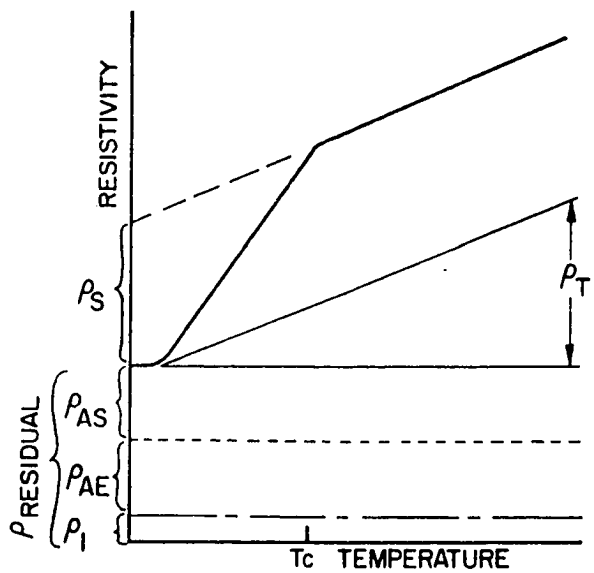
RESISTIVITY
ρ_S
ρ_T
$\rho_{RESIDUAL}$
ρ_{AS}
ρ_{AE}
ρ_1
Tc TEMPERATURE

this context to differentiate it from the residual resistivity, an experimentally determined quantity, which in alloys also includes several other contributions arising from alloying effects. Another common expression for this term is impurity resistivity, but this is too restrictive in its meaning, for the imperfection resistivity arises from a scattering of the conduction electrons by any deviations from the periodic potential of the lattice. J. M. Ziman (1960a) classifies these as point imperfections such as vacancies, interstials, chemical impurities, and isotopes; line imperfections such as dislocations; and surfaces of imperfection such as grain boundaries, twin boundaries, and stacking faults. Volume disorders such as those found in disordered solid solutions, which disrupt the periodicity of the lattice on a massive scale, are considered separately in Section 3.

The imperfection resistivity is commonly considered to be independent of temperature, as expressed by A. Matthiessen and C. Vogt (1864) in Matthiessen's rule, $\rho = \rho_I + \rho_T$, which was originally formulated on empirical grounds. This cannot be strictly true, because recombination of vacancies and interstials and coalescense of dislocations are known to be temperature dependent. The fluctuation of the resistivity due to such effects is small, however, and a more serious challenge to the validity of Matthiessen's rule has been raised by the behavior of dilute alloys of transition metals in the noble

metals. J. O. Linde (1958) has reviewed the experimental results as has A. N. Gerritsen (1956) who concludes that Matthiessen's rule holds as long as the temperature independent part is small compared to the temperature dependent part, and the solute impurity atoms do not measurably affect the solvent lattice.

The temperature dependent portion of the resistivity in a non-magnetic metal, ρ_T, arises from scattering of the conduction electrons by small deviations from perfect periodicity which are caused by thermal vibrations of the lattice. An analysis of various thermal vibrations of the lattice into normal modes of vibration, or standing waves, simplifies the description. Energy in these lattice waves is quantized and a quantum of lattice vibrational energy is termed a phonon, in analogy with the quantum of electromagnetic radiation, the photon. Attempts to compare the theory of lattice vibrations with a physically observable quantity, the specific heat, have required approximations and simplifications to reduce the formulae to dependence upon a single parameter. This parameter θ_D, the Debye temperature, which is proportional to the maximum frequency of a lattice wave, is a useful parameter by which to compare the energies of vibration of various solids. It must not, however, be regarded as an absolute quantity because of the simplifications of the theory required to derive it.

The description of the electron system is also a simplification of the real situation. The independent electron model considers the nuclei to be fixed at lattice points with the closed shells of electrons forming a charge cloud around the nucleus and rigidly attached to it. The valence electrons, which were confined to the region near the atom core in the free atom, are no longer localized, but free to move throughout the solid. Treating the conduction electrons in terms of their wave nature and introducing the periodicity of the lattice leads to the description of a metal proposed by F. Bloch (1928).

The interaction of the electron - phonon system, which gives rise to the scattering of conduction electrons and the observed resistance in metals, is quite complex; and theories dealing with it are of necessity an approximation to the real situation. As yet, an exact theory has not been proposed which can predict the magnitude of the resistivity to much better than a factor of two or three, for even the simplest case of the alkali metals.

Experimental results are most commonly compared to the Bloch - Grüneisen relation, formulated by F. Bloch (1930) as

$$\rho_T = 4(T/\theta)5\ J_5(\theta/T)\rho_\theta$$

where θ and ρ_θ are parameters and $J_5(\theta/T)$ is an integral of the Debye type

$$\int_0^{\theta/T} \frac{z^5 dz}{(e^z-1)(1-e^{-z})}$$

At temperatures greater than θ, this reduces to a linear temperature dependence, $\rho_T = (T/\theta)\,\rho_\theta$, in accord with experimental observations; while at low temperatures a T^5 dependence is predicted, $\rho_T = 497.6\,(T/\theta)^5\,\rho_\theta$, which is seldom observed. Tables of these functions were tabulated by E. Grüneisen (1933) and more recently reproduced by D. K. C. Mac Donald (1956) among others. The parameter θ, or θ_R, is nearly the same as the Debye temperature in many cases, although there are theoretical reasons to believe they should not be identical. M. Blackman (1955) has reviewed the current views regarding θ_R, and values of it for many metals have been tabulated by D. K. C. Mac Donald (1956), A. N. Gerritsen (1956), P. G. Klemens (1956) and J. M. Ziman (1960a).

2. Resistivity of a magnetic metal

A magnetic metal has, in addition to the scattering mechanisms previously described, another scattering process obviously related to the state of magnetic order in the metal. The experimentally observed temperature dependence for the total resistivity of a magnetic rare earth metal is illustrated in Figure 7. The resistivity increases more rapidly than in the previous case shown in Figure 6, until the magnetic ordering temperature is reached, after which the

curve flattens out and follows a linear temperature dependence with the same slope as that displayed by the non-magnetic metal.

Resistivity anomalies associated with the Curie temperatures of the magnetic transition metals were explained by N. F. Mott and H. Jones (1936) on the basis of changes in electronic structure when the metals were heated above the Curie temperature. Nickel, for example, can be described in terms of overlapping s and d bands. The s band carries most of the current and has a low density of states, i.e. a broad range of energies over which the available states are distributed. The d band, on the other hand, has a high density of states, i.e., a narrow energy band which must accomodate a large number of states. It enters into the conduction process mainly because there are a large number of vacant states near the Fermi level into which the s electrons can be scattered. Mott and Jones showed the probability that such a transition would occur was proportional to the density of states in the d band. Nickel is considered to have about 0.6 electron in the s band and 0.6 hole in the d band. Mott and Jones showed that the non-integral values of saturation magnetization observed experimentally could be explained if one postulated a polarization of d band electrons, i.e. an increase in the number with one type spin, say spin up. Since there are a fixed number of states in the d band the

electrons of opposite spin, spin down, are decreased in number and their Fermi level decreases. The unequal distribution is energetically stabilized by the exchange interaction which gives rise to the ferromagnetism. In the case of nickel, all vacant states for spin up electrons are filled, and the number of states near the Fermi level into which the s electrons can be scattered is reduced by a factor of two from the number of states available in the unmagnetized state. Thus the difference in electronic structure above and below the Curie temperature gives rise to an anomaly in the resistivity.

The observation of a resistivity anomaly at the Curie temperature of gadolinium by S. Legvold et al. (1953) evoked much interest, because an interpretation based upon the above mechanism conflicted with the generally accepted conceptions of the electronic structure of rare earth metals. The model of ferromagnetism proposed by W. Heisenberg (1928) also appeared inapplicable to the rare earth metals because the extension and shielding of the 4 f orbitals did not permit sufficient overlap for a direct exchange coupling. A growing literature concerned with explaining this and related effects in the rare earths has developed over the past eight years. One consequence of this study of the rare earths has been a re-investigation of the concepts of electronic structure in the transition metals, and doubt has been cast

on the validity of the model as described, except perhaps for cobalt and nickel.

The anomalous resistivity in gadolinium has been explained by B. R. Coles (1958) in the following manner:

At 0°K. the metal is in a ferromagnetic state with the spins of the unpaired 4 f electrons all perfectly aligned, and hence the conduction electrons are not scattered. As the temperature is increased, deviations from perfect alignment appear, and the periodic potential of the lattice is disrupted. The conduction electrons are scattered in proportion to the degree of misalignment, which continues to increase until the Curie temperature is reached. Above the Curie temperature the spins are completely disordered, and the resistivity from this source remains constant with further increases in temperature. The situation in an antiferromagnetic metal is similar, in that the scattering below the Néel temperature is dependent upon the presence of magnetic ordering, and not on the type of ordering. Resistivity arising from spin disorder of orientation has been termed spin-disorder resistivity, and in this paper is indicated by ρ_s.

This spin disorder resistivity is one manifestation of the exchange coupling between the conduction electrons and the unpaired spins in the 4 f shells which is believed to be the source of magnetism in the rare earths.

C. Zener (1951) and C. Zener and R. R. Heikes (1953) were the first to propose such a mechanism to explain certain discrepancies in the electrical and magnetic properties of the transition metals which were not explicable within the scope of existing theories. T. Kasuya (1956a) suggested that Zener's mechanism provided the best explanation of magnetism in rare earth metals, where the direct coupling between 4 f shells appeared very unlikely. He made a detailed calculation of the exchange coupling for gadolinium, the simplest case because spin-orbit coupling need not be considered. P. G. de Gennes (1958) suggested that the paramagnetic Curie temperatures of the heavy rare earths varied as $(g-1)^2 J(J+1)$, where g is the Lande g factor, and J is the total angular momentum of the trivalent ions. S. H. Liu (1961a) extended Kasuya's treatment of gadolinium to those metals where it was necessary to consider spin-orbit coupling, and arrived at the de Gennes relation starting from first principles. Others who have examined the problem are S. H. Liu (1961b) and R. J. Elliott (1961).

Matthias et al. (1958) found another example of the effects of this exchange interaction when they observed that one atom percent of various rare earths dissolved in lanthanum lowered the superconducting transition temperature by an amount proportional to the spin of the dissolved ions.

Recently K. A. Gschneidner et al. (1961) indicated that

a similar mechanism may be responsible for the lowering of the α-γ transition temperature of cerium in dilute alloys of cerium with various other rare earths.

R. Brout and H. Suhl (1959), after taking into account the spin-orbit coupling, arrived at the same relation for the spin dependence of the resistivity as that proposed by de Gennes for the Curie temperatures. They also pointed out that the lowering of the superconducting transition temperature in lanthanum alloys and the spin disorder resistivity arise from the same type of exchange interaction. H. Suhl and B. T. Matthias (1959) developed a theory for the phenomena observed in the superconducting lanthanum alloys.

T. Kasuya (1956b) was the first to interpret the resistivity anomalies of the magnetic rare earth metals in terms of a conduction electron - 4 f electron exchange interaction and points out that the spin disorder part would be constant above the magnetic ordering temperature.

G. S. Anderson and S. Legvold (1958) examined the experimental values of the resistivity of the heavy rare earths and evaluated the spin-disorder part above the ordering temperature by first extrapolating the linear portion of the curve from the paramagnetic region to $0^{\circ}K.$, and then subtracting the residual resistivity and a correction term derived from the Bloch-Grüneisen relation. These results were found to be proportional to $S(S+1)$, where S is the spin

quantum number for a trivalent ion. R. J. Weiss and A. S. Marotta (1959) performed essentially the same operation on resistivity data for Gd, Dy, and Er and also on Fe, Co, Ni, Cr, and several magnetic alloys of the transition metals. Upon plotting their results against $S(S+1)$ they found the rare earth data fell on a straight line with one slope, while the data for the transition metals and their alloys also fell on a straight line, but with a greater slope.

P. G. de Gennes and J. Friedel (1958) examined the anomalous part of the resistivity of gadolinium, concluding, as had Kasuya, that it arose from spin disorder effects, became constant above the Curie temperature, and tended to a T^2 temperature dependence at low temperatures. T. Kasuya (1959) expanded his original work to include the case of spin-orbit coupling and proposed transport equations for the electrical resistivity, thermal conductivity and thermoelectric power. He predicted a spin dependence of $(g-1)^2 J(J+1)$, and a temperature dependence of T^2 for a ferromagnetic and T^4 for an antiferromagnetic metal. I. Mannari (1959) examined the temperature dependence of the rare earths using a spin wave treatment to consider the perturbations of the spins at low temperatures. He likewise predicted temperature dependences of T^2 for a ferromagnetic and T^4 for an antiferromagnetic metal. J. Seiden (1961a, 1961b) and J. Seiden and M. Papoular (1961) have also

examined the resistivity behavior of the heavy rare earths and found a spin dependence of $(g-1)^2 J(J+1)$. Their calculations of the magnitude of the spin-disorder resistivity are in fair agreement with the experimentally determined values.

The most recent experimental results reported are those of R. V. Colvin *et al.* (1960), who derived their results from materials of higher purity than those available to Anderson and Legvold. Their values for ρ_s were plotted against both $S(S+1)$ and $(g-1)^2 J(J+1)$, (which reduces to $S^2(J+1)/J$ for the heavy rare earths), but their data did not fit either relation exactly.

In view of the investigations discussed above, it appears well established that the exchange interaction between the conduction electrons and unpaired 4 f shell electrons is important in explaining the cooperative magnetic phenomena in the rare earths, because it provides a mechanism of *indirect* interaction between the magnetic ions. The Heisenberg model of ferromagnetism is also based upon an exchange interaction, but this is between d shells in the transition metals, or between f shells for the rare earths, and is considered to be a *direct* interaction between the magnetic ions. This type of interaction is likely to be small in the rare earths because the 4 f orbital extensions and shielding are not commensurate with the overlap required.

As with all exchange interactions derived from the Heitler-London model of the chemical bond, the interaction arises from the Pauli exclusion principle and the indistinguishability of the electrons. To assure full understanding of this point let us review the Heitler-London model of the hydrogen molecule as discussed in C. A. Coulson (1958).

A hydrogen molecule consists of two hydrogen atoms A and B, each possessing an electron identified as 1 and 2. The energy of the system is greatly lowered if the configuration with electron 1 on atom B, and electron 2 on atom A, is considered as well as the configuration with 1 on A, and 2 on B. The terminology, exchange interaction, arose from this mathematical operation, for the electrons were said to change places. This is really a misnomer, because the exchange interaction arises because of the indistinguishability of the electrons, and hence the necessity to consider a combination of both configurations in the wave function of the system. The lowering of energy arises from the greater freedom of the electrons, for they now are free to move in the vicinity of both nuclei. When more complex systems are examined the spin of the electron must be considered, and anti-symmetric wave functions must be used to describe the system in accord with the Pauli exclusion principle. The spin quantum numbers enter via this restriction.

The exchange interaction between conduction electrons

and the 4 f shell electrons is based on the same general principles, except that in a magnetic material the state of lowest energy for the metal as a whole is assumed to be the one with as many spins as possible aligned rather than paired. The exchange interaction provides the energy necessary to stabilize this configuration. The spin dependent part of the Hamiltonian for the conduction electron - 4 f electron interaction is of the form $H = I \sum \vec{S}_f \cdot \vec{s}_c$, where I is the exchange integral, $\vec{S}_f$ the spin of the 4f electrons, and $\vec{s}_c$ the spin of the conduction electron. For those cases where spin-orbit coupling must be considered P. G. de Gennes (1958) and R. Brout and H. Suhl (1959) showed that $\sum \vec{S}_f$ could be replaced by the projection of $\vec{S}$ upon $\vec{J}$, namely $(g-1)\vec{J}$.

A physical picture of this substitution is as follows: The application of Russell-Saunders coupling gives $\vec{S}$ and $\vec{L}$ vectors for the spin and orbital angular momentum which are coupled together to give a $\vec{J}$ vector for the total angular momentum. These vectors precess in the magnetic field in the metal at a fast enough rate so that the conduction electron "sees" an average S which can be represented as the projection of $\vec{S}$ on $\vec{J}$, thus giving a Hamiltonian of the form $H = I\,(g-1)\,\vec{J} \cdot \vec{S}_c$.*

---

*Mackintosh, A. R., Physics Department, Iowa State University, Ames, Iowa. Interpretation of the physical model of the validity of the substitution of $(g-1)\vec{J}$ for $\sum \vec{S}_f$. Private communication. 1961.

The interaction between ions for indirect coupling of this type has been treated by M. A. Ruderman and C. Kittel (1954) and leads to a spin dependence of the form $(g-1)^2 J(J+1)$ which is seen in observations of the bulk properties of the materials. Since the basic interaction is related to the spin configuration of the magnetic ion, one would not expect a dependence upon the total angular momentum, J, or the magnetic moment, $g\sqrt{J}(J+1)$ even though these factors are experimentally observed in magnetic susceptibility and specific heat measurements. One should not be deceived by the appearance of the formula $(g-1)^2 J(J+1)$, for a glance at Figure 10 shows it is more closely related to $S(S+1)$ than $J(J+1)$.

3. Resistivity in a disordered solid solution alloy

The general form of the resistivity-temperature curve is pictured in Figure 8. The most noticeable difference between the resistivity of a pure metal and an alloy is the higher residual resistance. This arises from the massive perturbation of the lattice by a large number of "impurity" atoms. A composition dependence is also present, and L. Nordheim (1931) has shown this to follow the relation $\rho_{AE} = C \times (1-X)$, where ρ_{AE} indicates the resistivity arising from electrostatic deviations of the periodic potential caused by alloying, x and (1-x) are the mole fractions of the two components, and C is a constant characteristic of the alloy system. This gives

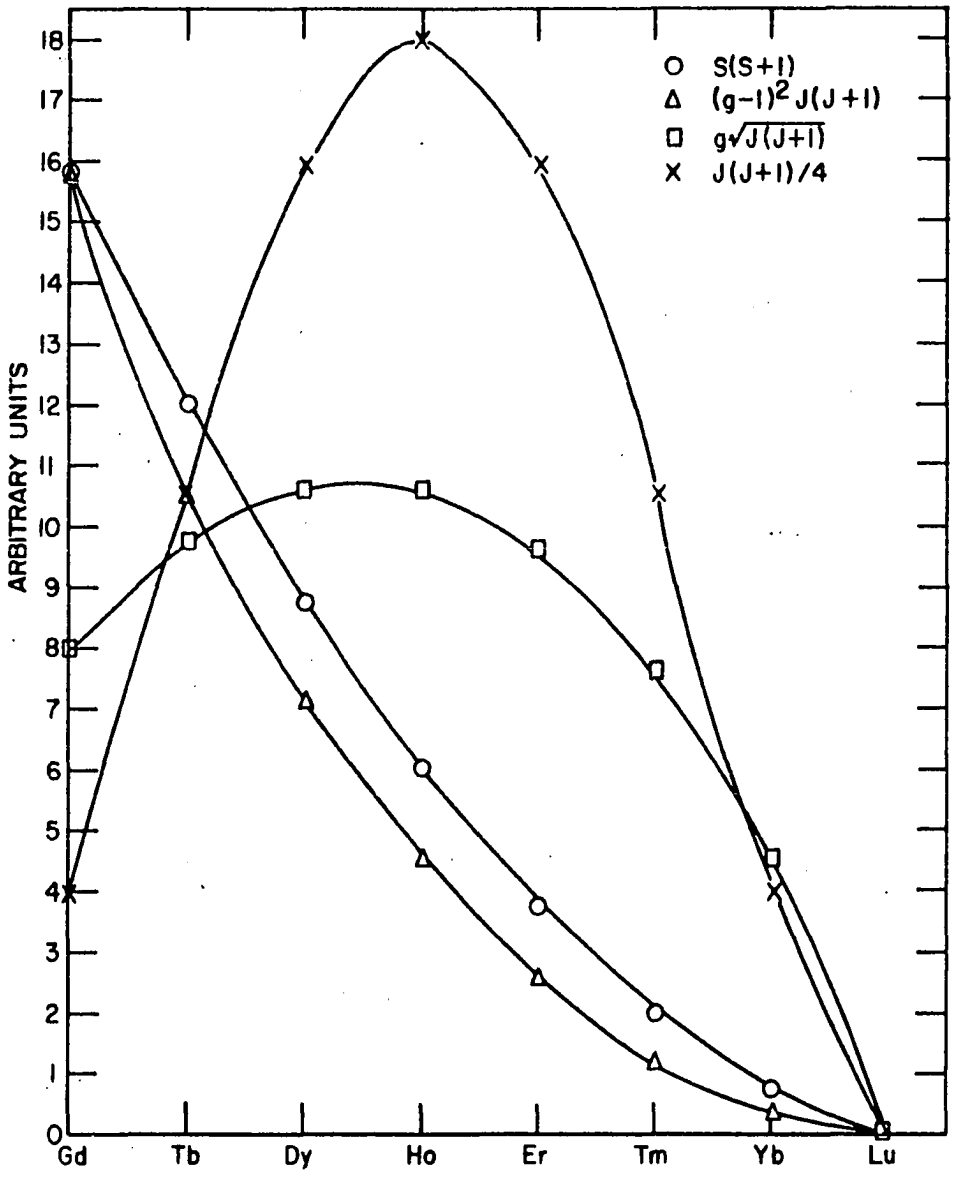

Figure 10. Values of several possible spin dependence relations [S(S+1), $(g-1)^2$ J(J+1), J(J+1)] and the magnetic moment ($g\sqrt{J(J+1)}$) for the trivalent rare earths Gd to Lu

rise to a symmetrical inverted parabola with the maximum at 50 atom percent composition. The assumptions to be satisfied are that the two metals have similar electronic structures, atomic sizes, and no change in crystal structure takes place in alloying. J. M. Ziman (1960a) gives the relation of the parameter C to the difference in potential an electron "sees" near an A atom and near a B atom. The derivation is as follows:

Let us define an average potential seen by each electron as

$$\overline{V} = x\, V_A + (1-x)\, V_B \quad ,$$

where x is as above, and V_A and V_B are the potentials at A and B atoms respectively. At the site of an A atom the potential deviates from the average by the amount

$$V_A - \overline{V} = (1-x)\,(V_A - V_B) = (1-x)V_{AB}$$

and at a B atom by

$$V_B - \overline{V} = -x\, V_{AB} \quad .$$

Other things being equal, the scattering by such a perturbing potential is proportional to the square of the matrix element, i.e. at an A site

$$\left|\int \psi k^* \, (V_A - \bar{V}) \, \psi k' \, d\vec{r}\right|^2 = (1-x)^2 \left|\int \psi k^* \, V_{AB} \, \psi k' \, d\vec{r}\right|^2$$

$$= (1-x)^2 \left|V_{AB}\right|^2$$

Since the density of A atoms is proportional to x, the contribution to the total electron scattering at these sites is

$$x(1-x)^2 \left|V_{AB}\right|^2 .$$

Adding the contribution of B atoms gives

$$[x(1-x)^2 + x^2(1-x)] \left|V_{AB}\right|^2$$

$$= x(1-x) \left|V_{AB}\right|^2$$

for the square of the matrix element at each site.

4. Resistivity of a disordered solid solution alloy, one component magnetic with localized magnetic electrons

The general shape of the resistivity-temperature curve is shown in Figure 9. The main difference from a combination of the results for a magnetic metal and a disordered alloy is an additional contribution to the residual resistivity. The additional resistivity, designated ρ_{AS}, arises from a spin-disorder scattering of the conduction electrons, because the magnetic atoms are distributed randomly over the lattice

sites by alloying.

Apparently J. Owen et al. (1956) were the first to recognize this effect and apply it to an interpretation of the properties of Cu-Mn alloys. R. W. Schmitt (1956) attempted to explain the resistance maxima observed in resistivity measurements of dilute alloys of the transition metals in noble metals by such a mechanism. K. Yosida (1957) expanded upon Schmitt's ideas and developed a more comprehensive theory for dilute alloys of manganese in copper. B. R. Coles (1958), in his review article, points out numerous other cases of transition metal alloys where it is apparent the spin-scattering mechanism can be invoked to explain anomalous resistivities, although the original authors of the various works did not realize the significance of their results.

T. Kasuya (1959), in his calculations of transport properties influenced by the exchange interaction between the conduction electrons and magnetic ions, predicted that dilute alloys containing a solute with localized spins should have a residual resistivity of $\rho = Cx\left\{A^2(0) + (g-1)^2\, j(j+1)J^2(0)\right\}$ where A(0) includes all interactions other than the exchange integral J(0), j is the total angular momentum quantum number, x is the concentration of solute, and $C = {}^3/_2 \frac{\pi m}{\hbar \zeta Ne^2}$ where ζ is the Fermi energy and N is the number of atoms per

unit volume.

B. Classical Conceptions of the Resistivity Behavior of Dilute Alloys

The work of J. O. Linde (1931, 1932) on various metal solutes dissolved in noble metal solvents was climaxed with the formulation of Linde's rule, $\Delta\rho = a+bZ^2$, where $\Delta\rho$ is the resistivity increase caused by one atom percent solute, a and b are constants for a given solvent metal, and Z is the valence difference between solute and solvent. This empirical rule held quite well for elements to the right of the noble metals on the periodic chart, but sizeable deviations were observed for the transition metals.

N. F. Mott (1936) calculated scattering cross sections for various solutes in dilute alloys, but the results were somewhat higher than the experimentally observed values. Better agreement was obtained by F. J. Blatt (1957), who took into account the strain in the lattice caused by the different ionic sizes of the solutes. J. Friedel (1956) considered the band structure of the transition metals in his interpretation of the anomalous behavior of the elements to the left of the noble metals in the periodic system.

The agreement between the experimental results and the calculated results of Mott should be substantially improved

by the use of a pseudo-potential, the difference between the kinetic energy and potential energy of the electron, such as discussed by M. H. Cohen and V. Heine (1961), and determining the scattering cross section from the difference between this pseudo-potential in the vicinity of a solvent and solute atom.

None of the methods discussed above, however, are capable of explaining the results observed in this investigation.

C. A Proposal by Mott and Stevens Concerning Electronic Structure of Ferromagnetic Metals

N. F. Mott and K. W. H. Stevens (1957) discussed the electronic structure of the transition metals in relation to their electrical and magnetic properties. They pointed out that there are certain fundamental differences between the electronic structures of the close-packed transition metals nickel and cobalt, and body centered cubic iron. These differences in the electronic structure are manifest in the behavior of the electrical resistivity in the neighborhood of the Curie temperature. The resistivities of cobalt and nickel, on the one hand, appear to be consistent with the original band structure proposed by N. F. Mott and H. Jones (1936); while the resistivity curve of iron, on the other

hand, is similar to that of gadolinium, and the electronic structure of iron might better be described in terms of localized d electrons. They propose that a distinction between magnetism of the collective electron type and the Zener type can be made by comparing the reduced resistivity vs. reduced temperature, (ρ/ρ_c vs. T/T_c) curves of ferromagnetic alloys of two representative materials.

The behavior predicted for the localized electron case is a superposition of the reduced resistivity - reduced temperature curves for the alloy and pure metal, both above and below the Curie temperature, while for the band model the two curves will diverge above the Curie temperature.

B. R. Coles is purported to have examined the behavior of iron and an Fe-Ru alloy,* but apparently has not yet published the results. A. I. Schindler et al. (1957) have published data applicable to the other case in their study of Ni-Pd alloys. In view of the uncertainties in the electronic structure of iron, it would be wise to examine as well a case known to be characteristic of the localized electron model, such as gadolinium and one of its ferromagnetic alloys.

---

*Information cited in footnote by N. F. Mott and K. W. H. Stevens (1957), p. 1380.

D. Additional Considerations

The resistivity-temperature curves for the light rare earth metals differ from those of the heavy rare earth metals in showing a pronounced curvature. R. J. Elliott (1954) has considered this phenomenon and proposed a mechanism whereby the crystal field of the lattice causes a Stark splitting of the energy levels of the ions. This would cause small deviations from the periodic potential of the lattice and give rise to an additional resistivity of the form $\rho = \rho_0 \operatorname{sech}^2(\Delta/2kT)$, where Δ is the energy difference between levels, and ρ_0 is a constant estimated to be about one micro ohm-cm. Addition of this extra contribution to that calculated with the Bloch-Grüneisen formula gives qualitative agreement with experimental results. Elliott's original calculations are not quantitatively correct, except possibly for lanthanum, because he was unaware of a low temperature region of magnetic ordering in praseodymium and neodymium, but his mechanism for explaining the curvature may have some merit.

The anisotropies of resistivity observed in single crystal studies can not be explained by any of the theories so far discussed. A. R. Mackintosh (ca. 1962) has recently considered the problem in terms of a free electron model of the Fermi surface; an approach which has been especially

successful in explaining the unusual resistivity behavior of the "c" axis single crystals of erbium. The Brillouin zone appropriate for a description of the rare earth metals is the single zone for a hcp. metal rather than a double zone. The spin-orbit coupling of the conduction electrons in hcp. metals has been shown to lift the degeneracy between the bands over the hexagonal face except along one line and hence gives rise to an energy gap not present in early calculations of the Brillouin zones of hcp. metals. In the reduced zone representation of the free electron Fermi surface the portion which will dominate most of the transport properties was found to lie in the third zone. In the case of erbium the occurrence of antiferromagnetic ordering introduces additional planes of energy discontinuity normal to the "c" axis which profoundly influences the geometry of the Brillouin zone. This change in geometry distorts the Fermi surface and decreases the conductivity parallel to the "c" axis, an effect which is seen in the sharp changes in slope of the resistivity curves for the "c" axis crystal. This model has been successful in qualitatively explaining other transport properties as well as the electrical conductivity but as yet quantitative information about the Fermi surface geometry of the rare earths has not been obtained.

V. EXPERIMENTAL RESULTS

The data obtained from x-ray diffraction and resistivity studies of rare earth alloys are presented in this part. The interpretation of the data is presented in Part VI.

A. X-Ray Diffraction Data

All alloy samples examined were found to possess the hexagonal close packed magnesium type crystal structure. The lattice constants were evaluated by means of the computer program described in Part III and are reported to $\pm$ .001 Å. The lattice constants, c/a ratio, and cell volumes are tabulated in Table 5, and the variation of c/a ratio and cell volume as a function of composition are illustrated graphically in Figure 11 and Figure 12 respectively. The variation of the c/a ratio for the pure metals as determined by F. H. Spedding *et al.* (1956) is also included in Figure 11.

B. Resistivity Data

1. Temperature dependence

The resistivity-temperature data for the thirteen alloys examined over the temperature range 4.2°K. to 310°K. is

Figure 11. c/a ratio vs. composition for the Gd-Lu, Tb-Lu, and Gd-Er alloy systems and for the metals Gd to Lu

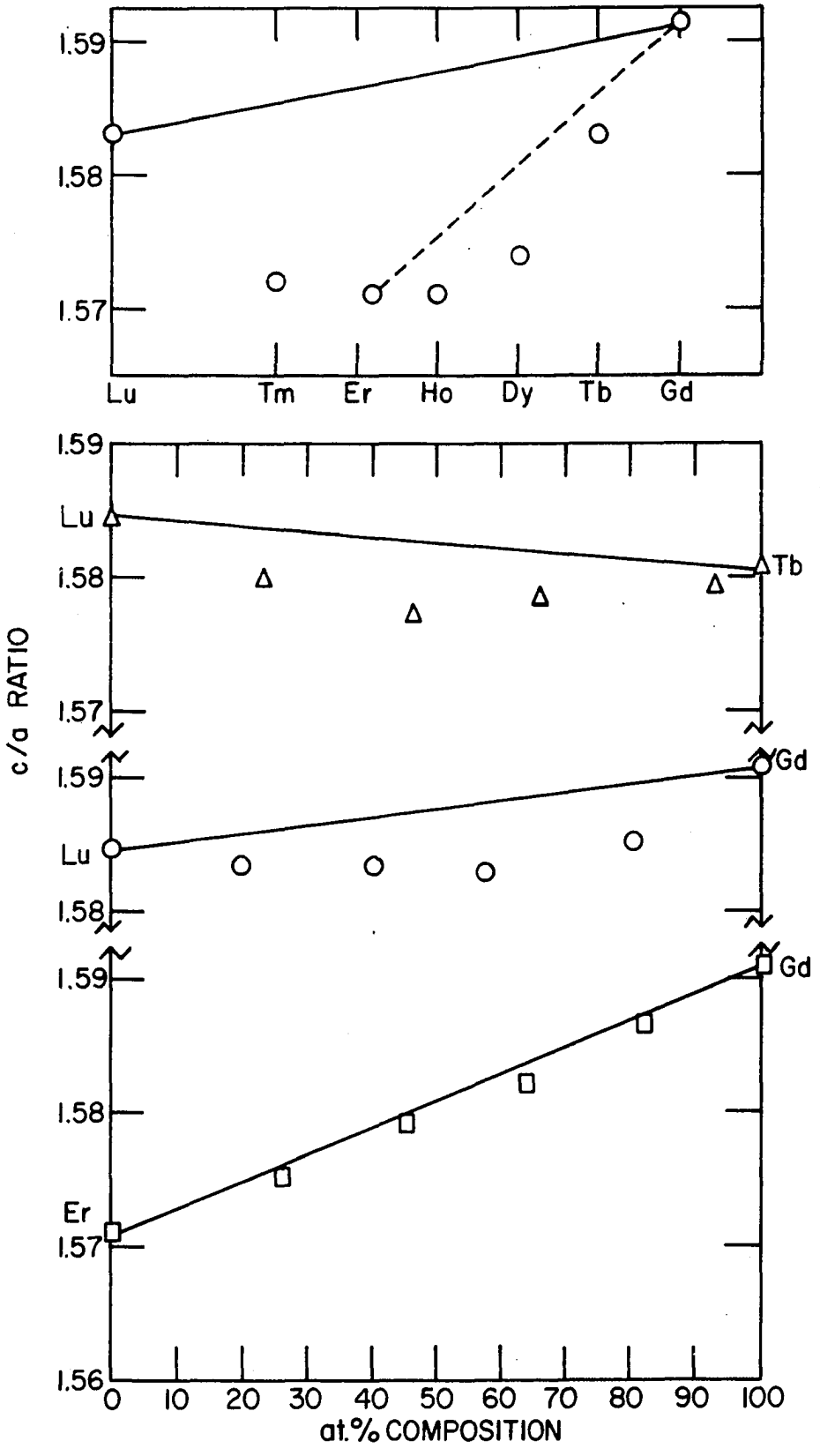
1.59
1.58
1.57
Lu
Tm
Er
Ho
Dy
Tb
Gd
c/a RATIO
Lu
Tb
Gd
Lu
Gd
Er
1.56
0
10
20
30
40
50
60
70
80
90
100
at.% COMPOSITION

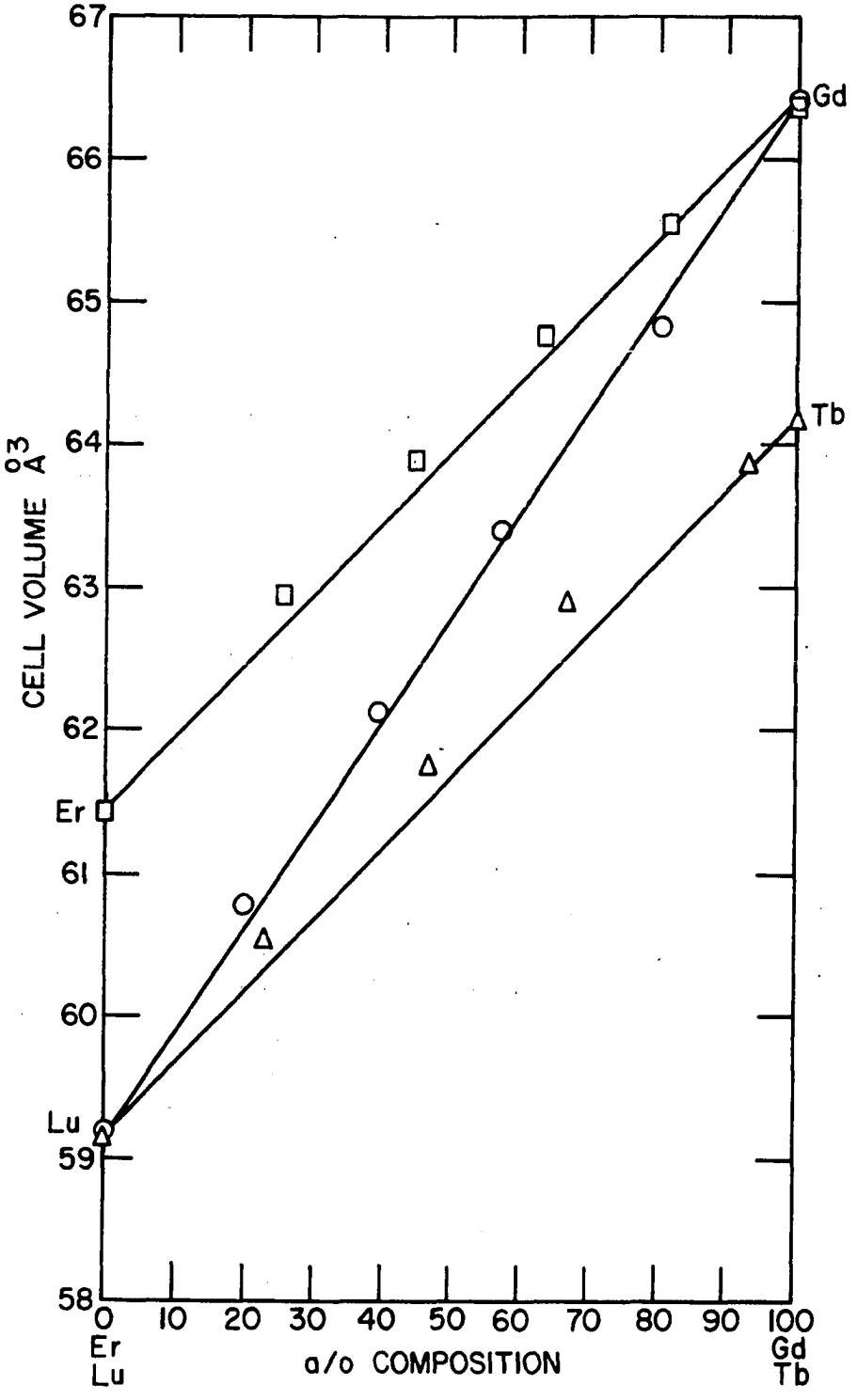

Figure 12. Cell volume vs. composition for the alloy systems Gd-Lu, Tb-Lu, and Gd-Er

Table 5. X-ray data

Sample	a_o Å	c_o Å	c/a	$V_{Å^3}$ [a]
Gd	3.639	5.789	1.5907	66.41
80.2 Gd-Lu	3.614	5.729	1.5851	64.82
57.3 Gd-Lu	3.589	5.681	1.5829	63.38
40.2 Gd-Lu	3.565	5.644	1.5832	62.11
20.0 Gd-Lu	3.539	5.604	1.5835	60.77
Lu	3.506	5.555	1.5845	59.14
Tb	3.606	5.698	1.5804	64.15
93.4 Tb-Lu	3.601	5.687	1.5793	63.85
66.7 Tb-Lu	3.583	5.655	1.5781	62.87
46.7 Tb-Lu	3.563	5.618	1.5771	61.75
23.3 Tb-Lu	3.537	5.587	1.5798	60.51
Lu	3.506	5.555	1.5845	59.14
Gd	3.639	5.789	1.5907	66.41
81.8 Gd-Er	3.626	5.753	1.5867	65.50
63.7 Gd-Er	3.615	5.719	1.5819	64.73
45.0 Gd-Er	3.601	5.686	1.5791	63.86
25.7 Gd-Er	3.587	5.650	1.5751	62.94
Er	3.561	5.594	1.5707	61.44

[a] $a_V = .866 a_o^2 c_o$.

tabulated in Tables 14 to 26 in the Appendix. The temperature dependent portion of the resistivity, (ρ - ρ residual), is plotted as a function of temperature in Figures 13, 14, 15 and 16 for each of the systems investigated. The abscissa's of the various curves are progressively displaced upward to provide a 10 micro ohm-cm. separation between the origins for the different curves and to facilitate comparison of the curves.

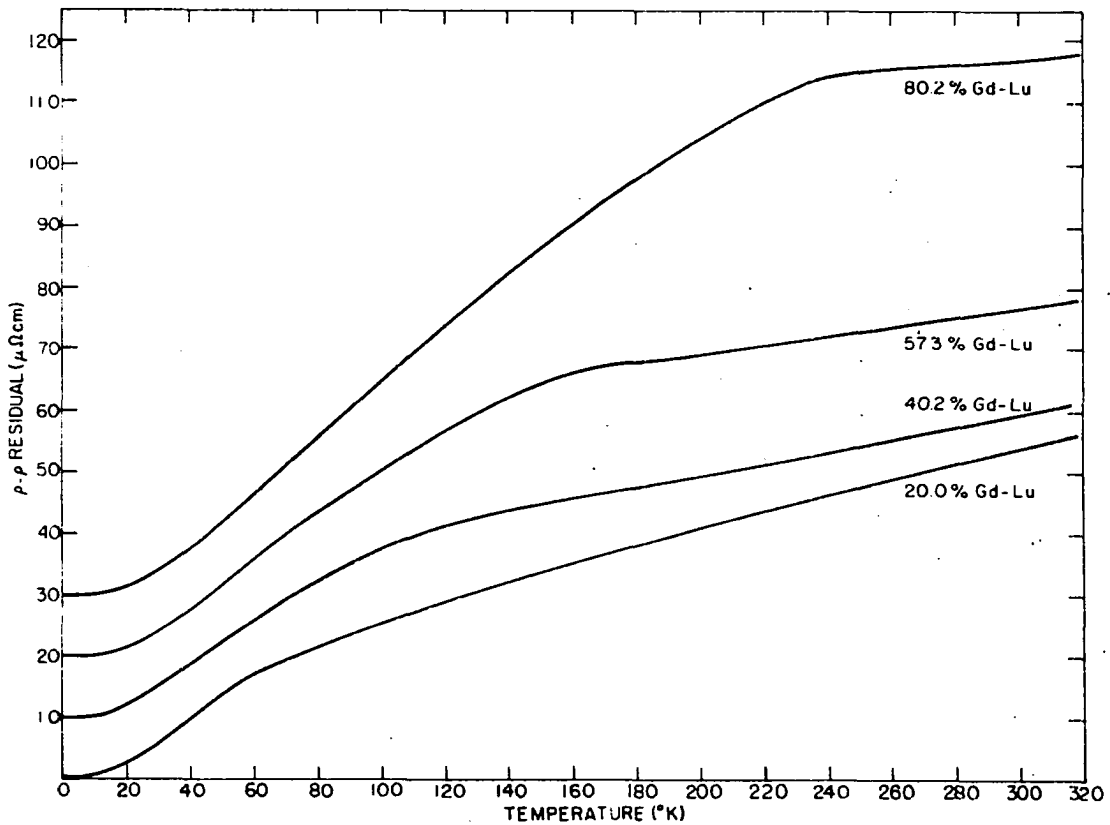

Figure 13. Resistivity vs. temperature for Gd-Lu alloys (residual resistivity subtracted)

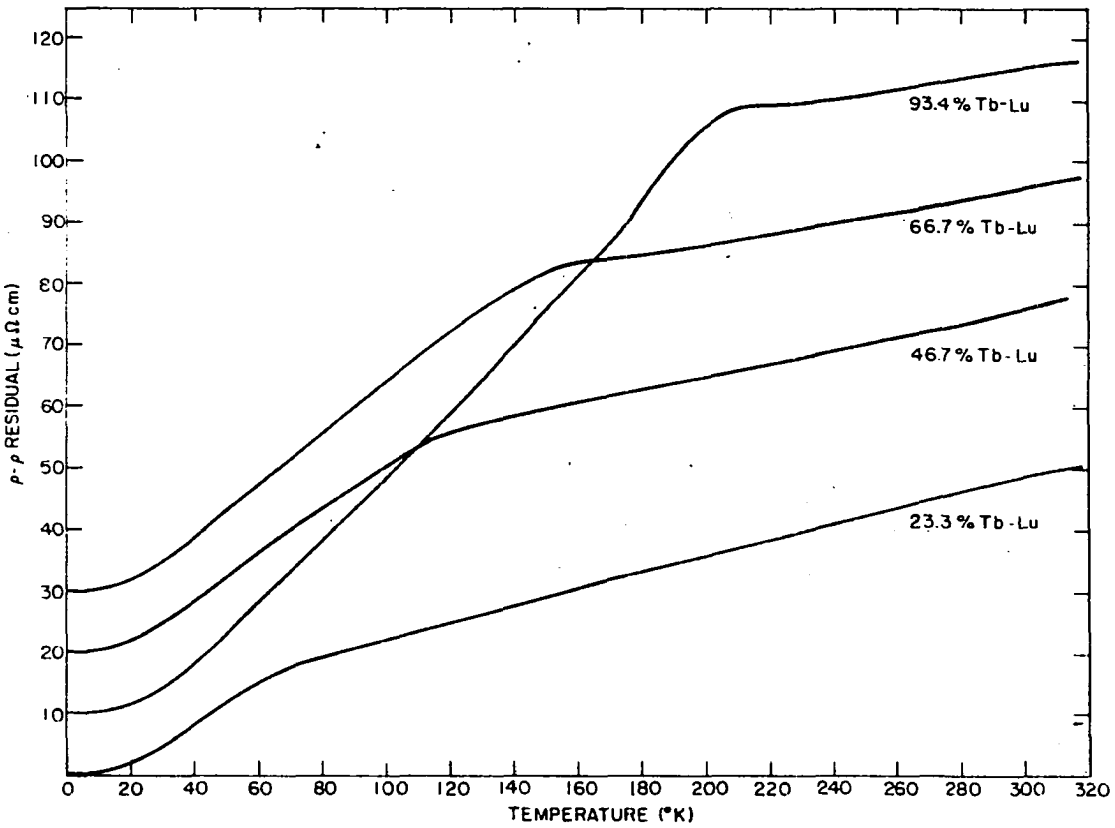

Figure 14. Resistivity vs. temperature for Tb-Lu alloys (residual resistivity subtracted)

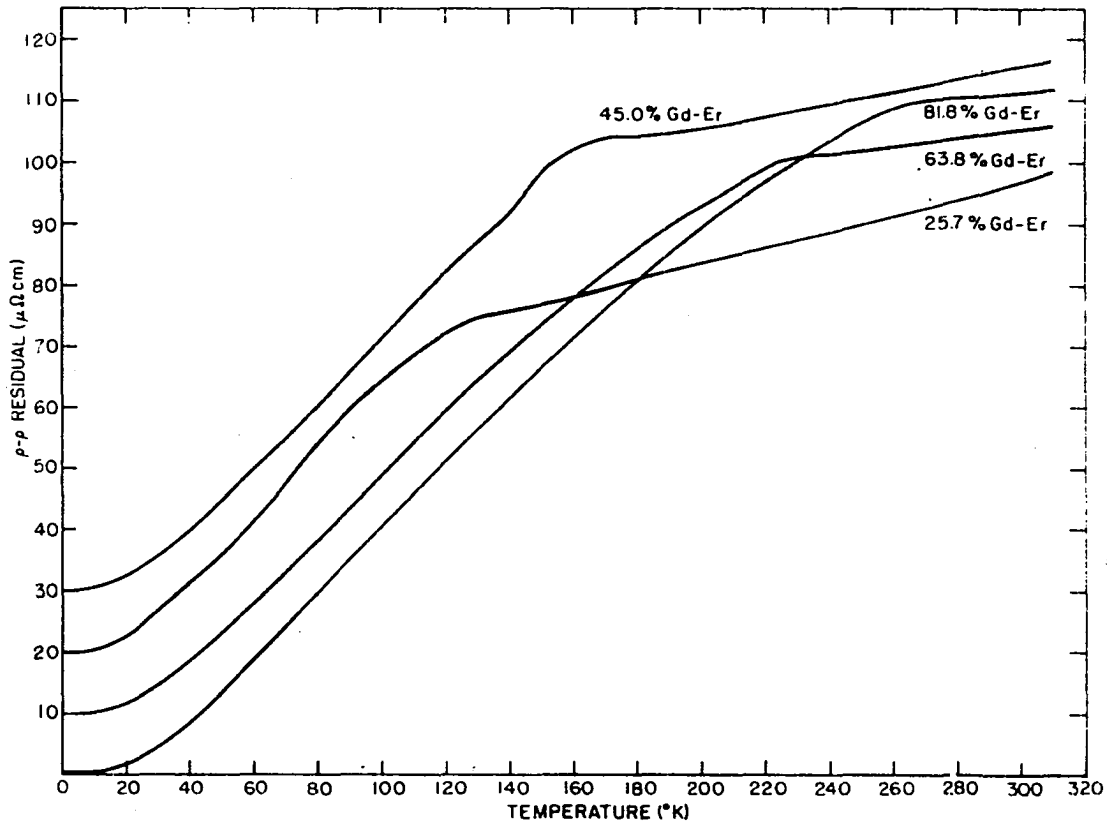

Figure 15. Resistivity vs. temperature for Gd-Er alloys (residual resistivity subtracted)

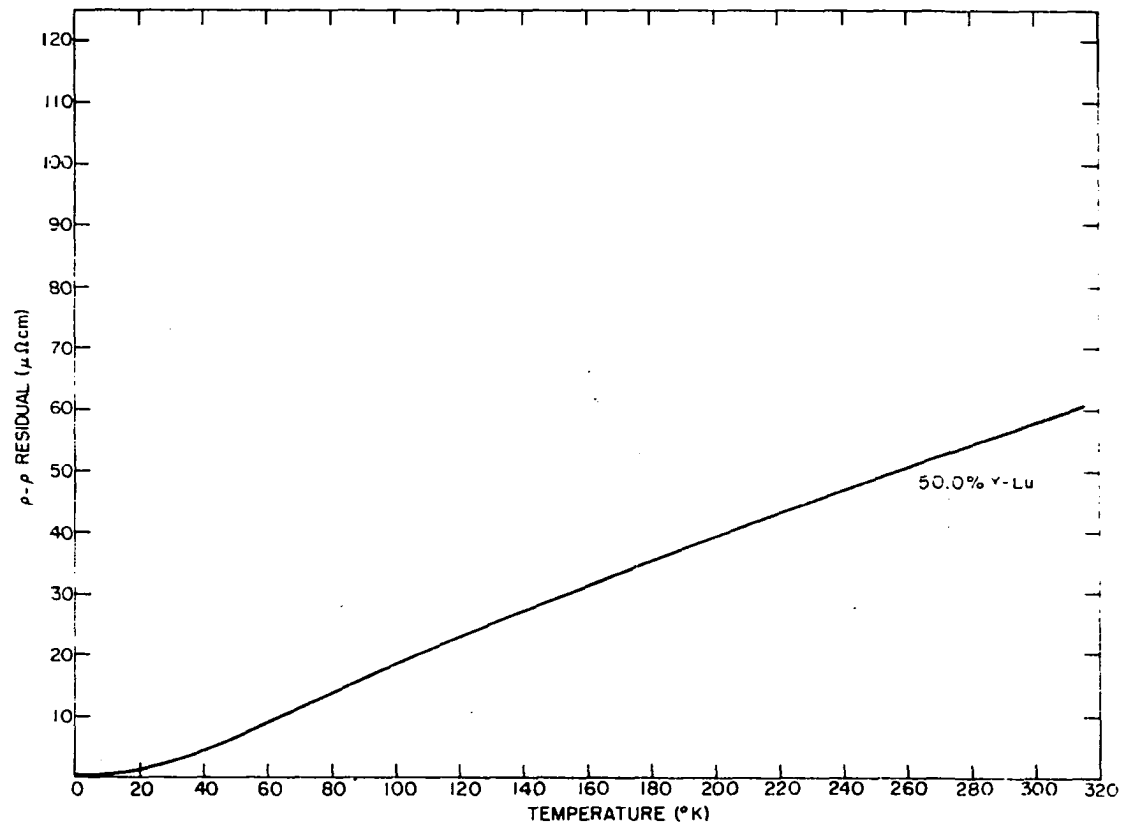

Figure 16. Resistivity vs. temperature for 50.0 atom percent Y-Lu alloy (residual resistivity subtracted)

The curves for the alloys display the same general behavior as those of the pure metals, exhibiting a change in slope at the highest magnetic transition temperature. Several of the alloys also have anomalies characteristic of the resistivity behavior at an antiferromagnetic-ferromagnetic transition temperature. The slopes of the resistivity curves in the paramagnetic region are seen to change gradually from alloy to alloy across the series.

The temperature dependence of the resistivity at low temperatures is a quantity of interest as was indicated in Part IV. If the resistivity is of the form $\rho = cT^n$ the exponent n can be determined from the slope of a plot of the logarithm of resistivity vs. the logarithm of temperature. Such plots were made for the heavy rare earths from the data of R. V. Colvin et al. (1960)*, M. A. Curry et al. (1960)*, and J. K. Alstad et al. (1961a, 1961b)*, and for the alloys examined in this investigation. The results are shown in Figures 17 to 22 and are summarized in Table 6. The scatter of the points in the region below 10°K. is rather large for most of the samples as a result of the expanded scale on the log-log plots and is not unusual for this region (cf. G. K. White and S. B. Woods (1959)).

---

*Legvold, S., Physics Department, Iowa State University, Ames, Iowa. Made available the raw data from these investigations. Private communication. 1961.

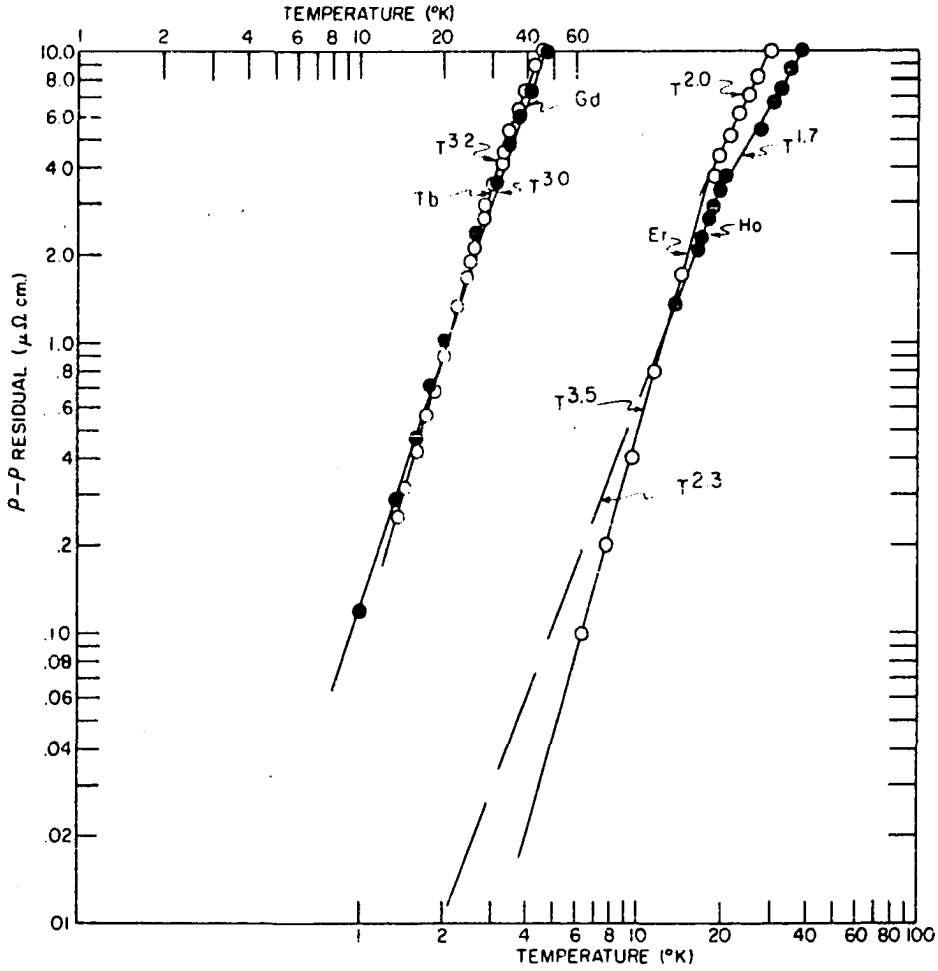

Figure 17. Determination of the temperature dependence of Tb, Gd, Er, and Ho (residual resistivity subtracted)

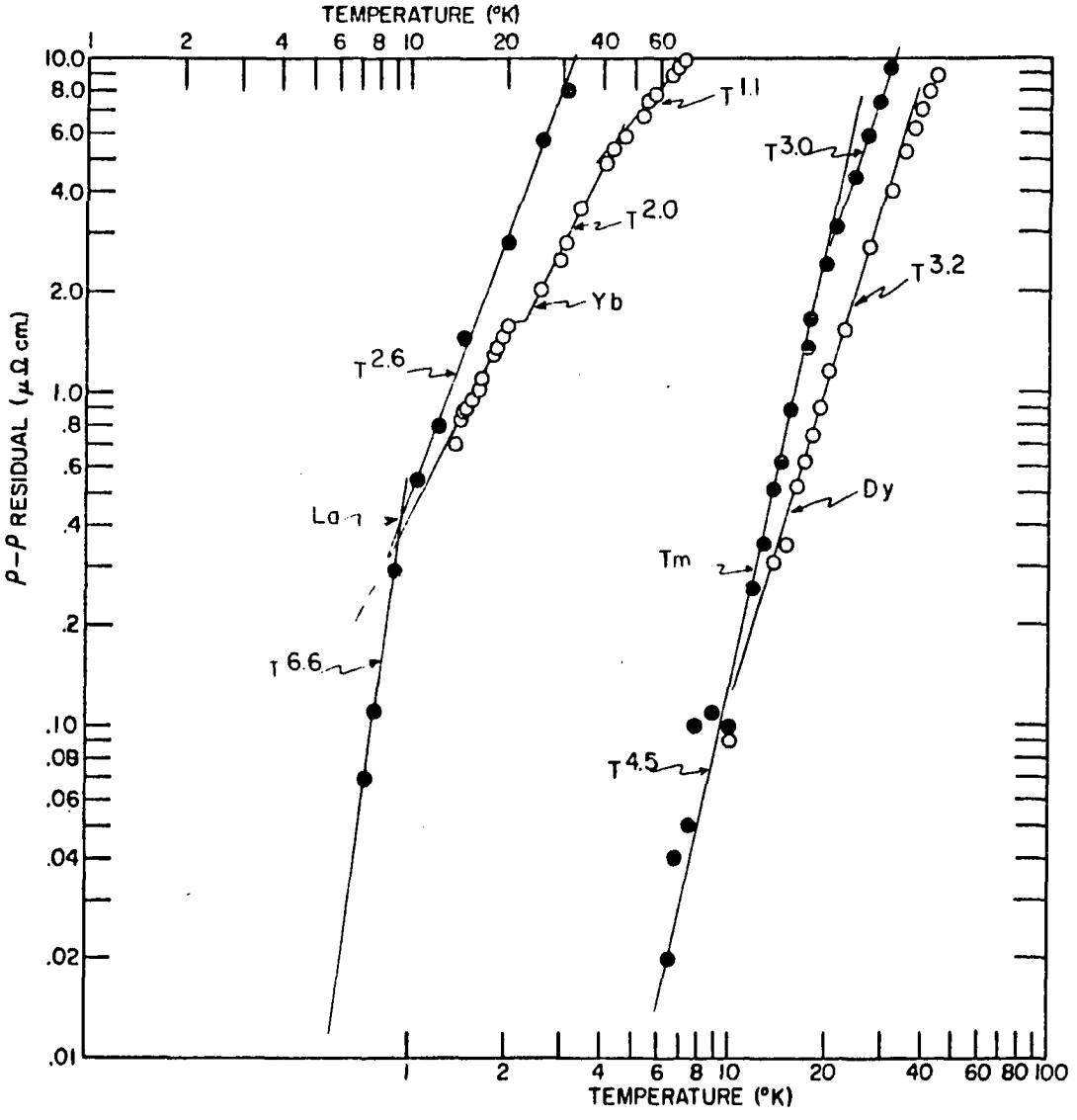

Figure 18. Determination of the temperature dependence of La, Yb, Tm, and Dy (residual resistivity subtracted)

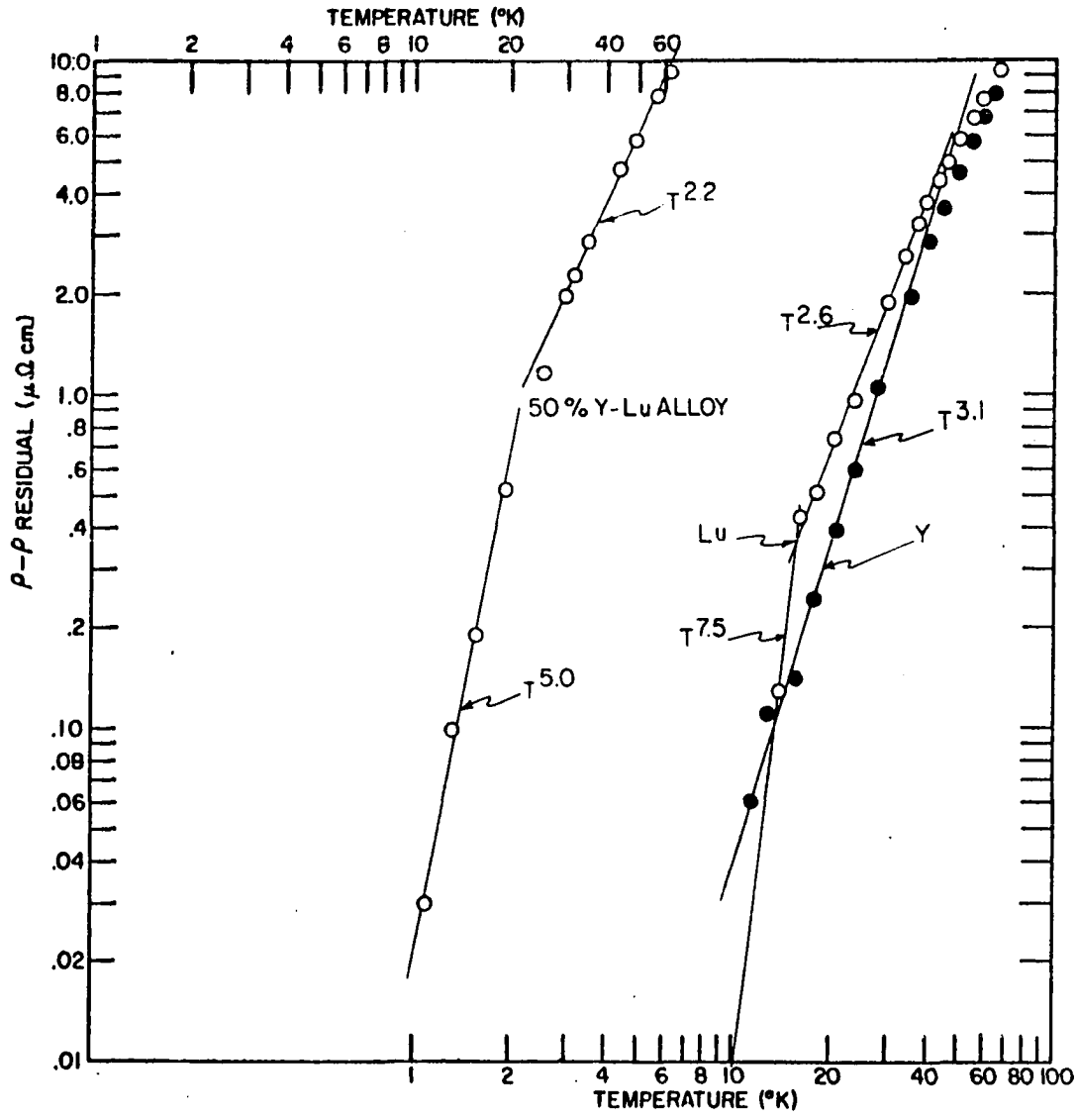

Figure 19. Determination of the temperature dependence of 50 percent Y-Lu, Lu, and Y (residual resistivity subtracted)

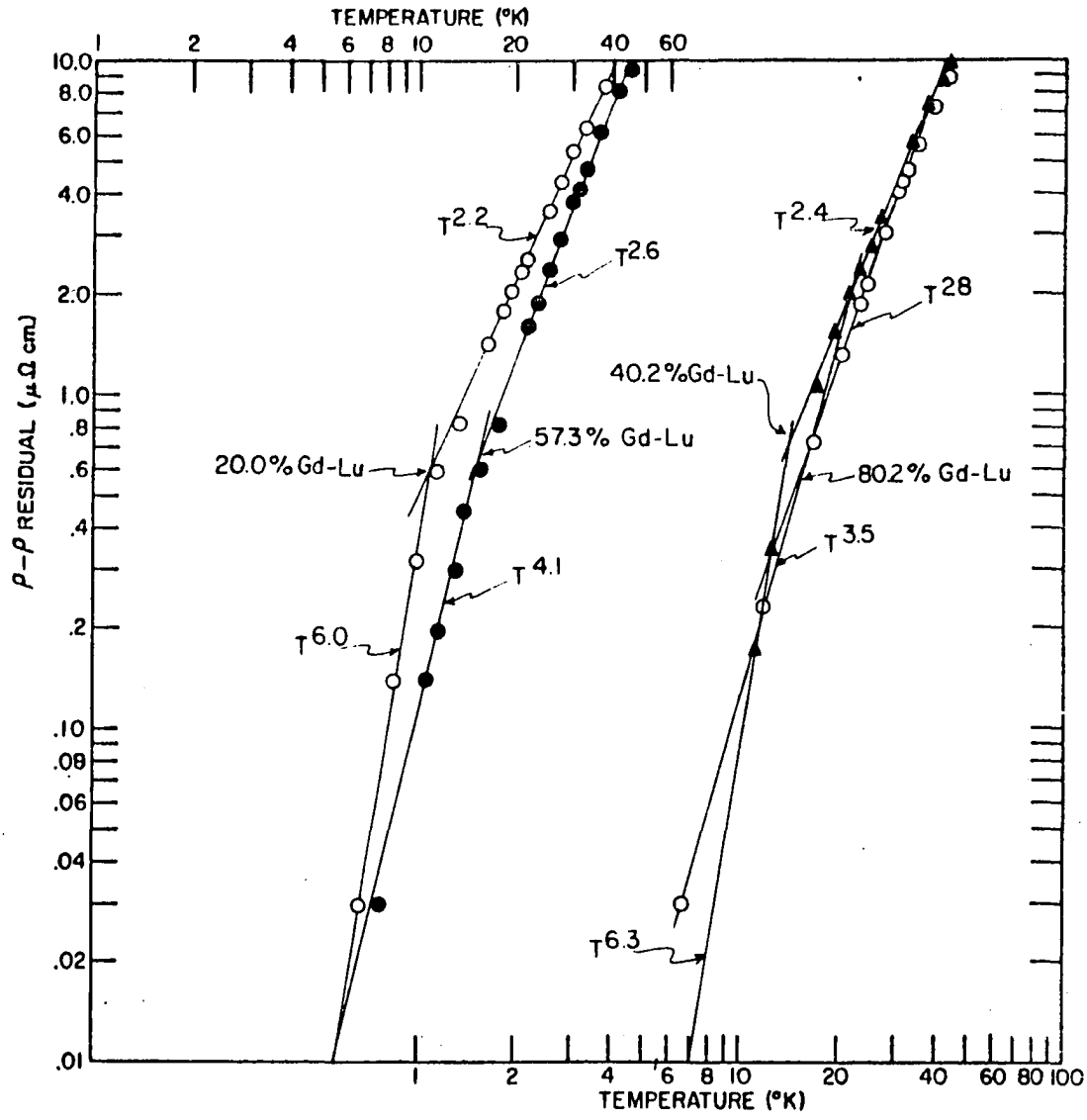

Figure 20. Determination of the temperature dependence of the Gd-Lu alloys (residual resistivity subtracted)

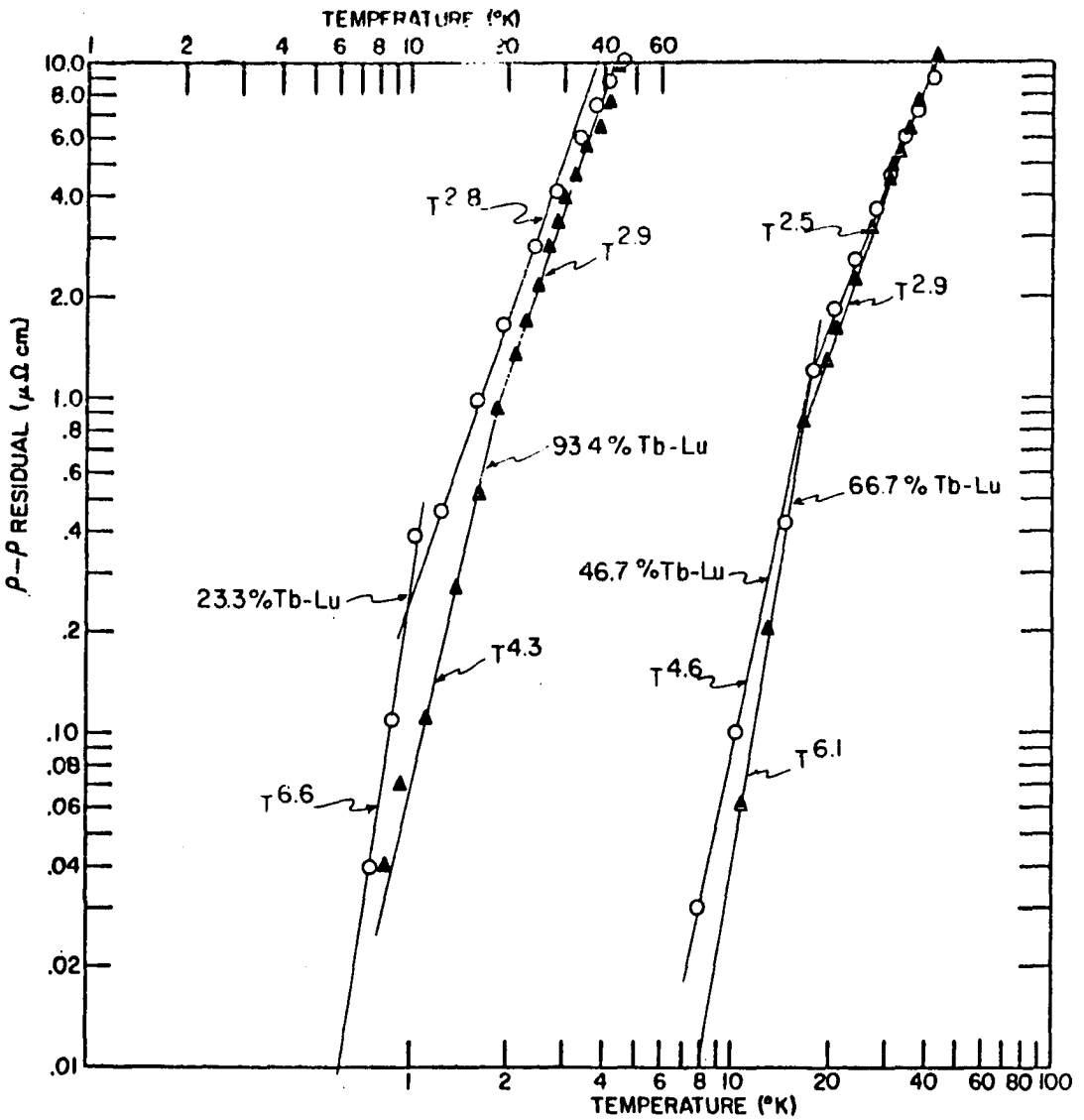

Figure 21. Determination of the temperature dependence of the Tb-Lu alloys (residual resistivity subtracted)

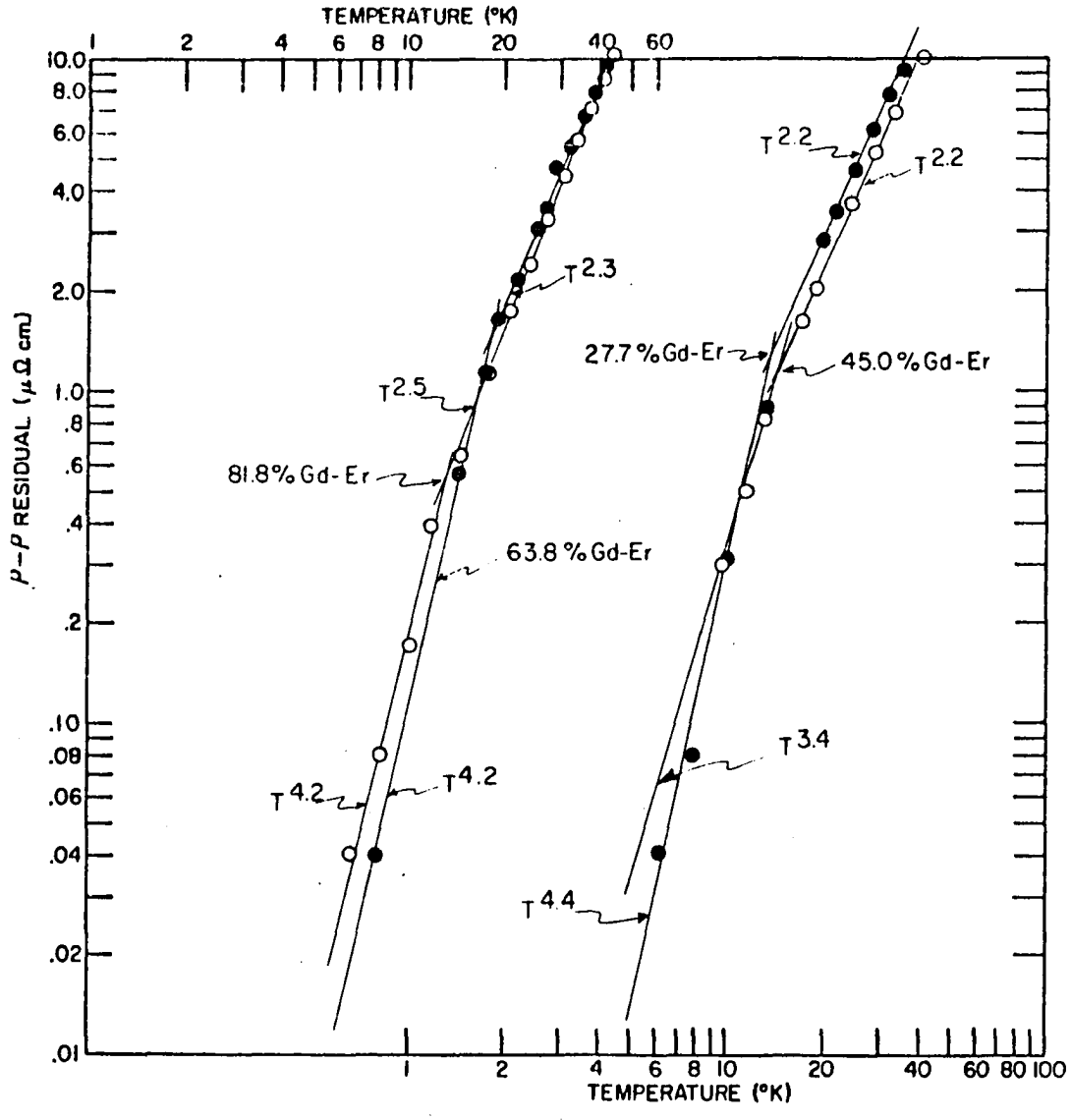

Figure 22. Determination of the temperature dependence of the Gd-Er alloys (residual resistivity subtracted)

Table 6. Summary of temperature dependence of the resistivity in the low temperature region

material	n	material	n	n'
Gd	3.0 (10-40°)[a]	80.2 Gd-Lu	3.5 (6-16)[a]	2.8 (17-35)[a]
Tb	3.2 (14-35)	57.3 Gd-Lu	4.1 (7-15)	2.6 (21-41)
Dy	3.3 (10-32)	40.2 Gd-Lu	6.3 (11-14)	2.4 (14-37)
Ho	2.3 (13-19)	20.0 Gd-Lu	6.0 (6-10)	2.2 (15-40)
Er	3.5 (6-18)	93.4 Tb-Lu	4.3 (11-18)	2.9 (18-34)
Tm	4.5 (6-21)	66.7 Tb-Lu	6.1 (11-17)	2.9 (17-35)
Yb	2.0 (14-40)	46.7 Tb-Lu	4.6 (8-17)	2.5 (17-37)
Lu	2.6 (18-40)	23.3 Tb-Lu	6.6 (7-10)	2.8 (12-29)
Y	3.1 (11-40)	81.8 Gd-Er	4.2 (6-13)	2.5 (13-37)
La	2.6 (9-26)	63.7 Gd-Er	4.2 (8-19)	2.3 (19-40)
		45.0 Gd-Er	3.4 (9-15)	2.2 (17-35)
		25.7 Gd-Er	4.4 (6-13)	2.2 (20-35)
		50.0 Y -Lu	5.0 (11-22)	2.2 (22-56)

[a]Temperature range in which n is observed.

2. Composition dependence

The residual resistivity of alloys is a composition dependent quantity for solid solution alloy systems. The values for this quantity were determined graphically from the resistivity-temperature curves; the residual resistivities were evaluated at the point where the resistivity-temperature curve tended to a constant value at low temperatures. This characteristically occurred at about 5-10°K., slightly higher than for the metals. Values of the residual resistivity so determined are listed in Table 7.

Table 7. Residual resistivities of alloys

Alloy	$\rho_{res.}$
80.2 Gd-Lu	50.3
57.3 Gd-Lu	81.7
40.2 Gd-Lu	79.6
20.0 Gd-Lu	55.9
93.4 Tb-Lu	20.2
66.7 Tb-Lu	61.6
46.7 Tb-Lu	68.4
23.3 Tb-Lu	42.7
81.8 Gd-Er	17.6
63.7 Gd-Er	29.0
45.0 Gd-Er	33.3
25.7 Gd-Er	28.3
50.0 Y -Lu	31.8

The variation of the total resistivity with composition for the alloy systems Gd-Lu, Tb-Lu, and Gd-Er is shown in Figures 23 and 24, at 50° intervals. The isotherms below the magnetic ordering temperature for all alloys in a system are seen to be quite symmetrical, while the isotherms above this temperature are seen to be unsymmetrical. The odd shape of some of the curves is due to the large difference in the temperature coefficient of the resistivity above and below the upper magnetic transition temperature.

The sharp change in slope of the resistivity-temperature curves at the upper magnetic transition temperature permits one to find the ordering temperature from resistivity data. According to the theories presented in Part IV, this point should correspond to a complete disordering of the ionic spins. In practice, the transition is not this simple, for a maximum in the resistivity-temperature curve is observed for many of the samples.

The change in slope of the resistivity-temperature curve is readily seen if one plots the slope, $\Delta \rho / \Delta T$, against temperature. A typical plot is shown in Figure 25. It is apparent that the transition from ordered to disordered state is not sharp, but occurs over about a 10° temperature interval. The mid-point of this transition range was taken for the ordering temperature tabulated in Table 8 for the alloys examined.

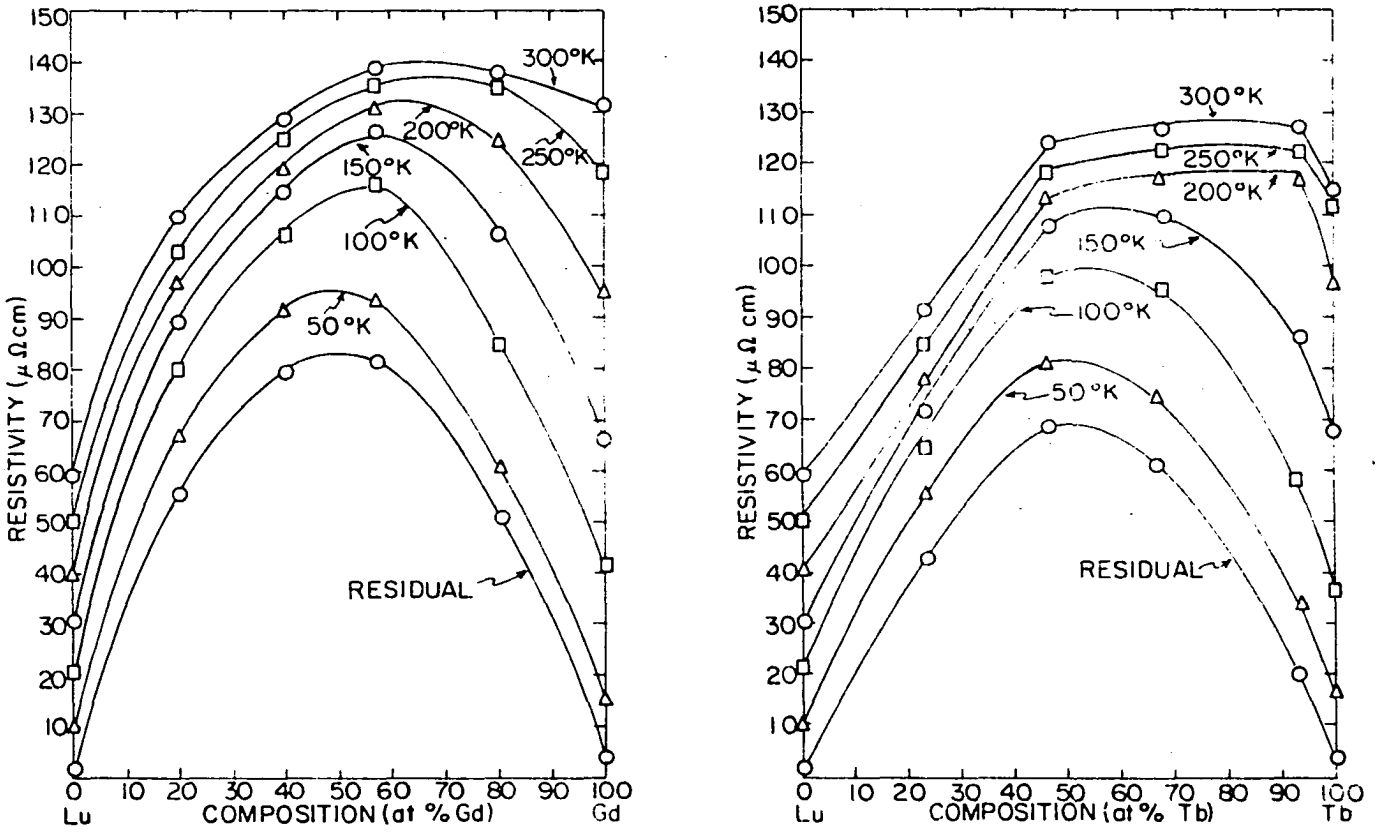

Figure 23. Resistivity vs. composition isotherms for Gd-Lu and Tb-Lu alloy systems

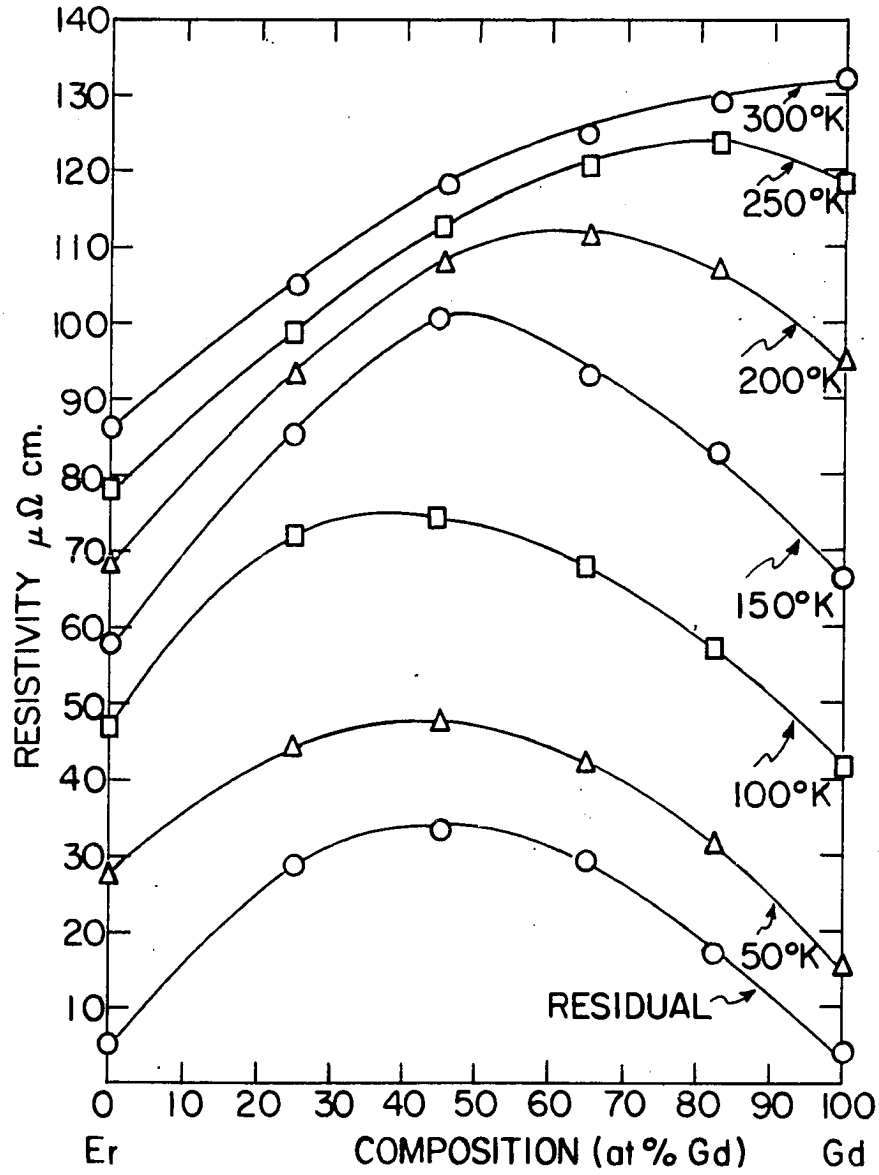

Figure 24. Resistivity vs. composition isotherms for the Gd-Er alloy system

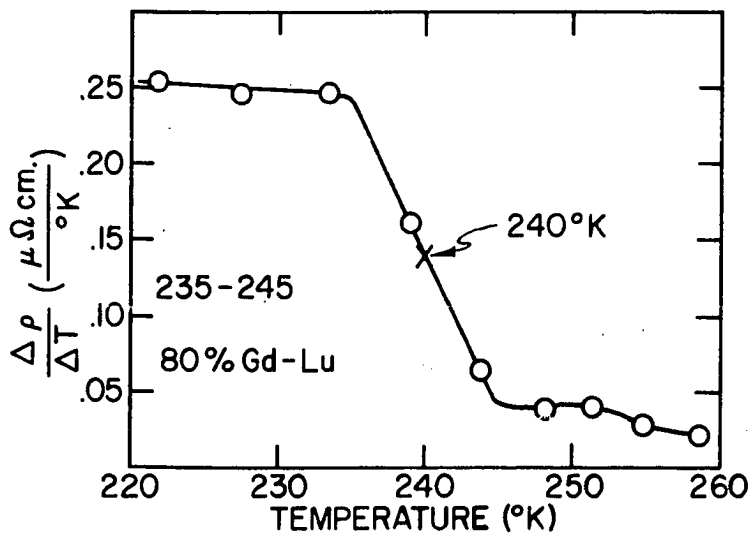

Figure 25. Graphical determination of the paramagnetic-magnetic ordering temperature for the 80% Gd-Lu sample

Table 8. Temperature of magnetic transition observed in resistivity-temperature curves

Alloy	θ_p °K.[a]	θ_{A-F} °K.[b]
80.2 Gd-Lu	240	---
57.3 Gd-Lu	167	?
40.2 Gd-Lu	121	?
20.0 Gd-Lu	61.0	?
93.4 Tb-Lu	211	181
66.7 Tb-Lu	157.5	?
46.7 Tb-Lu	120	?
23.3 Tb-Lu	63.5	?
81.8 Gd-Er	261.5	---
63.7 Gd-Er	225.5	---
45.0 Gd-Er	170.5	138
25.7 Gd-Er	128.5	70

[a] θ_p indicates the transition temperature between magnetic ordering and the paramagnetic region.

[b] θ_{A-F} indicates a possible antiferromagnetic-ferromagnetic transition temperature.

Several of the alloys also displayed behavior typical of that associated with a ferromagnetic-antiferromagnetic transition temperature and these values are also listed in Table 8. The variation of the upper magnetic ordering temperature with composition is shown in Figure 26.

The spin disorder resistivity, determined by an extrapolation of the linear portion of the ρ vs. T curve (the region above the ordering temperature) to T = 0°K., followed by a subtraction of the residual resistivity, is a

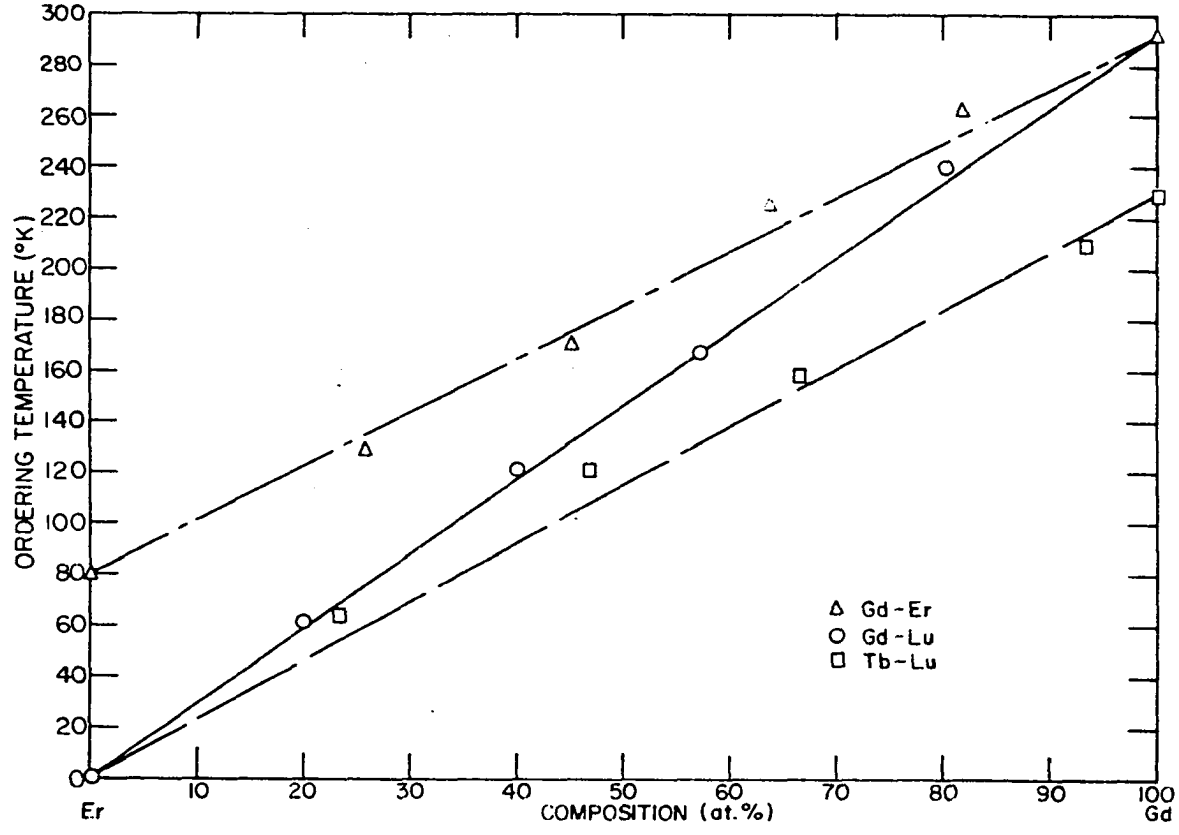

Figure 26. Ordering temperature vs. composition for the Gd-Lu, Tb-Lu, and Gd-Er alloy systems

quantity indicative of the magnitude of the conduction electron - magnetic ion interaction.

Values of the spin disorder resistivity so determined are tabulated in Table 9.

Table 9. Spin disorder resistivities of alloys

Alloy	ρ_s	Alloy	ρ_s
80.2 Gd-Lu	71.6	46.7 Tb-Lu	22.0
57.3 Gd-Lu	33.8	23.3 Tb-Lu	7.9
40.2 Gd-Lu	21.0	81.8 Gd-Er	94.9
20.0 Gd-Lu	7.7	63.7 Gd-Er	74.6
93.4 Tb-Lu	78.2	45.0 Gd-Er	55.6
66.7 Tb-Lu	35.2	25.7 Gd-Er	36.8

C. Dilute Alloys

The resistivities of some dilute alloys of various heavy rare earth metals dissolved in lutetium were measured at 4.2°K. to determine the increase in resistivity caused by the various solutes. The measurements were performed with the samples immersed in liquid helium to provide a uniform temperature for performing the experiment. The results are plotted in Figure 27.

The slopes of the lines for the various solutes in Figure 27 were used to evaluate the increase in resistivity for a given solute and the imperfection resistivities were

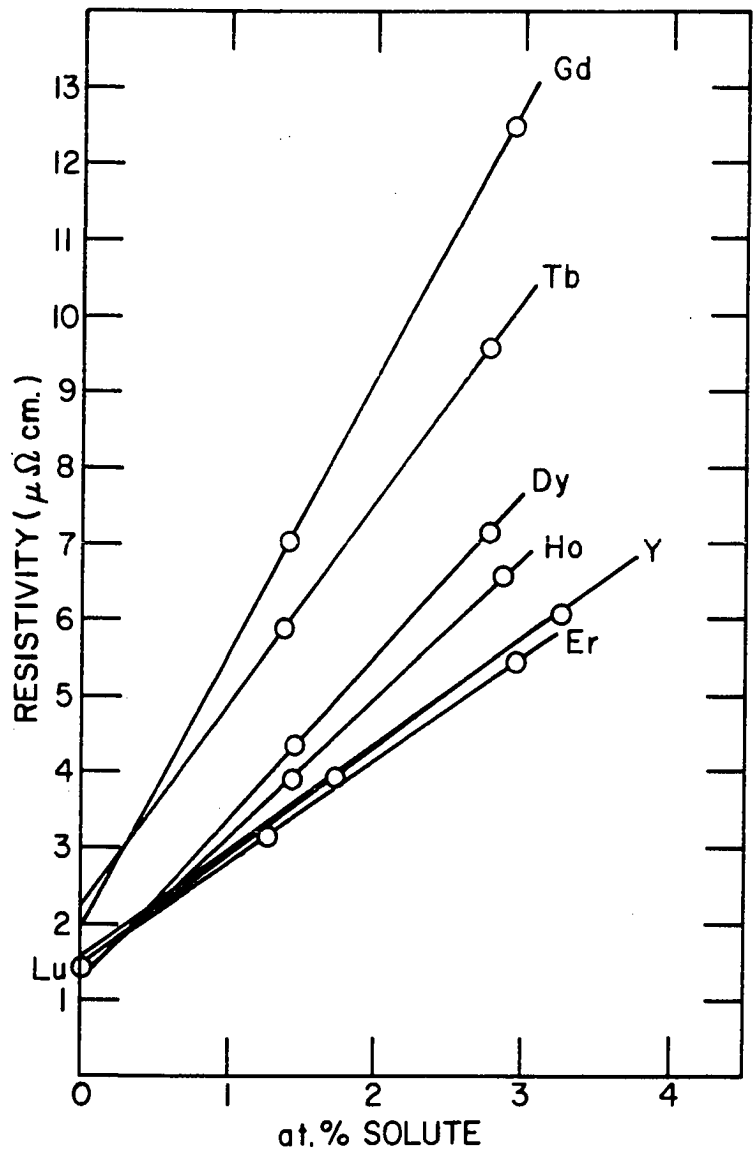

Figure 27. Resistivity at 4.2°K. of dilute alloys of lutetium with various rare earth solutes

evaluated from the data for the lutetium sample. The resistivity increase was then determined at 3 a/o composition and divided by 3 to give the results in terms of the conventionally reported increase of resistivity caused by 1 a/o solute. The raw data and $\Delta \rho$ are tabulated in Table 10. All resistivities are reported in micro ohm-cm.

Table 10. Resistivity data for dilute alloys

Sample	Measured	$\Delta \rho$/1% solute
1.4% Gd	7.02	3.58
2.9% Gd	12.47	
1.4% Tb	5.89	2.67
2.8% Tb	9.52	
1.4% Dy	3.93	2.11
2.8% Dy	6.55	
1.4% Ho	3.93	1.78
2.9% Ho	6.55	
1.3% Er	3.18	1.37
2.9% Er	5.46	
1.7% Y	3.91	1.43
3.3% Y	6.08	
Lu	1.43	----

VI. DISCUSSION

The results of this investigation are considered in this part under the three categories of phase relations, evidence of conduction electron - magnetic ion interaction in rare earth metals and alloys, and results chiefly of interest when compared to the properties of other metals.

A. Phase Relations

The information pertaining to phase equilibria obtained in this study established the existence of complete solid solubility in the Gd-Lu, Tb-Lu, and Gd-Er binary systems. Such a finding is not unexpected, for these systems satisfy the Hume-Rothery requirements for formation of extensive solid solutions; namely, similar valence, electronegativities, and crystal structures and a difference in metallic radii of less than 8%. The last of these requirements would appear to be the most critical for the systems investigated.

A study of the Gd-Y system by R. M. Valetta (1959) established the existence of complete solid solubility for a binary system of trivalent, hexagonal close packed rare earth metals with a size difference of about 0.05% between their metallic radii. The size factor for the Gd-Lu system, 3.9%, was the greatest for the systems examined in this study

and is well within the limits proposed by Hume-Rothery. A very recent study of the Sc-Y system by B. J. Beaudry* has revealed the existence of complete solid solubility in this system, where the size difference of 9.7% lies slightly outside the empirical limits suggested by Hume-Rothery.

The assumption that the rare earth metals will universally form complete solid solutions in binary systems among the elements of the group is of course unwarranted. R. M. Valetta (1959) demonstrated the importance of crystal structure in his studies of the La-Y and La-Gd systems.

Exploratory work on the Ce-Yb and La-Yb systems by F. A. Smidt (1960) showed the importance of valence in limiting the extent of solid solubility. The solubility limit for Yb in La was found to be less than 15% while the limit for Yb in Ce was estimated to be less than 5%. In contrast to the influence of valence in these systems, B. J. Beaudry* has found complete solid solubility in the Sc-Zr system, where the valences are +3 and +4 respectively.

The change of unit cell volume with composition for the various alloy systems in this study is shown in Figure 12. A slight positive deviation from a Vegard's law relation was noted for each of the alloy systems studied. The significance

---

*Beaudry, B. J., Ames Laboratory, United States Atomic Energy Commission, Ames, Iowa. Information on the phase equilibria in the Sc-Y and Sc-Zr alloy systems. Private communication. 1961.

of this is doubtful, because as pointed out by J. M. Sivertsen and M. E. Nicholson (1961), almost all metal solid solutions exhibit some type of deviation from Vegard's law. The behavior of the c/a ratio is more interesting, especially when compared to the change of c/a ratio across the heavy rare earth series as in Figure 11. The curve for the metals is observed to decrease from Gd to a minimum value at Ho and Er and then to increase again for Tm and Lu. A curve of similar shape is observed for the variation of c/a ratio with composition for the Gd-Lu and Tb-Lu systems. If one draws a line between the Gd and Er points on the graph for the metals, and expands the scale to match the composition axis for the alloy graphs, a less pronounced minimum would be observed. This coincides with the much smaller minimum seen in the variation of c/a ratio with composition in the Gd-Er system. A somewhat similar correlation between the spin disorder resistivities of alloys made up to a given average spin value, and metals of the same spin value, was noted in the resistivity measurements and is discussed in the next section.

Resistivity measurements are also capable of giving information about the phase equilibria in alloy systems. A. N. Gerritsen (1956) has summarized the characteristic behavior of the resistivity as a function of composition in various types of alloy systems. In general the resistivity

varies linearly across a two phase region, shows maxima at compounds, and curves across both primary and intermediate solid sclution regions. As shown in Figures 23 and 24, the residual resistivities of the alloy systems investigated in this study show the inverted parabola behavior characteristic of complete solid solubility.

B. Evidence of Conduction Electron - Magnetic Ion Interaction

The existence of an exchange interaction between the conduction electrons and the unpaired electrons in the 4f shell, henceforth to be called the s-f interaction, was well recognized before the present investigation was begun. The influence of the s-f interaction on the magnetic and electrical properties of the metals and on the superconducting transition temperature of lanthanum alloys was previously considered in Part IV.

The existence of another manifestation of this s-f interaction in rare earth alloys, namely an additional contribution to the residual resistivity due to random distribution of magnetic ions in the alloy lattice, and the relation of its magnitude to the spin of the magnetic component or components in the alloy, has been demonstrated in this study. The scattering of the conduction electrons to

give this additional contribution is similar to the mechanism responsible for the spin disorder resistivity in metals, and in fact its existence had been predicted, and several anomalous resistivities in transition metal compounds had been explained on this basis. The utilization of the unique materials available in the rare earth series, however, permits one to characterize this effect in much greater detail and evaluate the magnitude of the effect in comparison to the effects of a simple atomic disorder in solid solution alloys.

1. Experiments on dilute alloys

The most definitive experiment performed was the observation of the influence of various rare earth solutes on the residual resistivity of dilute alloys of lutetium. This experiment was of interest in two respects; defining the spin dependence of the s-f interaction and evaluating the exchange integral.

Although several theories have shown that the spin dependence of s-f interactions should vary as $(g-1)^2J(J+1)$, experimental verification of this prediction was lacking. Slight differences in the electronic structure of the conduction band and the magnetic ordering structure lead to scatter in the results when one attempts to compare the data for the rare earth series to a $(g-1)^2J(J+1)$ relation. The scatter in the results of the superconducting transition temperature experiments is more difficult to explain; perhaps

a mixture of the allotropic modifications of lanthanum was present in the samples. A comparison of the results from these experiments with the de Gennes relation is shown in Figure 28, while the data from the present experiment is compared with both the S(S+1) and the de Gennes relation in Figure 29. The advantage of examining a system where the effect of the s-f interaction can be observed without grossly perturbing the electronic structure of the system is immediately obvious.

T. Kasuya (1959) in his study of the effects of exchange interactions on the transport properties of metals and alloys predicted that the increase in resistivity in a dilute alloy above that of the solvent metal should be described by the expression

$$\rho = \frac{3}{2\hbar}\frac{\pi m}{\zeta}\frac{N_i}{N^2e^2}\left\{A^2(0) + (g-1)^2\, j(j+1)\, J^2(0)\right\}$$

where ζ is the Fermi energy, N_i/N the mole fraction of the solute, $\hbar$ Planck's constant/2π, e the electronic charge of the electron, m the electron mass, $A^2(0)$ a constant representing all interactions other than the exchange interactions $J^2(0)$, j the total angular momentum quantum number, and g the Lande g factor. A plot of the increase in resistivity for one atom percent solute over that of the

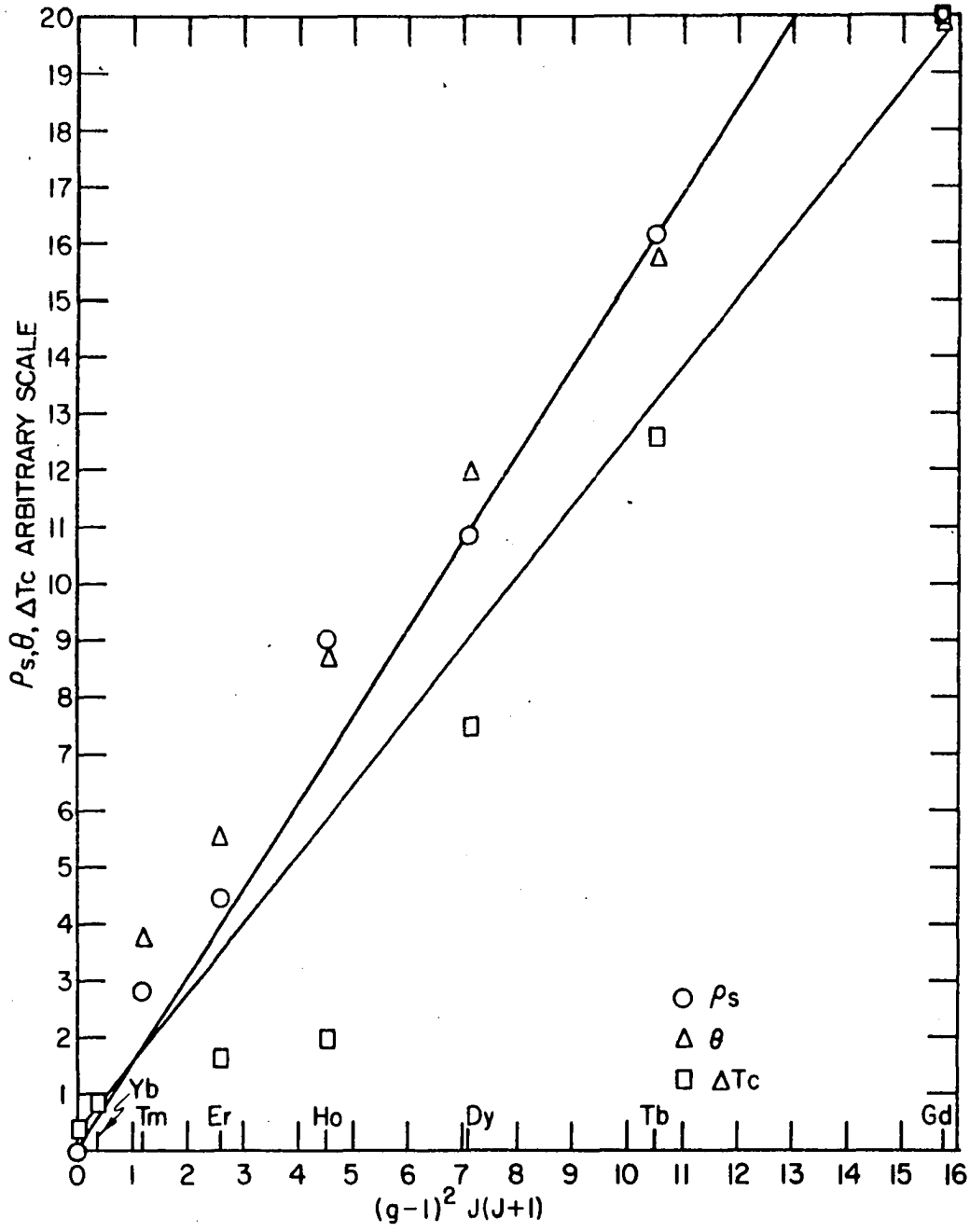

Figure 28. Previous attempts to show the spin dependence of the s-f interaction from the spin disorder resistivity, ρ_s; paramagnetic Curie temperature θ_p; and the lowering of the superconducting transition temperature of lanthanum alloys, ΔT_c

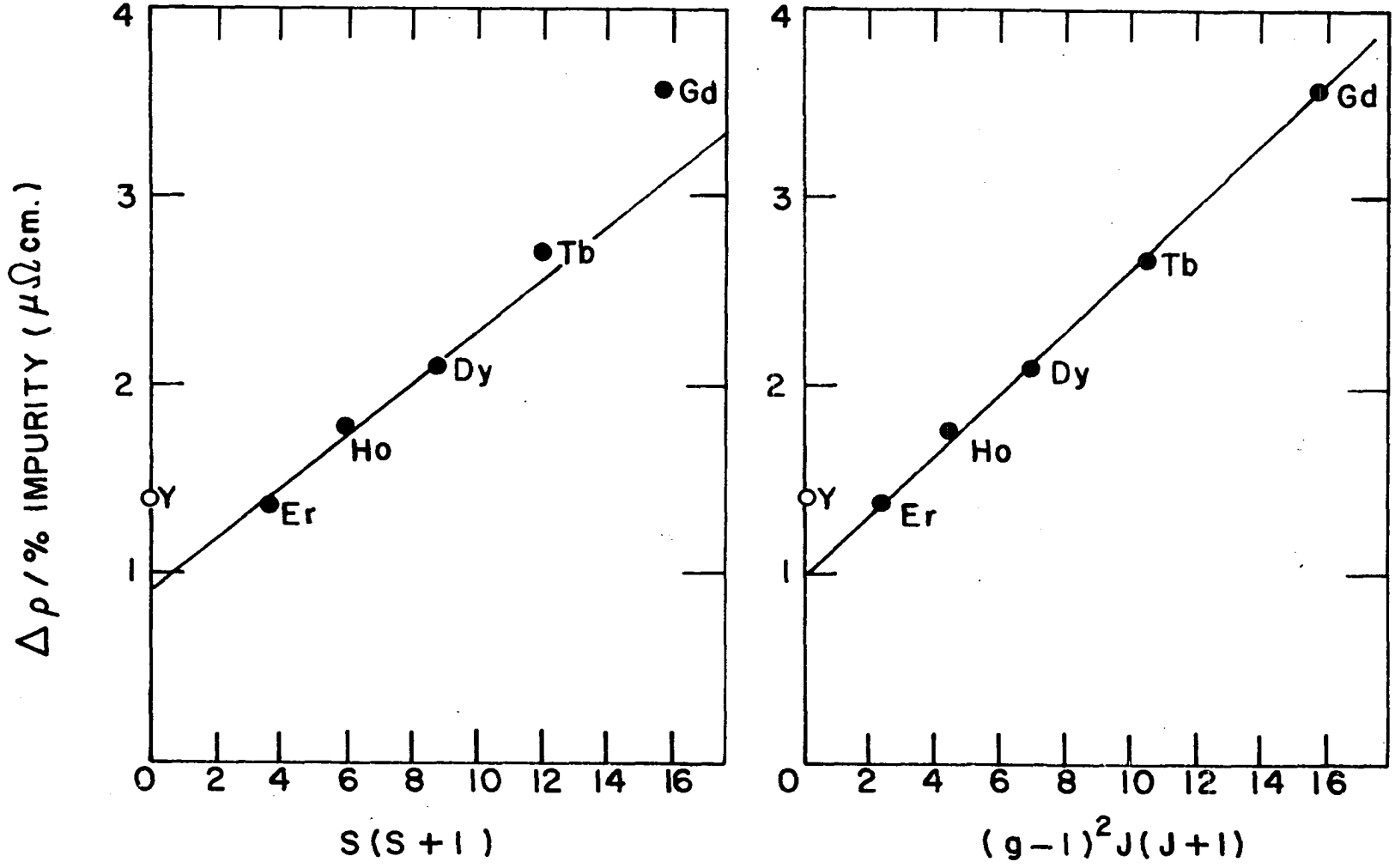

Figure 29. Determination of the spin dependence of the s-f interaction from the dilute alloy experiments

lutetium solvent vs. $(g-1)^2\ J)J+1)$ is shown in Figure 29. The intercept of the line with the resistivity axis gives $A^2(0)$, and $J^2(0)$ can be evaluated from the slope of the line.

An estimate of the Fermi energy at $0^oK.$ can be obtained from free electron theory as shown by A. J. Dekker (1958) from the relation,

$$E_F = \frac{h^2}{2m} \left(\frac{3n}{8\pi}\right)^{2/3} ,$$

where n is the number of free electrons per unit volume, m the electron mass, and h the Planck constant. Assuming lutetium has three free electrons, one finds a Fermi energy of 7.87 ev. Substitution of E_F for ζ in Kasuya's equation gives a value of 1.12 ev. for A(0) and .45 ev. for the exchange integral J(0). If one considers the ratio of $(g-1)^2\ j(j+1)\ J^2(0)/A^2(0)$ for gadolinium, a ratio of about 2.5/1 is obtained, indicating the magnitude of the s-f interaction in comparison to the coulombic interactions.

A similar equation for the spin disorder resistivity evaluated at its constant value above the ordering temperature,

$$\rho_s = 3/2 \frac{\pi m}{\hbar \zeta} \frac{1}{Ne^2} \left\{(g-1)^2\ j(j+1)\ J^2(0)\right\}$$

yields a value of 0.32 ev. for the exchange integral. The

slightly higher value observed for the dilute alloy experiments may be related to the fact that magnetic measurements of alloys invariably yield a higher magnetic moment per magnetic atom than in the pure metal. This has been attributed to a polarization of the conduction electrons by the magnetic ions, cf. L. F. Bates and M. M. Newmann (1958) and W. C. Thoburn *et al.* (1958).

It is of interest to examine these results for dilute rare earth alloys in relation to the existing concepts of the resistivity behavior of dilute alloys, cf. J. M. Ziman (1960a). Linde's rule states that $\rho = a + b Z^2$, where ρ is the increase of resistivity due to alloying, a is a constant varying with the row in the periodic table, b is another constant varying with the column in the table, and Z is the difference in valence between solute and solvent. Most studies of this type have been on transition metals using one of the noble metals as a solvent. Linde's rule is found to be valid for elements to the right of the noble metals but shows deviations to the left of the noble metals in the periodic table where there is uncertainty as to the valence of the various transition metals. For a series such as the heavy rare earths from Gd to Lu, Linde's rule would predict that each member of the series would increase the resistivity by the same amount, the $A^2(0)$ term in Kasuya's equation. The dependence of the constant "a" upon the row in the periodic

table is shown in this experiment by the fact that the point for yttrium in Figure 29 falls above the intercept of the line through the other points. Linde's rule makes no provision for the additional contribution to the resistivity from the s-f interactions for the rare earth series, and a similar s-d interaction should explain the anomalous values for some of the transition metal experiments, especially for manganese.

2. Variation of resistivity and ordering temperature with composition

The variation of the residual resistivity with composition in concentrated alloys was observed to follow Nordheim's rule quite well, thus justifying the assumptions that the sizes, crystal structure and electronic structure are similar for both components of the systems examined. The small deviations from symmetry observed (a shift of the maximum in the Gd-Er system by 5%) are attributed to subtle differences in the electronic structure of Gd and Er. This effect can also be seen from the differences in the temperature coefficients of resistivity.

The residual resistivity of the alloys studied in this investigation differed from the type for which Nordheim's rule was formulated, in that the composition dependent part of the residual resistivity was composed of two parts, ρ_{AE} and ρ_{AS}, the electrostatic deviations in the alloy and the

"magnetic spin" deviations. Since the sum of the two contributions is observed to follow a parabolic curve, and the conditions for ρ_{AE} to follow Nordheim's rule are better satisfied than in most solid solution alloys to which it has been applied, it would appear that the assumption of a similar behavior of ρ_{AS} is warranted. The conditions under which the parabolic behavior is followed, however, is limited to the low temperature region, for deviations begin to appear when the effects of ρ_s become measurable.

The variation of the highest magnetic ordering temperature (magnetic-paramagnetic) has been shown to vary approximately linearly with composition in the alloy systems in Figure 26. This behavior is similar to that observed by W. C. Thoburn et al. (1958) in their study of the magnetic properties of the Gd-Y system. The rather abrupt change from positive deviations from a linear behavior to negative deviations across the Gd-Er system is indicative of a change from ferromagnetic to antiferromagnetic ordering at about 50% composition.

Thoburn's results showed an interesting variation of the magnetic properties with composition which closely paralleled the change of magnetic properties across the rare earth series from Gd to Lu. This suggested the possibility that the type of magnetic ordering, the magnitude of the spin disorder resistivity, and the ordering temperature were

determined by S (or an average S for alloys), rather than being characteristic properties of a given metal. As many alloys as possible were made up with average spins corresponding to 20% Gd-Lu, 40% Gd-Lu, 57% Gd-Lu (also the spin of Ho), and 80% Gd-Lu so that a comparison of these properties could be made for alloys of the same average spin. It has since become evident that spin-orbit coupling must be taken into account and the actual spin dependence is determined by $(g-1)^2 J(J+1)$, so a direct comparison between these alloys was not possible.

This investigation has shown that although both the ordering temperature and spin disorder resistivity indicate the magnitude of the s-f interaction, both are affected by small differences in the metals which cause deviations from the predicted correlation with the de Gennes relation, and these differences do not affect them in the same way. An illustration of this point is shown in Figure 30 where θ, the highest ordering temperature, is plotted against ρ_s, the spin disorder resistivity, for the values of these quantities for the heavy rare earth metals. The values of ρ_s determined for the alloys, and the values for the metals, are shown in Figure 31 as a function of $(g-1)^2 J(J+1)$. The agreement for the alloys is seen to be about the same as for the metals except for Gd and the Gd-Lu alloys. H. E. Nigh has recently compared the results of studies of the resistivity of single

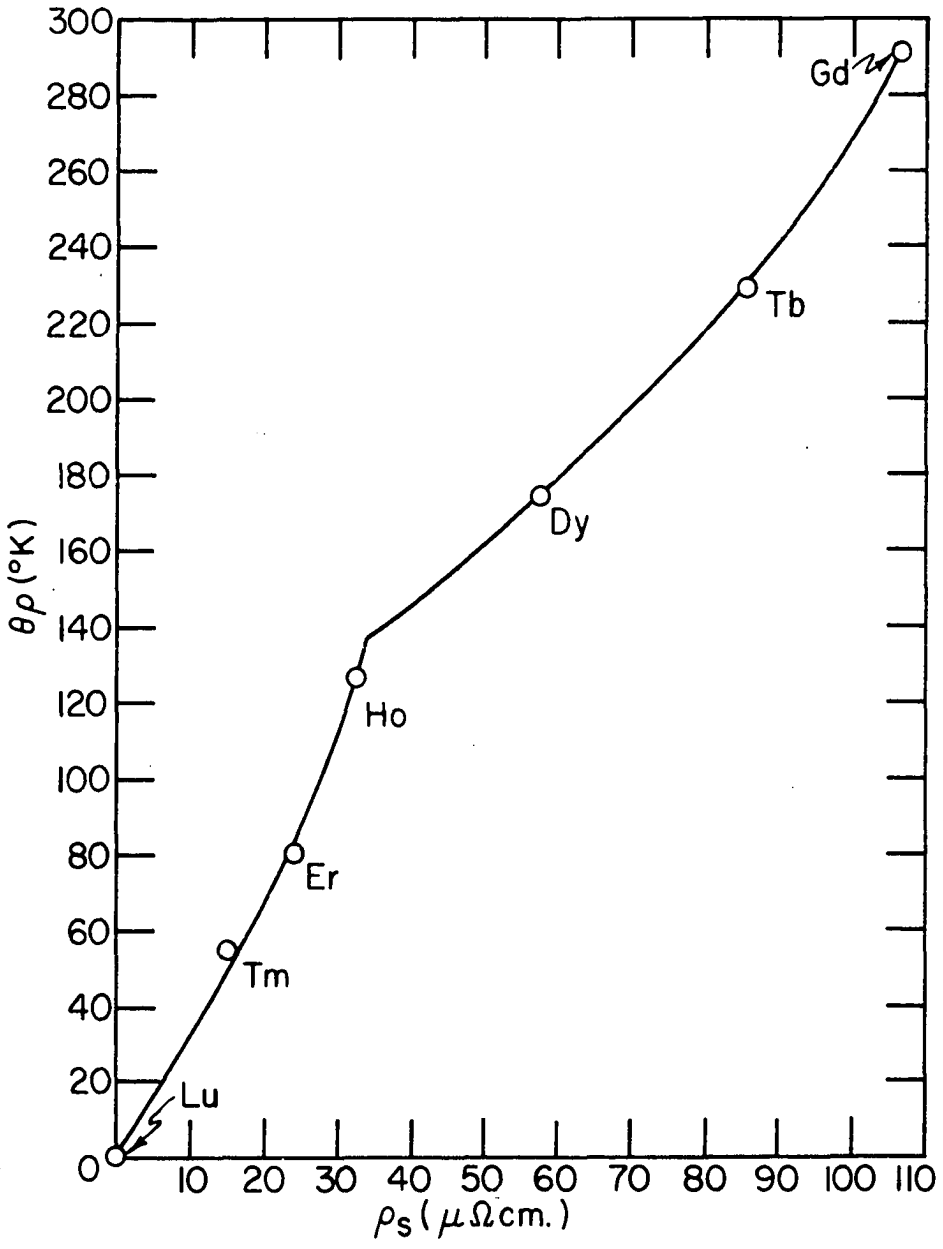

Figure 30. Paramagnetic Curie temperature vs. spin disorder resistivity for the metals Gd to Lu

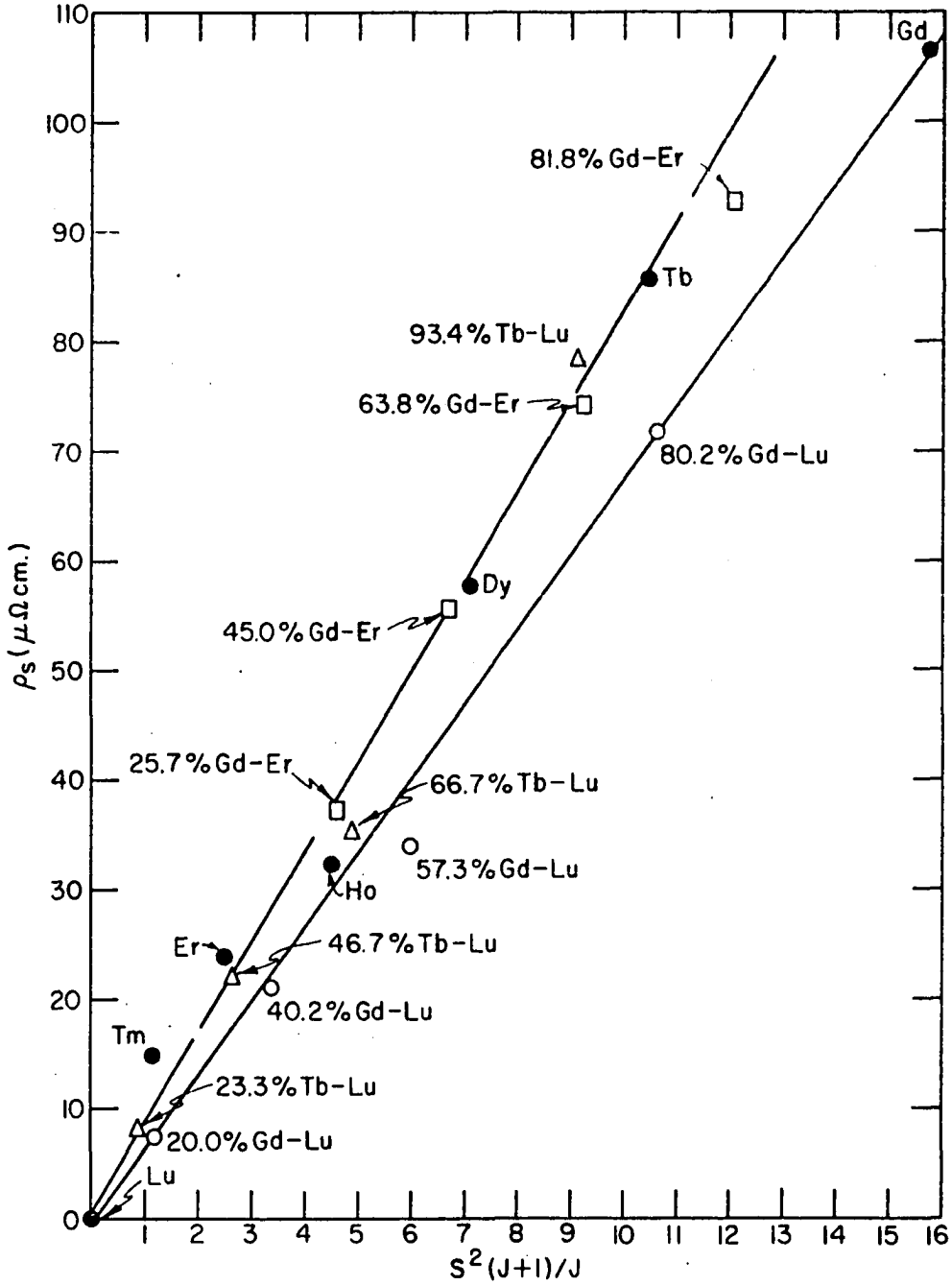

Figure 31. Spin disorder resistivities for the alloys and pure metals as a function of average values of $S^2(J+1)/J$ (the equivalent of $(g-1)^2 J(J+1)$ for the heavy rare earths)

crystals with the de Gennes relation* and finds that an evaluation of ρ_s from the "a" axis data fits a straight line except for gadolinium.

There are several possible explanations why the point for gadolinium is less than the expected value. B. R. Coles (1958) pointed out the similarity between the ρ_s curve and the magnetic entropy curve for erbium; both rise sharply to the upper magnetic ordering temperature and then level off when the magnetic disorder is complete. M. Griffel et al. (1954) observed that the magnetic entropy of gadolinium did not attain its theoretical value of $S_{mag} = R \ln(2J+1)$ at 355°K. Such behavior is indicative of the existence of short range order above the Curie temperature. Since the resistivity measurements covered approximately the same temperature range, the low values of ρ_s might arise from the same source. However, the ρ_s values for the Gd-Lu alloys are also observed to be less than expected, and measurements on them were made well above the Curie temperatures. Another obvious difference between gadolinium and the other heavy rare earths is the ferromagnetic ordering at the upper transition temperature, and the absence of a ferromagnetic-

---

*Nigh, H. E., Physics Department, Iowa State University of Science and Technology, Ames, Iowa. Information concerning the agreement of the spin disorder resistivities of single crystals with the de Gennes relation. Private communication. 1961.

antiferromagnetic transition at lower temperatures.

There do not appear to be any changes in slope in the resistivity-temperature curves for the Gd-Lu alloys below the paramagnetic region. Such anomalies were observed in two Gd-Er alloys and one of the Tb-Lu alloys, and are believed to be caused by ferromagnetic-antiferromagnetic transitions similar to the type observed in the metals. In conclusion, there appears to be a definite correlation between the average spin of an alloy and its spin disorder resistivity, but the magnitude of the s-f interaction is influenced by several unknown factors which do not permit quantitative comparisons.

3. Temperature dependence of the resistivity and magnetic ordering

I. Mannari (1959), as well as several others, has considered the temperature dependence of the resistivity of ferromagnetic and antiferromagnetic rare earth metals using a spin wave model to describe the perturbations of the spins from a state of alignment at low temperatures. He concluded that a ferromagnetic metal should follow a T^2 temperature dependence for the spin disorder part of the resistivity. The determination of the temperature dependence of the total resistivity at low temperatures was shown in Figures 17 to 19. The results for Gd, Tb, Dy, Ho, and Er, which are ferromagnetic at low temperatures, were approximately T^3 in

their behavior, while Tm which is antiferromagnetic at low temperatures showed a $T^{4.5}$ behavior.

The total resistivity at low temperatures (less than about 20°K.) includes a contribution from thermal vibrations of the lattice which the Bloch-Grüneisen relation predicts should show a T^5 dependence. The total resistivity should then be of the form $\rho = aT^2 + bT^5$ for a ferromagnet, and $\rho = aT^4 + bT^5$ for an antiferromagnet. Thus a plot of ρ/T^2 vs. T^3 should give a straight line in the region where this relation holds for a ferromagnet, and ρ/T^4 vs. T should give a straight line for the antiferromagnetic case. The results of such plots are shown in Figure 32 for Gd, Tb and Dy and in Figure 33 for thulium. The results are seen to be in accord with theory over the range 10-20°K., although a comparison of the "a" constants is probably not meaningful because the estimate of the residual resistivity required to determine ρ is not sufficiently accurate. The results for Ho and Er are not shown because magnetic transitions in this temperature range limit the applicable data.

C. Behavior of Rare Earth Metals and Alloys in Comparison to Transition Metals and Alloys

The effects of the s-f interaction were shown to cause several effects unique to the rare earth elements in the

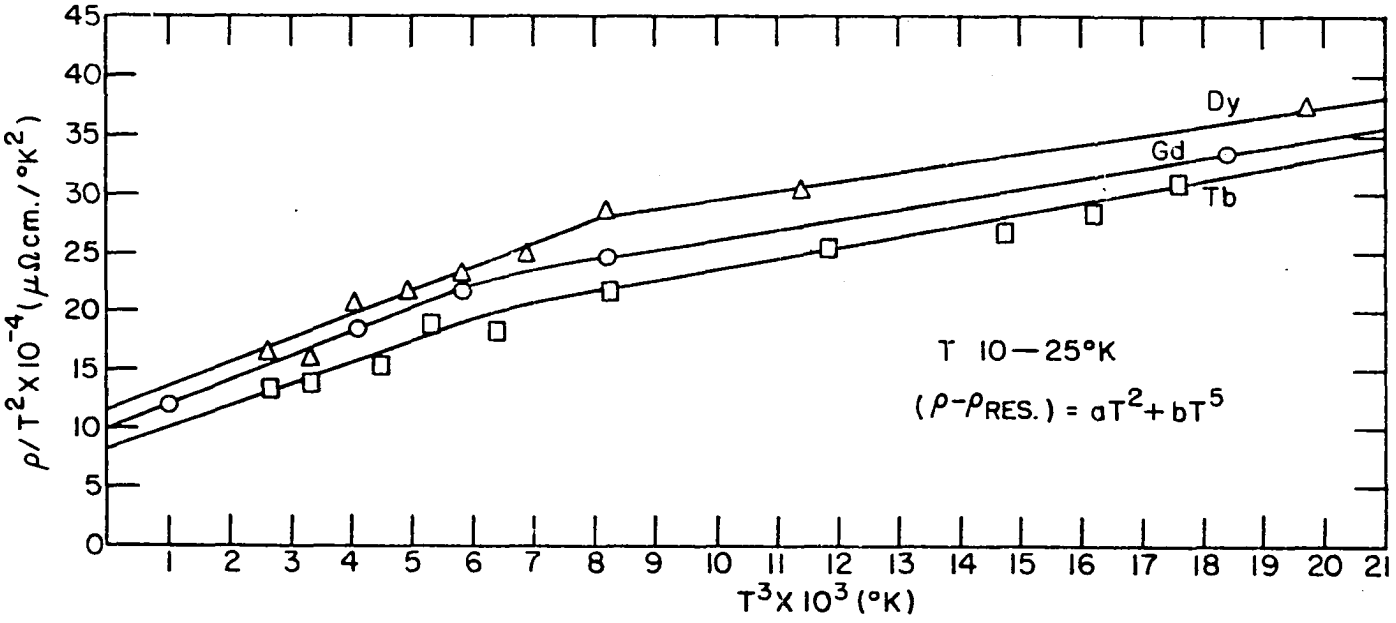

Figure 32. Graphical determination of the existence of a T^2 term in the resistivity of Gd, Tb and Dy in the ferromagnetic region

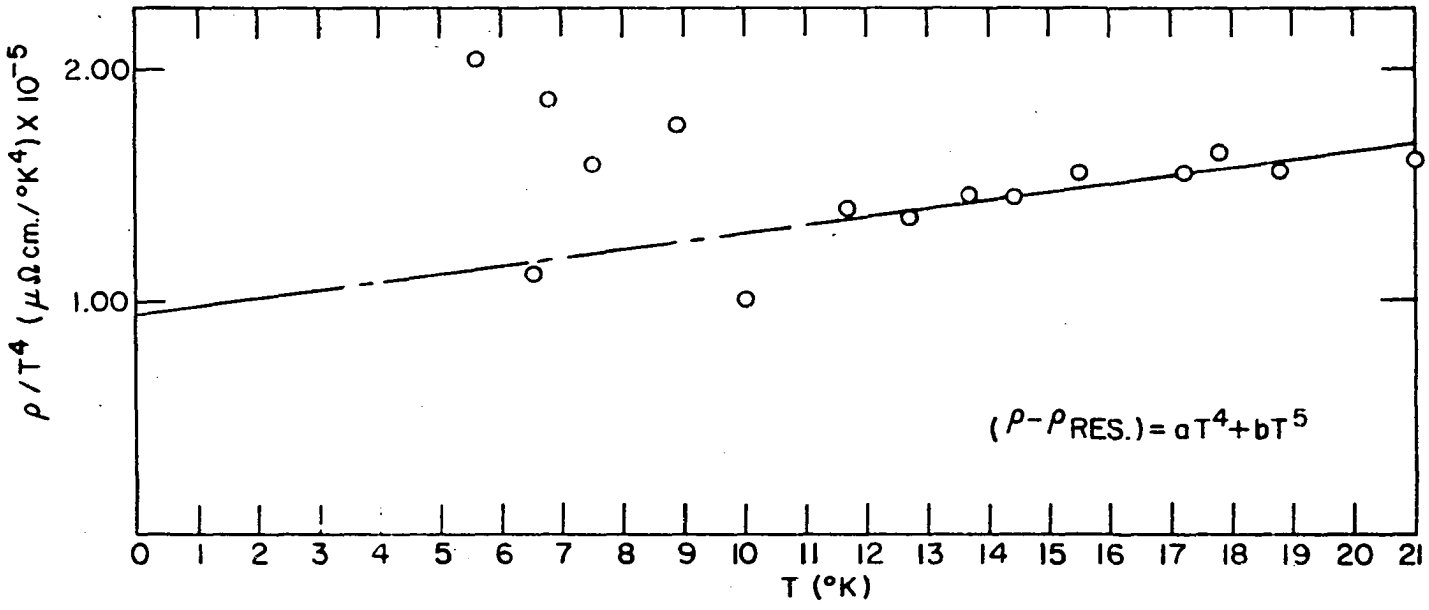

Figure 33. Graphical determination of the existence of a T^4 term in the resistivity of thulium in the antiferromagnetic region

preceding section, but the study of the rare earths is also of interest in regard to information they might contribute which would lead to a better understanding of the transition metals and the metallic state in general.

1. The proposal of Mott and Stevens

One such application is the proposal by Mott and Stevens discussed in Part IV. To summarize briefly, they proposed that the fundamental difference between the band model of a ferromagnet and the localized electron model should be reflected in the behavior of the resistivity in the neighborhood of the Curie temperature. Specifically, a comparison of the reduced resistivity - reduced temperature curves for a ferromagnetic metal, and an alloy of this metal with a paramagnetic metal of similar electronic structure, should yield superimposed curves for the localized electron model and diverging curves above the Curie temperature for the band model. The work of A. I. Schindler et al. (1956, 1957) on Ni and Ni-Pd alloys provides an example of the band model behavior. A confirmation of the predicted behavior for a localized electron model was provided in this work by a comparison of Gd and an 80% Gd-Lu alloy as shown in Figure 34. The slight deviation of the curves above the Curie temperature is attributed to small differences in the electronic structure of Gd and Lu.

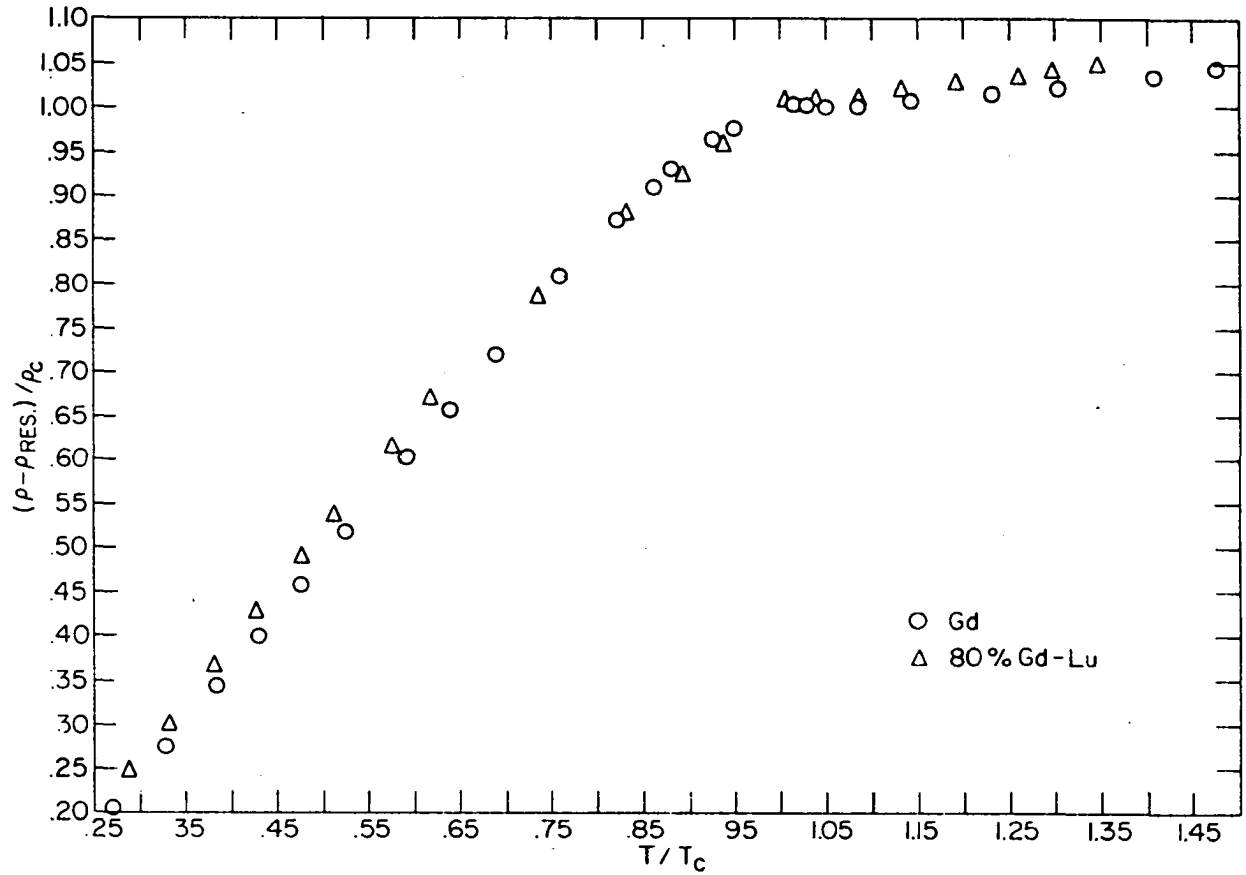

Figure 34. Test of Mott and Stevens proposal for a magnetic metal with localized electrons in an unfilled shell

2. The Ziman R parameter

J. M. Ziman (1960a, 1960b, 1961) has been active in furthering the use of the "ordinary" transport properties (electrical conductivity, thermal conductivity, thermoelectric power, and Hall coefficient) in interpreting the electronic structure of metals. Admittedly, these properties are not capable of resolving the intricate geometry of the Fermi surface, as are the De Haas - van Alphen effect, cyclotron resonance, anomalous skin effect, etc. However, they are capable of showing some of the major effects of the Fermi surface, and can be observed under more easily obtainable conditions of temperature, magnetic fields and sample purity as well as on alloys. For these reasons Ziman advocates a comprehensive study of the transport properties to better define the complicated interactions between electrons, phonons, and imperfections which govern the transport properties. The lack of a complete understanding of these processes at present limits the quantitative interpretation of the transport properties to the alkali metals at best.

To utilize the store of knowledge accumulated on the electrical properties of metals Ziman relates a parameter R to the area of the Fermi surface. This parameter is basically the inverse of the $\sigma/M\theta^2$ parameter suggested by Mott and Jones, but has been modified to relate more directly

to the area of the Fermi surface; the derivation of the equations is shown by J. M. Ziman (1960a). The final result gives

$$R = \frac{5.04\ e^2\ M\ k\theta^2 \rho}{\pi^3\ \hbar^3\ N_o\ D\ T} = 8.125 \times 10^9 \left[\frac{M\theta\ \rho}{D\ T}\right]$$

where e is the charge of an electron, M the molecular weight, k the Boltzmann constant, θ the Debye temperature, ρ the resistivity from phonon scattering, $\hbar$ the Planck constant/2π, T the temperature, N_o Avagadroes number, and D the Debye radius given by $(6\pi^2 N)^{1/3} = 3.90\ N^{1/3}$ where N is the number of atoms per unit volume (density$\cdot N_o/M$). The values of R shown in Table 11 are those given by Ziman with the following exceptions: Mn, which was corrected for a spin disorder of 112 micro ohm-cm; V, Re, and Hf for which G. K. White and S. B. Woods (1958) give data for purer samples; and the rare earths which were calculated from the data of R. V. Colvin et al. (1960), J. K. Alstad et al. (1961a, 1961b) and M. A. Curry et al. (1960). The resistivities for the rare earths were evaluated at 300°K. after correction for residual resistivity and spin disorder resistivities. The values of θ_D used were taken from the compilation by K. A. Gschneidner (1961) except for scandium which was estimated with the Lindemann melting point formula $\theta_D = B\ T_M^{\frac{1}{2}}\ A^{-5/6}\ D_o^{1/3}$ where B is an empirical constant equal to 120, T_M is the melting

Table 11. Values of the parameter R for the metals

Group I		Group II		Group III		Group IV		Group V	
Li	1.63	Be	3.76	Al	1.98	Sn	7.12	As	21.1
Na	1.04	Mg	2.36			Pb	7.12	Sb	38.0
K	2.08	Ca	2.30	Ga	3.12			Bi	82.0
Rb	1.61	Sr	11.3	In	4.26				
Cs	2.78	Ba	27.0	Tl	5.76				
Cu	1.67	Zn	3.94						
Ag	1.59	Cd	4.42						
Au	2.73	Hg	7.66						

Transition metals

Ti	31.1	Zr	58.3	Hf	48.7
V	28.3	Nb	27.6	Ta	28.1
Cr	22.8	Mo	13.1	W	17.5
Mn	56.3	Tc	--	Re	47.8
Fe	18.3	Ru	23.0	Os	19.7
Co	10.6	Rh	11.4	Ir	17.2
Ni	11.4	Pd	15.4	Pt	20.0

Rare earth metals

Sc	52	Sm	37.4	Er	55.1
Y	53.6	Eu	14	Tm	49.8
La	30.9	Gd	21.0	Yb	9.6
Ce	36.2	Tb	21.0	Lu	54.8
Pr	23.6	Dy	27.7		
Nd	24.8	Ho	39.2		

point, A the atomic weight, and D the density; the value obtained for scandium was 308°K. A check of the accuracy of this method of estimating θ_D is indicated by the value of 201°K. obtained for yttrium compared to the value of 218°K.

from specific heat measurements.

The periodic nature of the R parameter is apparent in Figure 35. Variations within the rare earth group are rather larger than one might expect, but as will be shown later, for large values of R, the parameter is very sensitive to slight variations in the electronic structure. The divalence of Eu and Yb gives lower values of R than the trivalent metals and the effect of crystal structure on the Ce and Sm values is also noticeable. The large variation within the heavy rare earth group is not so easily explained, but it does faithfully reproduce the observed differences in the temperature coefficient of resistivity in the paramagnetic region (R is easily seen to be proportional to $d\rho/dT$). There is a correlation between R and the c/a ratio, for R increases as c/a decreases from Gd to Er, and then R decreases as c/a increases for thulium. Lutetium, however, does not follow this trend. The above interpretation is dependent upon the validity of the assumption that the c/a ratio affects the number of electrons overlapping the zone boundary in the c direction.

The free electron model provides a good approximation to the behavior of the alkali metals and noble metals. A. V. Gold (1958), for example, showed that the free electron model qualitatively explained the De Haas - van Alphen data for lead. The parameter R is also based upon a free electron

Figure 35. Ziman R parameter for the metallic elements

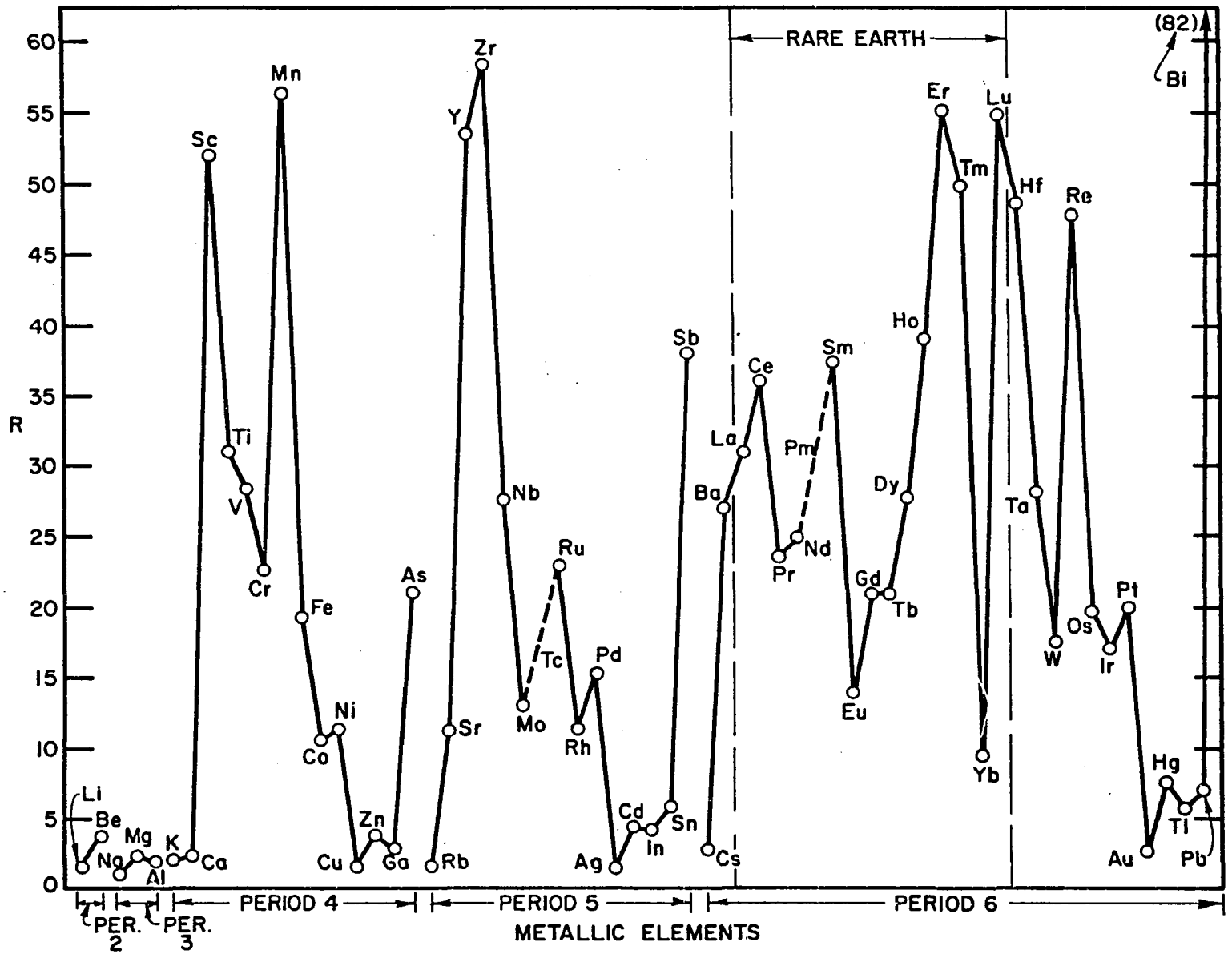
R
60
55
50
45
40
35
30
25
20
15
10
5
0
RARE EARTH
(82)
Bi
Li
Be
Na
Mg
Al
K
Ca
Sc
Ti
V
Cr
Mn
Fe
Co
Ni
Cu
Zn
Ga
As
Rb
Sr
Y
Zr
Nb
Mo
Tc
Ru
Rh
Pd
Ag
Cd
In
Sn
Sb
Cs
Ba
La
Ce
Pr
Nd
Pm
Sm
Eu
Gd
Tb
Dy
Ho
Er
Tm
Yb
Lu
Hf
Ta
W
Re
Os
Ir
Pt
Au
Hg
Tl
Pb
PERIOD 4
PERIOD 5
PERIOD 6
PER. 2
PER. 3
METALLIC ELEMENTS

model and is proportional to the quantity $N_a^{2/3}\ (S_{free}/S)^2$, where N_a is the number of conduction electrons per atom, S is the area of the Fermi surface, and S_{free} is the area of a spherical Fermi surface calculated from the free electron model ($S_{free} = 1.205 \times 10^2\ n^{2/3}$ where n is the number of conduction electrons per unit volume). The equality of the relation holds quite well for the third period elements Na, Mg, and Al, but deviations grow increasingly greater as one considers higher or lower periods. J. M. Ziman (1960b) has shown that the deviations in the group IA and IB elements are related to the anisotropies of the Fermi surface which have been directly observed in Fermi surface measurements on these elements. Anisotropy of the Fermi surface reduces the electron velocity in certain directions which decreases the conductivity, increases the effective potential for scattering by phonons, and also increases the scattering contribution from "umklapp" processes. Another factor which would decrease the Fermi surface area (or increase R) is the reduction of area when the Fermi surface touches the Brillouin zone boundary, since Fermi surface areas touching a zone boundary do not contribute to conduction.

Considering the above factors which affect the interpretation of the results, it is obvious that the following tabulation of the ratio S/S_{free} and the corresponding values of the effective number of carriers,

$N_{eff.}$, must be regarded only as a qualitative interpretation. In defense of the calculations, it would seem that any deviations would affect the rare earths in the same way and differences among the members of the series certainly reflect facts which must be explained in any future theories. In addition, a proportionality constant can be added to the R equation after the Fermi surface of one of the members has been studied, which should allow one to predict the behavior of the remainder of the series.

A perusal of the table shows that although there are large differences in the parameter R, these actually correspond to rather small differences in the Fermi surface area and effective number of carriers. The sensitivity of the electrical properties of the rare earth metals to impurity content is also easily explained on the basis of these calculations.

An independent check of the validity of these speculations is afforded by the measurements of the electronic specific heats of La, Y and Lu by L. D. Jennings et al. (1960). The value of this quantity for lutetium was found to be 95×10^{-4} joules/mole deg.^{2}. This can be used to find the density of states,

$$N(E_F) = 3\gamma/\pi^2 k^2 V_A = 1.592 \times 10^{31}\ \gamma/V_A \quad ,$$

where γ is the electronic specific heat, k the Boltzmann

Table 12. Electronic structure parameters for rare earth metals

Element	Crystal structure	R	S/S_{free}	$N_{eff.}$
La	hex.	30.9	.259	.40
Ce	fcc	36.2	.239	.35
Pr	hex.	23.6	.297	.49
Nd	hex.	24.8	.289	.47
Sm	rhomb.	37.4	.235	.34
Eu	bcc	14	.34	.4
Gd	hcp.	21.0	.314	.53
Tb	hcp.	21.0	.314	.53
Dy	hcp.	27.7	.274	.43
Ho	hcp.	39.2	.230	.33
Er	hcp.	55.1	.194	.26
Tm	hcp.	49.8	.204	.28
Yb	fcc	9.6	.407	.52
Lu	hcp.	54.8	.195	.26
Y	hcp.	53.6	.197	.26
Ca*	fcc	2.30	.83	1.52
Al*	fcc	1.98	1.01	3.04

*Included as examples of metals with valences similar to one or more of the rare earths.

constant, and V_A the atomic volume. A comparison with the $N(E_F)$ calculated from a free electron model,

$$N(E_F) = 2.55 \times 10^{26} n^{1/3}$$

where n is the number of conduction electrons per unit volume, gives the effective mass parameter, or an effective number of carriers. The calculations for lutetium give:

$$\frac{N(E_F)_\gamma}{N(E_F)_{calc.}} = \frac{85.2 \times 10^{33}}{12.5 \times 10^{33}} = \frac{m^*}{m} = 6.8 = \frac{3}{N_{eff.}}$$

$$N_{eff.} = .44$$

This gives agreement with the .26 carrier obtained from conductivity data which is really quite good considering the assumptions used in the calculations. Corresponding calculations for La and Y yield values of $N_{eff.}$ of .47 and .51 respectively.

3. Temperature dependence of resistivity at low temperatures

While the resistivities of most metals follow a linear temperature dependence for temperatures greater than the Debye temperature, in accordance with the predictions of the Bloch-Grüneisen relation, the low temperature behavior shows much more variation from the predicted T^5 behavior. This is especially true of the transition elements, as shown by the excellent work of G. K. White and S. B. Woods (1959), who found temperature dependences ranging from T^2 to T^5 for various elements of the transition series as shown in Table 13. They pointed out that there is an apparent correlation between a T^2 temperature dependence, attributed to electron-electron interactions, and large values of the electronic specific heat.

The temperature dependence of the rare earth metals Y,

Table 13. Exponent of T in low temperature resistivities of transition metals

Period 4		Period 5		Period 6	
Element	n	Element	n	Element	n
Ti	5.3 (15°K)[a]	Zr	4.5 (13°K)[a]	Hf	4.7 (10°K)[a]
V	3.4 (12°K)	Nb	2.7 (12°K)	Ta	3.8 (8°K)
Cr	3.2 (15°K)	Mo	5.1 (20°K)	W	4.0 (20°K)
Mn	2.0	Tc	--- ---	Re	4.6 (10°K)
Fe	3.3 (20°K)	Ru	4.7 (25°K)	Os	4.7 (25°K)
Co	3.3 (15°K)	Rh	4.6 (20°K)	Ir	4.7 (12°K)
Ni	3.1 (15°K)	Pd	3.2 (10°K)	Pt	3.7 (10°K)
Cu	5.1 (10°K)	Ag	4.7 (10°K)	Au	5.1 (10°K)

[a]The number in parentheses indicates the lowest temperature at which the exponent n is observed.

Lu, and Yb should yield additional information about the low temperature conductivity for the elements at the beginning of the transition series. As previously discussed, the part of the resistivity due to thermal vibrations is only part of the total resistivity for those metals which exhibit magnetic ordering at low temperatures. The results of the temperature dependence determinations for Lu, Y, and Yb were shown to be $T^{2.6}$, $T^{3.1}$, and $T^{2.0}$ respectively, which is characteristic of transition metal behavior and indicative of a possible electron-electron interaction such as suggested by White and Woods. The total resistivity for such behavior would be composed of two terms, $\rho = a' T^2 + bT^5$. This is similar to the formula for the ferromagnetic metals but the constant

"a'" should be smaller than the "a" in that equation. A plot of this equation for Y and Lu is shown in Figure 36. The results are somewhat surprising in that the intercept for the lutetium data indicates a T^2 contribution of the same magnitude as that found for the ferromagnetic metals and a rather small T^5 contribution for both yttrium and lutetium. As previously emphasized however, the "a" constant is very sensitive to the value chosen for the residual resistivity and might easily be in error by 5 units. The yttrium data is more consistent with the expected behavior in the range 10-20°K. and in addition has more points in the temperature range of interest. The low temperature "tail" below 10°K. is highly unusual and if it is real would indicate a minimum in the bT^5 part of the resistivity.

Ytterbium is unusual, in that it shows a T^2 dependence over a wide temperature range. Unfortunately no data were found for the low temperature dependence of other divalent metals, such as Ca, Sr, or Ba, so it was not possible to determine if this type of behavior is characteristic of a divalent metal.

D. Suggestions for Further Work

There are several interesting problems which this study has suggested, ranging from some aspects of alloying theory

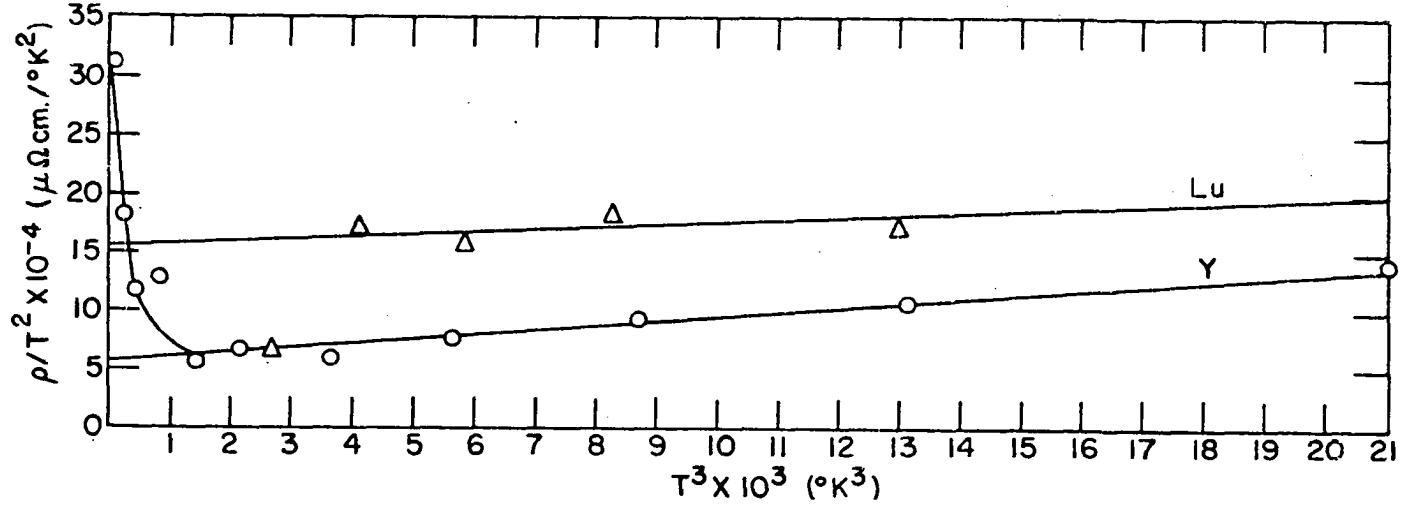

Figure 36. Graphical determination of the existence of a T^2 term in the low temperature resistivity of yttrium and lutetium

to a better understanding of the conduction processes in metals. Several alloy systems might profitably be studied by the techniques used in this investigation. The intermediate phase found in binary systems between light and heavy rare earths has been found to form at a characteristic c/a ratio intermediate to the two sub-groups. The sensitivity of the conductivity to the change in c/a ratio in the heavy rare earth group indicates that this would be a useful tool in investigating this phase. Another alloy system of interest is the Sc-Zr system between a trivalent and quadrivalent metal. The deviations from Nordheim's rule in this system should be pronounced and such a study might also provide information about how the electronic structure changes at the beginning of the transition series.

The study of dilute alloys using light rare earth elements for solutes might also be examined to determine the validity of de Gennes relation for these elements. Another phase of dilute alloys which might be investigated is the existence of magnetic ordering at low temperatures. R. A. Hein et al. (1959), for example, found dilute alloys of gadolinium disolved in lanthanum to have Curie temperatures ranging from 1°K. for 1 atom percent gadolinium to 3°K. for 5 atom percent gadolinium. Still another aspect of dilute alloys of interest is the possibility of the

existence of giant thermopowers in dilute rare earth alloys similar to those found in dilute alloys of iron dissolved in copper.

VII. SUMMARY

The examination of the electrical resistivity at low temperatures in several rare earth solid solution alloy systems has led to a better understanding of the conduction processes in rare earth metals and alloys. As the first such investigation on rare earth alloys it has yielded information about the variation of the resistivity with composition; information which is enhanced in value if one regards the behavior of these systems to be characteristic of the localized electron model of a magnetic metal. The properties of such metals are known to be influenced by the s-f exchange interaction and hence the characterization of the change of these properties with dilution of the magnetic metal was of interest. The electrical resistivity was admittedly a complex property to examine and interpret because of the many factors which influence it, but the use of metals with similar electronic structures and lattices permitted one to effect a more meaningful separation of these factors than is often possible.

In addition to the benefits cited above, which were largely envisioned before the investigation was begun, a different manifestation of the s-f exchange interaction was observed as an additional contribution to the residual resistivity of the magnetic alloys. This effect was

attributed to the random distribution of magnetic atoms in the alloy lattice and the attendent introduction of an additional scattering mechanism. The spin dependence of this effect was characterized in a series of dilute alloys of lutetium which provided the first experimental confirmation of the predicted spin dependence for the s-f exchange interaction. The exchange integral was evaluated using an estimate of the Fermi energy calculated from a free electron model, and was found to be 0.45 ev.

A qualitative comparison of the "normal" temperature dependent portion of the resistivities of the heavy rare earth metals (after correction for the spin disorder scattering, imperfection scattering, and differences in elastic constants) showed a correlation with the c/a ratio of the metals, and yielded a value of approximately 0.5 effective carriers per atom; a value which compares favorably with the observed electronic specific heat data and the free electron model of the Fermi surface proposed for the rare earths.

VIII. BIBLIOGRAPHY

Adcock, F. 1931. Iron and Steel Inst. (London) 124, 99.

Adenstedt, H. K., J. R. Pequinot, and J. M. Raymer. 1952. Trans. Am. Soc. Metals 44, 990.

Alstad, J. K., R. V. Colvin, S. Legvold, and F. H. Spedding. 1961a. Phys. Rev. 121, 1637.

_____, _____, _____, and _____. 1961b. Phys. Rev. 123, 418.

Ames, S. L. and A. D. Mc Quillan. 1954. Acta Met. 2, 831.

Anderson, G. S. and S. Legvold. 1958. Phys. Rev. Letters 1, 521.

_____, _____, and F. H. Spedding. 1958a. Phys. Rev. 109, 243.

_____, _____, and _____. 1958b. Phys. Rev. 109, 1257.

Bates, L. F. and M. M. Newmann. 1958. Proc. Phys. Soc. (London) 72, 345.

_____ and R. D. Barnard. 1961a. Proc. Phys. Soc. (London) 77, 691.

_____ and _____. 1961b. Proc. Phys. Soc. (London) 78, 361.

Beckman, [Initial not given]. 1911. [Title not given]. Unpublished thesis. Upsala. (Original not available). Cited in Mott, N. F. and H. Jones. 1936. The Theory of the Properties of Metals and Alloys. p. 299. Dover Publications, Inc., New York, N. Y.

Blackman, M. 1955. "Specific Heat of Solids." In Flügge, S., ed. Encyclopedia of Physics. Vol. 7, Pt. 1. pp. 325-381. Springer-Verlag, Berlin.

Blatt, F. J. 1957. Phys. Rev. 108, 285.

Bloch, F. 1928. Z. Physik 52, 555.

Bloch, F. 1930. Z. Physik 59, 208.

Born, H. J., S. Legvold, and F. H. Spedding. 1961. J. Appl. Phys. 32, 2543.

Braun, K., R. Kieffer, and K. Sedlatschek. 1959. "Beitrag zur Technologies der Tantal-Wolfram Legierungen." In Benesovsky, F., ed. Plansee Proceedings, 3rd Plansee Seminar "De Re Metallica", Reutte/Tyrol, Austria, June 22-26, 1958. pp. 264-276. Metallwerk Plansee Ag., Reutte/Tyrol, Austria.

Bridgman, P. W. 1952. Proc. Am. Acad. Arts Sci. 81, 211.

_____. 1953. Proc. Am. Acad. Arts Sci. 82, 97.

_____. 1954. Proc. Am. Acad. Arts Sci. 83, 1.

_____. 1955. Proc. Am. Acad. Arts Sci. 84, 111.

Broniewski, W. and W. Pietrek. 1935. Compt. rend. 201, 206.

Brout, R. and H. Suhl. 1959. Phys. Rev. Letters 2, 387.

Carlson, O. N., J. A. Haefling, F. A. Schmidt, and F. H. Spedding. 1960. J. Electrochem. Soc. 107, 540.

Carter, F. E. 1928. Trans. Am. Inst. Mining, Met., Petrol. Engrs. 28, 759.

Chevenard, P. 1926. J. Inst. Metals 36, 39.

Cohen, M. H. and V. Heine. 1961. Phys. Rev. 122, 1821.

Coles, B. R. 1958. Advances in Phys. 7, 40.

_____. 1960. "Electrical and Magnetic Measurements on Alloys." In National Physical Laboratory, ed. Physical Chemistry of Metallic Solutions and Intermetallic Compounds, Symposium. Vol. 1, pp. 62-74. Chemical Publishing Co., Inc., New York, N. Y.

Colvin, R. V. 1958. "Electrical Resistivity of Tb, Ho, and Er." Unpublished M. S. Thesis. Library, Iowa State University of Science and Technology, Ames, Ia.

_____, S. Legvold, and F. H. Spedding. 1960. Phys. Rev. 120, 741.

Coulson, C. A. 1958. Valence. 2nd ed. Oxford University Press, London.

Curry, M. A., S. Legvold, and F. H. Spedding. 1960. Phys. Rev. 117, 953.

Daane, A. H., C. E. Habermann, and D. H. Dennison. ca. 1962. "Distillation of Rare Earth Metals." In Lundin, C. E. and J. F. Nachman, eds. Denver Research Institute, University of Denver, University Park, Denver, Colo. Proceedings of 2nd Rare Earth Conference, Glenwood Springs, Colo., Sept. 24-27, 1961. [Publisher unknown.]

Dean, R. S., J. R. Long, T. R. Graham, E. V. Potter, and E. T. Hayes. 1945. Trans. Am. Soc. Metals 34, 443.

De Boer, J. H. and P. Clausing. 1930. Physica 10, 267.

de Gennes, P. G. 1958. Compt. rend. 247, 1836.

_____ and J. Friedel. 1958. J. Phys. and Chem. Solids 4, 71.

Dekker, A. J. 1958. Solid State Physics. Prentice Hall, Inc., Englewood Cliffs, N. J.

Elliott, R. J. 1954. Phys. Rev. 94, 564.

_____. 1961. Phys. Rev. 124, 346.

Esch, V. and A. Schneider. 1944. Z. Electrochem. 50, 268.

Friedel, J. 1956. Can. J. Phys. 34, 1190.

Gebhardt, E. and W. Koster. 1940. Z. Metallk. 38, 262.

Geibel, W. 1911a. Z. anorg. allg. Chem. 70, 240.

_____. 1911b. Z. anorg. allg. Chem. 70, 242.

Gerritsen, A. N. 1956. "Metallic Conductivity; Experimental Part." In Flügge, S., ed. Encyclopedia of Physics. Vol. 19. pp. 137-226. Springer-Verlag, Berlin.

Gold, A. V. 1958. Phil. Trans. Roy. Soc. London 251A, 85.

Green, R. W., S. Legvold, and F. H. Spedding. 1961. Phys. Rev. 122, 827.

Griffel, M., R. E. Skochdopole, and F. H. Spedding. 1954. Phys. Rev. 93, 657.

Grube, G. and H. Kästner. 1936. Z. Electrochem. 42, 156.

Grüneisen, E. 1933. Ann. Phys. Ser. 5, 16, 530.

Gschneidner, K. A., Jr. 1961. Rare Earth Alloys. D. Van Nostrand Company, Inc., Princeton, N. J.

_____, R. R. McDonald, and R. O. Elliott. 1961. Phys. Rev. Letters 6, 218.

_____ and R. Smoluchowski. 1961. "Concerning the Valences of Ce Allotropes." Multilithed paper. Los Alamos Scientific Laboratory, Los Alamos, N. M.

Habermann, C. E. 1960. "The Purification of Yttrium Metal by Distillation." Unpublished M. S. Thesis. Library, Iowa State University of Science and Technology, Ames, Ia.

Hake, R. R., D. H. Leslie, and T. G. Berlincourt. 1961. J. Phys. Chem. Solids 20, 177.

Hall, P. M., S. Legvold, and F. H. Spedding. 1959a. Phys. Rev. 116, 1446.

_____, _____, and _____. 1959b. Phys. Rev. 117, 971.

Hansen, M. 1958. Constitution of Binary Alloys. 2nd ed. McGraw-Hill Book Co., Inc., New York, N. Y.

Hein, R. A., R. L. Falge, Jr., B. T. Matthias, and E. Corenzwit. 1959. Phys. Rev. Letters 2, 500.

Heisenberg, W. 1928. Z. Physik 49, 619.

James, N. R., S. Legvold, and F. H. Spedding. 1952. Phys. Rev. 88, 1092.

Jennings, L. D., R. E. Miller, and F. H. Spedding. 1960. J. Chem. Phys. 33, 1849.

Johansson, C. H. and J. O. Linde. 1927. Ann. Physik, Ser. 4, 82, 449.

_____ and _____. 1930. Ann. Physik, Ser. 5, 5, 762.

_____ and _____. 1936. Ann. Physik, Ser. 6, 25, 1.

Kasuya, T. 1956a. Progr. Theoret. Phys. (Kyoto) 16, 45.

_____. 1956b. Progr. Theoret. Phys. (Kyoto) 16, 58.

_____. 1959. Progr. Theoret. Phys. (Kyoto) 22, 227.

Kevane, C. J., S. Legvold, and F. H. Spedding. 1953. Phys. Rev. 91, 1372.

Klemens, P. G. 1956. "Thermal Conductivity of Solids at Low Temperatures." In Flügge, S., ed. Encyclopedia of Physics. Vol. 14, pp. 198-281. Springer-Verlag, Berlin.

Kurnakow, N. S. and A. J. Nikitinsky. 1914. Z. anorg. allg. Chem. 88, 151.

Legvold, S., F. H. Spedding, F. Barson, and J. F. Elliott. 1953. Rev. Mod. Phys. 25, 129.

Levitas, A. 1955. Phys. Rev. 99, 1810.

Linde, J. O. 1931. Ann. Physik, Ser. 5, 10, 52.

_____. 1932. Ann. Physik, Ser. 5, 15, 219.

_____. 1937. Ann. Physik, Ser. 6, 30, 151.

_____. 1958. Physica, Supplement, 24, S109.

Liu, S. H. 1961a. Phys. Rev. 121, 451.

_____. 1961b. Phys. Rev. 123, 470.

Lock, J. M. 1957. Phil. Mag., Ser. 8, 2, 726.

Mac Donald, D. K. C. 1956. "Electrical Conductivity of Metals and Alloys at Low Temperatures." In Flügge, S., ed. Encyclopedia of Physics. Vol. 14, pp. 137-197. Springer-Verlag, Berlin.

Mackintosh, A. R. ca. 1962. "The Electronic Structure of the Rare-Earth Metals." In Lundin, C. E., and J. F. Nachman, eds. Denver Research Institute, University of Denver, University Park, Denver, Colo. Proceedings of 2nd Rare Earth Conference, Glenwood Springs, Colo. Sept. 24-27, 1961. [Publisher unknown.]

Mannari, I. 1959. Progr. Theoret. Phys. (Kyoto) 22, 227.

Masumoto, H. 1927. Sci. Repts. Tohoku Univ. 16, 321.

Matthias, B. T., H. Suhl, and E. Corenzwit. 1958. Phys. Rev. Letters 1, 92.

Matthiessen, A. and C. Vogt. 1864. Ann. Physik, Ser. 2, 122, 19.

Mott, N. F. 1936. Proc. Cambridge Phil. Soc. 32, 281.

_____ and H. Jones. 1936. The Theory of the Properties of Metals and Alloys. Dover Publications, Inc., New York, N. Y.

_____ and K. W. H. Stevens. 1957. Phil Mag., Ser. 8, 2, 1364.

Nordheim, L. 1931. Ann. Physik, Ser. 5, 9, 607.

North American Philips Co., Inc. ca. 1948. "Tungsten, Molybdenum and Wire Products." (Original not available). Cited in Archer, R. S., J. Z. Briggs, and C. M. Loeb, Jr., eds. 1948. Molybdenum. p. 318. Climax Molybdenum Co., New York, N. Y.

Owen, J., M. Browne, W. D. Knight, and C. Kittel. 1956. Phys. Rev. 102, 1501.

Rinck, E. 1936. Compt. rend. 203, 255.

_____. 1937. Compt. rend. 205, 135.

Roberts, L. M. and J. M. Lock. 1957. Phil. Mag., Ser. 8, 2, 811.

Ruderman, M. A. and C. Kittel. 1954. Phys. Rev. 96, 99.

Savitskii, E. M. and V. F. Terekhova. 1958. Zhur. Neorg. Khim. 3, 756.

Schindler, A. I., R. J. Smith, and E. I. Salkovitz. 1956. J. Phys. Chem. Solids 1, 39.

_____, _____, and _____. 1957. Phys. Rev. 108, 921.

Schmitt, R. W. 1956. Phys. Rev. 103, 83.

Seiden, J. 1961a. Compt. rend. 252, 1922.

_____. 1961b. Compt. rend. 252, 3550.

_____ and M. Papoular. 1961. Compt. rend. 253, 812.

Sivertsen, J. M. and M. E. Nicholson. 1961. "The Structure and Properties of Solid Solutions." In Chalmers, B., ed. Progress in Materials Science, Vol. 9, pp. 305-389. Pergamon Press, New York, N. Y.

Slater, J. C. 1956. "Band Theory of Bonding in Metals." In American Society for Metals. Theory of Alloy Phases. pp. 1-12, American Society for Metals, Cleveland, Ohio.

Smidt, F. A. 1960. Information about the phase equilibria in the Yb-Ce and Yb-La alloy systems. (Unpublished research notebook No. FAS-2) United States Atomic Energy Commission, Ames Laboratory, Document Library, Ames, Ia.

Spedding, F. H. and A. H. Daane. 1954. J. Metals 6, 504.

_____, _____, and K. W. Herrmann. 1956. Acta Cryst. 9, 559.

_____, _____, and _____. 1957. J. Metals 9, 895.

_____, _____, G. Wakefield, and D. H. Dennison. 1960. Trans. Am. Inst. Mining, Met., Petrol. Engrs. 218, 608.

_____, J. J. Hanak, and A. H. Daane. 1958. Trans. Am. Inst. Mining, Met., Petrol. Engrs. 211, 239.

_____, _____, and _____. 1961. J. Less Common Metals 3, 110.

_____ and J. E. Powell. 1954. J. Metals 6, 1131.

Strandburg, D. L. 1961. "Electrical and Magnetic Properties of Holmium Single Crystals." Unpublished Ph. D. Thesis. Library, Iowa State University of Science and Technology, Ames, Ia.

Suhl, H. and B. T. Matthias. 1959. Phys. Rev. 114, 977.

Svensson, B. 1932. Ann. Physik, Ser. 5, 14, 699.

Thoburn, W. C., S. Legvold, and F. H. Spedding. 1958. Phys. Rev. 110, 1298.

Valentiner, S. and G. Becker. 1934. Z. Physik 93, 795.

Valetta, R. M. 1959. "Structures and Phase Equilibria of Binary Rare Earth Metal Systems." Unpublished Ph. D. Thesis. Library, Iowa State University of Science and Technology, Ames, Ia.

Weiss, R. J. and A. S. Marotta. 1959. J. Phys. Chem. Solids. 9, 302.

White, G. K. and S. B. Woods. 1959. Phil. Trans. Roy. Soc. London 251A, 35.

Wilson, A. H. 1936. The Theory of Metals. 1st ed. University Press, Cambridge.

Yosida, K. 1957. Phys. Rev. 107, 396.

Zener, C. 1951. Phys. Rev. 81, 440.

_____ and R. R. Heikes. 1953. Rev. Mod. Phys. 25, 191.

Ziman, J. M. 1960a. Electrons and Phonons. Oxford University Press, London.

_____. 1960b. "'Ordinary' Transport Properties and the Shape of the Fermi Surface." In Harrison, W. A. and M. B. Webb, eds. Proceedings of the International Conference on the Fermi Surface, Cooperstown, N. Y., Aug. 22-24, 1960. pp. 296-305. John Wiley and Sons, New York, N. Y.

_____. 1961. Advances in Phys. 10, 1.

IX. ACKNOWLEDGEMENTS

The author wishes to express his appreciation to Dr. A. H. Daane for his advice and counsel not only during the course of this investigation but during his entire graduate career. The author is also greatly indebted to Dr. S. Legvold, both for his interest in the investigation and for the use of his apparatus, and to Dr. A. R. Mackintosh for many informative discussions and suggestions concerning the phenomena observed in this investigation.

Acknowledgements are also due Messers. C. E. Habermann for preparing the metals, A. R. Kooser for machining the samples, and H. E. Nigh and J. K. Alstad for indoctrination and assistance in the use of the apparatus. Finally, the author wishes to thank his wife, Lee, whose patience, sacrifices, and unselfish dedication to his goals have contributed immeasurably to the success of his graduate study.

X. APPENDIX

The data from the resistivity-temperature measurements on the alloys examined in this investigation are tabulated in the appendix. The resistivity values are recorded to two decimal places for convenience in determining relative changes in the resistivity but the absolute accuracy is an order of magnitude less.

Table 14. Resistivity-temperature data for 20.0% Gd-Lu

Resistivity micro ohm-cm.	Temperature °K.	Resistivity micro ohm-cm.	Temperature °K.
56.04	4.2	79.82	92.7
55.98	4.6	80.55	96.5
55.94	5.0	81.25	100.7
55.98	6.6	81.91	104.3
56.11	7.8	82.81	108.4
56.11	8.4	83.26	111.6
56.27	9.8	83.83	115.8
56.54	11.4	84.65	120.2
56.77	13.2	85.29	124.8
57.37	16.1	86.05	129.9
57.73	18.0	86.87	134.9
57.97	19.2	87.64	140.3
58.26	20.8	88.40	145.4
58.46	21.6	89.29	150.3
59.49	25.2	89.99	156.1
60.28	27.4	90.89	161.7
61.21	29.6	91.65	167.2
62.20	32.3	92.44	172.8
64.29	37.0	93.30	179.2
66.83	43.9	94.13	184.5
67.93	47.1	95.46	194.4
69.02	50.0	96.51	202.0
70.18	52.9	97.58	209.4
71.34	56.2	98.57	216.7
73.39	63.8	99.66	224.9
74.29	66.8	101.02	235.1
74.92	69.1	101.81	241.1
75.39	71.3	103.50	253.4
75.74	73.2	104.47	261.0
76.28	75.4	105.89	272.4
76.81	77.4	106.82	279.1
77.74	81.3	107.87	187.7
78.24	84.0	109.20	298.1
78.56	86.1	110.09	305.9
79.23	89.0	111.65	317.7

Table 15. Resistivity-temperature data for 40.2% Gd-Lu

Resistivity micro ohm-cm.	Temperature °K.	Resistivity micro ohm-cm.	Temperature °K.
79.76	4.4	104.17	88.7
79.73	4.6	104.42	90.8
79.56	5.1	104.92	92.3
79.60	5.6	105.71	95.9
79.56	6.2	106.30	98.7
79.66	6.9	107.02	101.6
79.66	7.9	107.81	104.6
79.69	9.0	108.46	107.5
79.73	11.0	109.74	112.8
79.90	12.3	110.07	115.5
80.59	17.0	110.23	117.5
81.07	19.2	110.76	120.6
81.53	21.4	111.19	124.2
81.89	23.0	111.67	128.4
82.26	25.0	112.46	134.3
82.93	26.9	112.95	139.3
85.14	33.1	113.58	144.8
86.78	37.0	113.94	148.4
87.99	40.9	114.39	152.5
89.21	43.6	114.70	156.8
90.13	46.5	115.05	160.8
91.31	49.6	115.42	164.9
92.42	52.8	116.11	171.0
93.24	55.0	116.62	176.8
93.90	57.1	117.15	182.3
94.39	59.3	117.55	187.9
95.57	61.8	118.24	193.8
96.06	63.9	118.63	199.8
97.28	67.2	119.12	205.0
98.43	70.5	119.81	210.2
99.31	73.7	120.29	216.5
100.95	78.1	121.16	222.3
101.94	81.8	121.64	228.4
102.55	83.7	122.17	234.0
103.32	86.4	122.82	239.7

Table 15. (Continued)

Resistivity micro ohm-cm.	Temperature °K.
123.48	246.0
124.01	251.4
124.53	257.2
124.79	261.2
125.42	266.9
126.04	272.9
126.76	278.9
127.52	284.7
127.84	290.7
128.47	296.7
129.03	302.3
129.62	308.8
130.27	315.4
130.89	322.0

Table 16. Resistivity-temperature data for 57.3% Gd-Lu

Resistivity micro ohm-cm.	Temperature °K.	Resistivity micro ohm-cm.	Temperature °K.
81.94	4.2	105.13	80.0
81.91	4.3	105.53	81.6
81.83	4.7	106.25	83.0
81.79	5.0	106.85	84.6
81.75	5.3	107.71	86.9
81.75	5.6	108.57	89.0
81.72	6.6	108.98	90.3
81.75	7.6	109.58	92.0
81.68	8.8	110.34	94.2
81.86	10.5	110.67	96.3
81.91	11.4	111.73	98.7
82.02	13.0	112.43	100.8
82.17	13.8	113.00	102.5
82.32	15.5	113.78	104.8
82.54	17.8	114.46	107.1
83.33	21.6	115.21	109.2
83.60	23.2	116.11	112.7
84.08	25.2	117.38	116.5
84.65	27.0	118.25	119.4
85.51	29.6	119.08	122.3
85.84	31.0	120.40	126.6
86.59	32.7	121.10	129.3
87.83	36.0	121.74	131.7
89.74	41.0	122.71	134.9
91.06	44.6	123.23	137.4
92.48	48.1	123.69	139.7
93.87	51.3	124.44	142.8
94.40	52.8	125.15	146.8
95.71	55.9	126.01	150.2
96.87	58.4	126.95	154.5
98.60	62.4	127.74	159.4
99.91	65.8	128.34	163.4
100.89	68.4	128.82	166.4
102.58	72.9	129.02	168.6
104.11	76.4	129.28	171.6

Table 16. (Continued)

Resistivity micro ohm-cm.	Temperature °K.
129.35	173.5
129.65	176.1
129.76	179.1
130.21	182.1
130.31	184.0
130.44	187.2
130.67	190.6
131.00	194.4
131.15	199.4
131.45	203.2
131.75	207.2
131.94	211.2
132.12	213.8
132.65	217.1
132.80	220.9
132.99	224.3
133.18	227.7
133.66	231.4
133.88	236.5
134.34	241.2
134.60	246.3
135.16	252.4
135.62	258.2
136.06	264.9
136.78	270.8
137.22	276.7
137.57	281.9
138.05	287.8
138.43	293.4
139.10	301.2
139.70	309.9
140.45	317.9

Table 17. Resistivity-temperature data for 80.2% Gd-Lu

Resistivity micro ohm-cm.	Temperature °K.	Resistivity micro ohm-cm.	Temperature °K.
50.32	4.2	88.84	107.7
50.30	4.4	91.60	114.0
50.31	5.3	93.54	118.5
50.30	6.0	95.59	123.3
50.33	6.7	97.84	128.7
50.56	8.4	98.94	131.3
50.53	11.7	102.10	138.9
51.01	16.6	104.93	146.0
51.60	20.3	106.59	150.0
52.14	23.2	110.92	161.2
52.41	24.5	114.20	169.6
53.31	30.6	116.62	176.5
54.31	30.6	119.33	184.4
54.45	31.3	122.13	192.9
54.93	32.4	124.27	199.8
55.82	35.2	126.47	207.3
57.49	39.3	128.09	213.1
59.12	43.2	129.75	219.1
60.64	46.7	131.17	224.7
61.93	49.8	132.53	230.2
63.06	32.1	134.11	236.6
64.12	54.4	134.89	241.4
65.47	57.3	135.19	246.2
66.93	60.3	135.33	250.0
68.43	63.6	135.45	253.0
69.53	65.9	135.55	256.8
70.83	68.5	135.63	260.6
72.33	71.7	135.80	264.7
73.85	75.1	136.04	269.7
75.70	79.2	136.13	274.0
77.64	83.5	136.28	278.0
79.37	86.5	136.40	281.6
81.17	90.7	136.66	286.2
83.25	95.3	136.89	291.4
86.15	101.8	137.13	296.9

Table 17. (Continued)

Resistivity micro ohm-cm.	Temperature °K.
137.44	302.1
137.64	306.3
137.92	311.0
138.20	316.6
138.58	322.8

Table 18. Resistivity-temperature data for 23.3% Tb-Lu

Resistivity micro ohm-cm.	Temperature °K.	Resistivity micro ohm-cm.	Temperature °K.
42.88	4.2	63.49	92.7
42.66	5.8	64.09	96.6
42.66	6.0	64.81	101.5
42.70	7.6	65.51	107.4
42.77	8.8	66.66	114.6
43.05	10.4	67.64	121.9
43.12	12.6	68.76	129.9
43.64	16.2	69.90	137.0
44.65	19.4	70.98	145.0
45.46	24.3	72.20	153.4
46.74	28.5	73.49	161.9
48.65	33.8	74.43	169.3
50.15	37.8	75.54	177.4
51.52	41.6	76.76	186.6
52.84	45.6	77.98	195.9
54.20	49.5	79.20	204.8
55.21	52.5	80.42	214.5
56.50	56.6	81.57	223.7
57.50	60.0	82.83	233.2
58.30	62.6	84.15	243.2
58.72	64.8	85.14	251.2
59.35	67.2	86.24	260.2
59.90	69.9	87.53	269.9
60.36	72.2	88.64	278.9
60.85	74.9	89.86	288.5
61.44	78.1	90.93	297.8
61.86	81.4	92.30	208.0
62.27	84.0		
62.77	87.0		
63.11	89.8		

Table 19. Resistivity-temperature data for 46.7% Tb-Lu

Resistivity micro ohm-cm.	Temperature °K.	Resistivity micro ohm-cm.	Temperature °K.
68.53	4.2	103.20	115.9
68.53	5.1	103.94	119.4
68.46	5.8	104.65	123.3
68.39	6.7	105.00	126.4
68.43	7.8	105.64	130.6
68.50	10.1	106.17	134.5
68.82	14.4	106.45	138.1
69.59	17.5	106.81	141.9
70.20	20.1	107.16	145.7
70.97	23.5	107.59	149.0
72.02	27.1	108.15	152.9
72.95	30.0	108.47	156.2
74.33	33.8	108.86	159.7
75.43	36.7	109.39	163.6
77.31	41.6	109.89	167.3
78.26	44.4	110.20	170.8
79.32	46.1	110.70	175.3
80.56	50.5	111.34	180.1
82.05	54.2	111.94	184.6
83.32	57.3	112.18	188.4
84.77	60.9	112.61	192.4
85.58	63.4	113.10	196.7
87.28	67.6	113.60	201.0
88.45	70.9	114.13	205.6
89.76	74.5	114.52	210.5
90.78	77.4	114.94	215.9
93.33	84.4	115.47	221.0
94.18	87.1	115.93	226.4
95.56	90.9	116.64	231.8
96.62	94.0	117.28	236.8
98.07	98.0	117.92	242.3
99.06	101.8	118.48	247.8
100.30	105.1	119.05	253.5
101.32	109.0	119.68	259.5
102.32	112.4	120.36	265.4

Table 19. (Continued)

Resistivity micro ohm-cm.	Temperature °K.
120.99	271.1
121.56	276.6
122.20	282.6
122.94	288.5
123.61	294.3
124.07	300.0

Table 20. Resistivity-temperature data for 66.7% Tb-Lu

Resistivity micro ohm-cm.	Temperature °K.	Resistivity micro ohm-cm.	Temperature °K.
61.82	4.2	86.48	77.7
61.58	5.0	87.21	79.7
61.55	5.7	88.17	81.9
61.55	6.6	89.53	85.2
61.55	7.7	90.66	88.0
61.55	9.0	91.93	91.1
61.61	10.8	93.12	94.0
61.75	12.9	94.35	97.1
62.28	16.6	95.91	100.7
62.81	19.5	97.44	103.6
63.11	21.0	98.27	106.5
63.71	23.7	99.61	109.8
64.74	26.8	100.86	113.1
65.27	28.5	102.39	116.9
65.91	30.2	103.79	120.5
66.33	31.4	105.06	123.8
66.90	32.9	106.41	127.7
67.76	34.9	107.88	131.5
69.06	37.5	109.24	135.7
70.49	40.9	110.43	139.6
71.75	43.7	111.60	143.6
72.89	46.5	112.60	147.5
74.08	49.4	113.52	151.2
75.07	51.7	114.16	154.9
76.08	54.1	114.66	158.4
77.60	57.6	115.05	162.0
78.76	60.3	115.23	165.7
79.63	62.0	115.23	169.2
80.13	63.4	115.39	173.1
81.12	65.6	115.62	177.2
82.36	68.2	115.82	181.1
83.22	70.1	116.12	185.0
84.51	73.5	116.35	188.7
85.42	75.6	116.68	193.0
86.21	77.5	117.12	197.4

Table 20. (Continued)

Resistivity micro ohm-cm.	Temperature °K.
117.51	202.3
118.01	207.5
118.38	212.2
118.75	217.0
119.15	222.4
119.67	227.9
120.21	233.3
120.78	239.2
121.33	245.1
122.03	250.5
122.50	256.4
123.14	262.3
123.66	267.4
124.29	273.4
124.83	279.2
125.42	284.8
126.15	291.3
126.79	298.1
127.35	304.5
127.99	311.0
128.51	316.0

Table 21. Resistivity-temperature data for 93.4% Tb-Lu

Resistivity micro ohm-cm.	Temperature °K.	Resistivity micro ohm-cm.	Temperature °K.
20.38	4.4	53.70	90.7
20.18	5.2	55.61	94.4
20.11	6.8	57.74	98.3
20.15	8.3	59.42	101.6
20.18	9.4	61.55	105.5
20.22	11.2	63.26	108.7
20.38	13.9	65.09	112.1
20.62	16.2	65.76	113.4
21.02	18.4	67.91	117.5
21.43	21.0	70.14	121.5
21.80	22.7	71.76	125.2
22.23	24.7	76.37	133.0
22.88	26.5	77.59	135.4
23.38	28.3	81.43	142.4
23.99	29.9	84.12	147.0
24.69	32.0	85.90	150.2
25.67	34.3	90.05	157.7
27.42	38.1	95.03	166.8
28.66	40.9	98.44	172.7
30.08	43.9	100.02	175.7
31.64	47.3	103.73	181.4
33.25	50.6	110.19	189.7
34.30	52.9	113.36	195.8
35.81	55.9	116.46	202.1
37.09	58.4	118.41	207.0
38.34	60.7	120.00	214.1
39.65	63.2	119.92	218.4
41.60	67.1	120.00	222.7
43.19	70.2	120.10	226.5
44.84	73.5	120.23	230.2
46.65	77.1	120.50	235.3
47.00	77.5	120.74	238.6
48.41	80.4	120.90	241.8
50.33	84.0	121.21	245.8
51.84	87.1	121.35	249.8

Table 21. (Continued)

Resistivity micro ohm-cm.	Temperature °K.
121.61	252.6
122.05	256.9
122.43	261.8
122.86	266.0
123.23	271.6
123.77	277.2
124.31	281.7
124.84	286.6
125.15	290.4
125.92	298.6
126.36	303.5
126.90	309.4
127.14	314.7
128.22	322.1
Recheck	
96.18	168.2
100.19	175.1
101.60	177.7
105.67	182.9
107.13	184.4
108.98	187.1
107.10	183.1
109.76	187.9
111.54	190.6
113.53	194.6
115.15	198.2
116.76	201.8
117.87	205.0
119.15	209.1
119.97	214.1

Table 22. Resistivity-temperature data for 25.7% Gd-Er

Resistivity micro ohm-cm.	Temperature °K.	Resistivity micro ohm-cm.	Temperature °K.
28.34	4.5	81.60	123.8
28.34	5.2	82.64	127.9
28.38	6.1	83.22	131.2
28.42	7.9	83.56	134.0
28.65	9.9	83.79	136.6
29.23	13.2	84.06	139.8
29.97	16.2	84.52	144.0
31.15	19.7	84.99	147.4
31.80	21.8	85.33	150.9
32.92	24.8	85.79	154.4
34.38	28.0	86.18	156.5
36.07	31.3	86.64	160.7
37.65	34.7	87.45	165.3
39.92	40.0	87.79	168.4
40.95	42.5	88.25	171.8
42.19	45.3	88.72	175.8
43.57	48.2	89.14	179.1
45.49	51.8	89.83	183.5
47.57	55.9	90.48	187.6
49.11	58.6	91.18	193.7
51.11	62.1	91.83	198.5
53.49	66.3	92.72	205.0
56.07	70.7	93.21	210.4
59.14	75.5	94.10	216.4
62.45	79.9	94.83	222.6
62.83	80.5	95.60	228.3
64.68	83.5	96.48	234.0
66.60	86.9	97.10	240.0
69.72	92.8	97.94	244.9
71.41	96.8	98.64	250.6
73.76	102.0	99.37	256.1
75.41	106.2	100.10	261.7
76.83	110.2	100.75	267.6
78.95	115.3	101.59	273.9
80.56	120.3	101.94	276.3

Table 22. (Continued)

Resistivity micro ohm-cm.	Temperature °K.
102.87	281.9
103.48	287.3
104.29	293.1
104.94	299.0
105.83	306.5

Table 23. Resistivity-temperature data for 45.0% Gd-Er

Resistivity micro ohm-cm.	Temperature °K.	Resistivity micro ohm-cm.	Temperature °K.
33.41	4.5	90.72	131.0
33.29	5.4	92.61	135.1
33.72	6.4	94.50	139.0
33.84	7.5	97.93	144.1
33.60	9.5	101.05	148.5
33.80	11.2	103.14	152.7
34.12	12.9	104.52	157.1
34.91	16.7	105.35	160.5
35.34	18.5	105.94	163.4
36.96	23.7	106.57	166.6
38.53	28.0	107.05	170.2
40.15	32.2	107.28	174.0
43.31	39.7	107.40	179.0
46.38	46.2	107.60	183.4
47.64	49.4	107.87	188.3
48.99	52.0	108.15	192.8
50.45	54.9	108.43	196.8
52.34	58.5	108.86	202.3
54.86	63.3	109.25	207.6
57.55	68.2	109.65	212.6
60.66	73.9	110.20	217.8
63.30	79.2	110.79	223.4
62.44	77.1	111.42	228.6
65.47	82.9	111.82	233.3
68.91	89.0	112.29	238.0
70.72	92.5	112.76	243.2
72.69	96.1	113.32	248.6
74.31	99.2	113.87	253.6
76.52	103.2	114.38	259.2
78.81	107.4	115.09	265.1
80.30	111.0	115.64	271.0
82.83	114.9	116.04	276.3
84.96	119.1	116.67	282.1
86.85	123.1	117.30	288.2
88.94	127.4	117.89	293.8
		118.48	299.4
		119.09	305.2

Table 24. Resistivity-temperature data for 63.8% Gd-Er

Resistivity micro ohm-cm.	Temperature °K.	Resistivity micro ohm-cm.	Temperature °K.
29.08	4.2	73.53	109.8
29.01	4.8	75.86	114.4
29.08	5.9	78.04	118.7
29.12	7.9	80.98	123.9
29.12	10.1	83.12	128.4
29.65	14.2	85.87	134.3
30.27	17.6	88.16	139.3
30.72	20.0	90.57	144.6
31.22	22.0	92.82	149.5
32.10	25.1	95.08	154.7
32.67	27.0	97.37	160.4
33.71	28.9	99.63	165.4
34.43	32.0	101.92	171.1
35.65	35.1	104.02	176.7
37.03	38.2	106.16	182.4
38.56	41.9	108.34	188.4
39.63	44.4	109.64	192.2
40.89	47.2	110.90	110.9
42.65	50.8	111.97	199.4
44.75	55.0	113.12	203.0
46.58	58.6	114.30	206.7
48.34	61.8	115.49	210.5
50.10	65.3	116.79	215.0
52.81	70.5	118.12	219.4
54.80	74.2	119.31	233.9
56.56	77.7	119.77	228.8
56.48	77.4	119.96	232.7
58.16	80.7	120.26	236.6
59.58	83.4	120.45	240.4
61.76	87.4	120.57	244.2
63.67	91.0	120.87	248.2
65.62	94.7	121.26	254.0
67.76	98.6	121.45	258.2
69.44	102.0	122.25	263.8
71.54	105.8	122.29	269.1

Table 24. (Continued)

Resistivity micro ohm-cm.	Temperature °K.
122.59	275.2
122.86	280.8
123.43	286.2
123.78	292.2
124.24	298.1
124.70	303.6
125.19	309.9

Table 25. Resistivity-temperature data for 81.8% Gd-Er

Resistivity micro ohm-cm.	Temperature °K.	Resistivity micro ohm-cm.	Temperature °K.
17.61	4.3	58.60	101.1
17.61	4.9	60.53	104.7
17.62	5.7	62.16	107.6
17.65	6.6	63.92	110.9
17.69	8.2	65.74	114.5
17.78	10.1	68.21	119.1
17.90	11.7	70.37	123.4
18.24	14.6	72.94	127.8
18.72	18.0	75.47	133.0
19.33	20.9	77.69	137.5
19.99	24.0	80.33	142.6
20.89	27.1	82.64	147.2
21.99	30.3	85.08	152.0
23.23	33.6	87.35	156.8
24.60	36.9	89.70	161.6
26.18	40.5	92.11	166.6
27.81	43.9	94.42	171.4
29.43	47.3	96.52	176.0
30.62	49.8	98.96	181.4
32.47	53.3	100.94	185.9
33.86	56.0	103.01	191.0
35.03	58.1	105.01	195.8
36.77	61.4	107.29	201.2
38.69	64.8	109.42	206.6
40.40	67.9	111.24	211.3
41.71	70.4	113.27	216.9
43.86	74.3	115.28	222.7
45.61	77.2	117.20	228.2
47.56	80.9	119.04	234.0
48.58	82.8	120.71	239.6
50.12	85.6	122.43	245.5
51.57	88.2	123.97	251.1
53.15	91.1	125.49	256.8
54.79	94.2	126.72	262.5
56.60	97.5	126.98	266.3

Table 25. (Continued)

Resistivity micro ohm-cm.	Temperature °K.
127.15	270.1
127.36	273.8
127.50	276.8
127.65	279.7
127.83	283.6
128.03	287.5
128.25	291.4
128.46	295.2
128.66	299.0
129.03	304.8
129.37	310.4

Table 26. Resistivity-temperature data for 50.0% Y-Lu

Resistivity micro ohm-cm.	Temperature °K.	Resistivity micro ohm-cm.	Temperature °K.
31.88	4.2	54.53	121.6
31.85	5.2	55.65	126.9
31.85	6.2	56.71	131.7
31.82	8.0	57.97	138.0
31.85	10.8	59.10	142.9
31.92	13.2	60.22	148.4
32.01	15.7	61.55	154.5
32.34	19.2	62.67	160.0
32.97	25.4	63.96	166.3
33.73	29.6	64.89	170.6
34.07	31.8	65.92	176.0
34.66	35.0	67.14	182.2
36.52	43.2	68.92	189.6
37.57	48.1	70.41	196.9
39.60	56.6	71.94	204.9
40.92	62.0	73.49	212.5
41.95	66.5	74.88	219.8
43.11	71.2	76.41	227.7
43.97	75.1	77.90	235.3
44.60	77.5	79.39	242.8
46.05	83.8	80.78	250.1
46.88	87.2	82.21	257.9
47.78	91.2	83.21	257.9
48.67	95.1	85.15	273.1
49.50	98.8	86.27	280.6
50.22	102.0	87.86	288.3
51.08	105.7	89.32	296.3
51.91	109.6	90.68	303.7
52.64	112.9	92.20	311.5
53.40	116.6		